Advances in Virology

Virus Budding/Host Interactions

Guest Editors: Ronald N. Harty, Anthony P. Schmitt, Fadila Bouamr, Carolina B. Lopez, and Claude Krummenacher

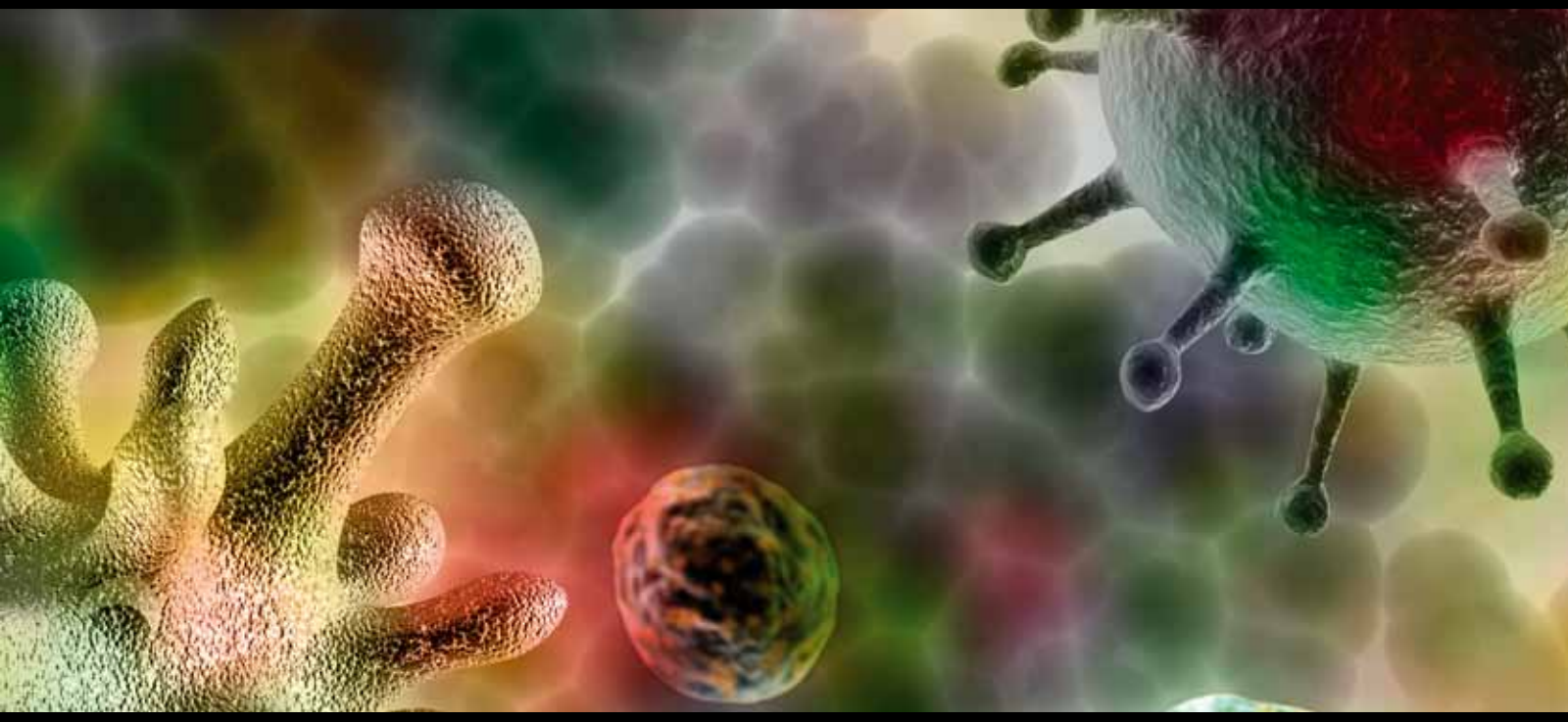

Virus Budding/Host Interactions

Advances in Virology

Virus Budding/Host Interactions

Guest Editors: Ronald N. Harty, Anthony P. Schmitt,
Fadila Bouamr, Carolina B. Lopez,
and Claude Krummenacher

Editorial Board

Contents

Hindawi Publishing Corporation
Advances in Virology
Volume 2011, Article ID 963192, 2 pages
doi:10.1155/2011/963192

Editorial
Virus Budding/Host Interactions

Ronald N. Harty,[1] Anthony P. Schmitt,[2] Fadila Bouamr,[3] Carolina B. Lopez,[1] and Claude Krummenacher[4]

[1] *Department of Pathobiology, School of Veterinary Medicine, University of Pennsylvania, Philadelphia, PA 19104, USA*
[2] *Center for Molecular Immunology and Infectious Disease, Department of Veterinary and Biomedical Sciences, The Pennsylvania State University, University Park, PA 16802, USA*
[3] *Laboratory of Molecular Microbiology, NIAID, NIH, Bethesda, MD 20892, USA*
[4] *Department of Biochemistry, School of Dental Medicine, University of Pennsylvania, 240 S. 40th Street, Philadelphia, PA 19104, USA*

Correspondence should be addressed to Ronald N. Harty, rharty@vet.upenn.edu

Received 22 August 2011; Accepted 22 August 2011

Viruses have developed unique and oftentimes complex molecular mechanisms to ensure efficient egress of mature virions from infected cells. Over the years, virologists have begun to unravel and appreciate the intricate roles of both viral and host proteins in this process, and particularly the specific recruitment of host factors to promote efficient budding of infectious virus. A better understanding of these virus-host interactions and the mechanisms of virus budding not only will provide fundamental insights into the functions of both viral and host proteins, but also will lead to the emergence of novel strategies to inhibit virion egress and spread. In this special issue on virus budding/host interactions, we have invited both review articles to summarize recent findings in the field as well as original research articles to provide new insights into this late stage of virus replication.

The first paper of this special issue is a review article that focuses on the current knowledge of arenavirus budding and the critical role that the small RING finger Z protein plays in this process. S. Urata and J. C. de la Torre present a comprehensive discussion on the structure and function of Z and highlight the various L-domain motifs conserved in arenavirus Z proteins and in the matrix proteins of other emerging RNA viruses. Viral L-domains are of particular interest since they mediate recruitment of host proteins to promote virus budding and, as such, constitute attractive and potentially broad-spectrum targets for antiviral drugs designed to inhibit virus egress. Indeed, the authors discuss several strategies and ongoing efforts to identify and screen candidate budding inhibitors.

The viral L-domain/host interaction theme continues in the second paper, where Y. Liu et al. have utilized a bimolecular complementation (BiMC) approach to detect, localize, and follow filovirus VP40-host complexes in live mammalian cells in real time. The authors postulate that adaptation of the BiMC approach to the study of virus-host interactions and budding may help address gaps in our understanding of the dynamics, kinetics, and trafficking patterns of virus-host complexes involved in the budding process. In addition, the BiMC approach was used in conjunction with the more established filovirus VP40 virus-like particle (VLP) budding assay to test candidate small molecule inhibitors (identified by *in silico* screening) of L-domain/host interactions for their ability to inhibit particle release.

The mechanisms by which viral and host proteins are trafficked and/or targeted to the site of budding are of great interest. The third paper summarizes experimental data in support of a model for assembly and budding of influenza virus from viral bud zones and raft-enriched domains at the plasma membrane. Indeed, assembly and budding at raft domains appears to be a characteristic shared by several RNA virus families. M. Veit and B. Thaa discuss the raft-targeting features of the hemagglutinin (HA) and neuraminidase (NA) glycoproteins of influenza virus, along with the critical roles of M1 and M2 proteins in orchestrating virus assembly and in membrane bending/particle scission, respectively.

Little is known about the role of human respiratory syncytial virus (HRSV) glycoproteins during assembly and budding of mature virions. In the fourth paper, M. Batonick and G. W. Wertz address this gap by engineering recombinant viruses and using microscopic and biochemical analyses to demonstrate that deletion of the G and F proteins affected the incorporation of other viral proteins into budding virions; however, their absence did not directly affect the efficiency of virion egress. Thus, this study ascribes a novel role for the G and F glycoproteins during the late stage of HRSV replication.

In the fifth paper, Snyder et al. describe a novel and intriguing cell lysis system utilized by two archaeal viruses, *Sulfolobus* turreted icosahedral virus (STIV) and *Sulfolobus islandicus* rod-shaped virus 2 (SIRV2). The authors demonstrate that the STIV c92 protein forms unique pyramid-like structures on the cell surface through which newly assembled virions are released during cell lysis. The authors speculate that this new lysis system may be common within other archaeal viral populations present in acidic hot springs.

Ronald N. Harty
Anthony P. Schmitt
Fadila Bouamr
Carolina B. Lopez
Claude Krummenacher

Hindawi Publishing Corporation
Advances in Virology
Volume 2011, Article ID 180326, 9 pages
doi:10.1155/2011/180326

Review Article

Arenavirus Budding

Shuzo Urata[1,2] and Juan Carlos de la Torre[2]

[1] *Department of Emerging Infectious Disease, Institute of Tropical Medicine, Nagasaki University, 1-12-4 Sakamoto, Nagasaki 852-8523, Japan*
[2] *Department of Immunology and Microbial Science, The Scripps Research Institute, 10550 North Torrey Pines Road, La Jolla, CA 92037, USA*

Correspondence should be addressed to Juan Carlos de la Torre, juanct@scripps.edu

Received 19 February 2011; Accepted 23 May 2011

Academic Editor: Fadila Bouamr

Several arenaviruses cause hemorrhagic fever disease in humans and pose a significant public health concern in their endemic regions. On the other hand, the prototypic arenavirus LCMV is a superb workhorse for the investigation of virus-host interactions and associated disease. The arenavirus small RING finger protein called Z has been shown to be the main driving force of virus budding. The budding activity of Z is mediated by late (L) domain motifs, PT/SAP, and PPXY, located at the C-terminus of Z. This paper will present the current knowledge on arenavirus budding including the diversity of L domain motifs used by different arenaviruses. We will also discuss how improved knowledge of arenavirus budding may facilitate the development of novel antiviral strategies to combat human pathogenic arenaviruses.

1. Introduction

Arenaviruses are enveloped viruses with a bisegmented negative strand (NS) RNA genome with coding capability for four known genes: nucleoprotein (NP), surface glycoprotein precursor (GPC), polymerase (L), and matrix-like (Z) proteins. Despite their limited genome and proteomic complexity, arenaviruses are able to exhibit very different phenotypic infection outcomes ranging from long-term subclinical chronic infections on their natural rodent hosts [1] to hemorrhagic fever (HF) disease in humans, infected through mucosal exposure to aerosols or by direct contact of abrade skin with infectious material. Thus, Lassa virus (LASV), the causative agent of Lassa fever (LF) is estimated to infect several hundred thousand individuals yearly in its endemic regions of West Africa, resulting in a high number of LF cases associated with high morbidity and significant mortality. Likewise, Junin virus (JUNV) causes Argentine HF, a severe illness with hemorrhagic and neurological manifestations and a case fatality of 15–30%, whereas the Machupo (MACV) and Guanarito (GTOV) arenaviruses emerged as causative agents of HF in Bolivia and Venezuela, respectively. On the other hand, the prototypic arenavirus, lymphocytic choriomeningitis virus (LCMV), is a superb workhorse for the investigation of virus-host interactions including mechanisms of virus control and clearance by the host immune defenses, as well as viral counteracting measures leading to chronic infection and associated disease [2, 3]. Moreover, evidence indicates that the globally distributed prototypic arenavirus LCMV is a neglected human pathogen of clinical significance, especially in cases of congenital infection. In addition, LCMV poses a special threat to immunocompromised individuals, as illustrated by cases of transplant-associated infections by LCMV with a fatal outcome in the USA and Australia. Public health concerns about arenavirus infections are aggravated by the lack of licensed vaccines and current therapy being limited to the use of the nucleoside analog ribavirin, which is only partially effective, requires early and intravenous administration for optimal activity, and can cause significant side effects. Therefore, it is important to develop novel and effective antiarenaviral strategies, a task that should be facilitated by a better understanding of the arenavirus molecular and cell biology.

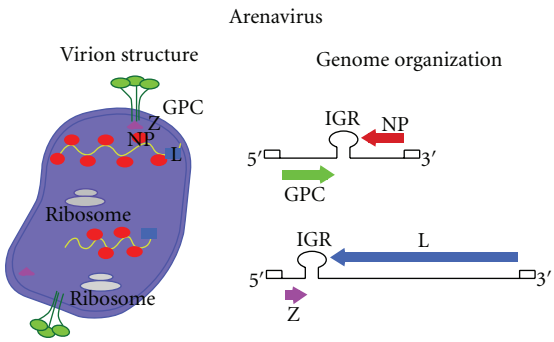

Figure 1: Arenavirus virion structure and genome organization. Arenaviruses are enveloped viruses with a bisegmented negative strand RNA genome. Each genome segment uses an ambisense-coding strategy to direct the synthesis of two viral polypeptides. The S (ca 3.5 kb) segment encodes for the viral nucleoprotein (NP) and glycoprotein precursor (GPC). GPC is posttranslational processed by the cellular protease S1P into the mature virion surface GP1 and GP2. The L (ca 7.3 kb) segment encodes for the virus RNA-dependent RNA polymerase (L) and a small RING finger protein (Z) that is functionally the arenavirus counterpart of the matrix (M) protein found in many enveloped negative strand RNA viruses. IGR, noncoding intergenic region.

The arenavirus small RING finger Z protein has been shown to be the main driving force of budding. This paper will examine our current understanding of arenavirus budding and discuss potential implications for the development of novel targeting strategies to combat human pathogenic arenaviruses.

2. Arenavirus Genome Organization and Life Cycle

Arenaviruses are enveloped viruses with a bisegmented negative strand (NS) RNA genome and a life cycle restricted to the cell cytoplasm. Virions are pleomorphic but often spherical and covered with surface glycoprotein spikes. Both the large, L (ca 7.3 kb) and small, S (ca 3.5 kb) genome RNA species use an ambisense-coding strategy to direct the synthesis of two polypeptides in opposite orientation, separated by a noncoding intergenic region (IGR) with a predicted folding of a stable hairpin structure [1] (Figure 1). The S RNA encodes the viral glycoprotein precursor, GPC, (ca 75 kDa) and the nucleoprotein, NP, (ca 63 kDa), whereas the L RNA encodes the viral RNA-dependent RNA polymerase (RdRp, or L polymerase) (ca 200 kDa) and a small (ca 11 kDa) RING finger protein Z that is functionally the counterpart of the matrix (M) protein found in many enveloped NS RNA viruses.

Consistent with a broad host range and cell-type tropism, a highly conserved and widely expressed cell surface protein α-Dystroglycan (α-DG) has been identified as a main receptor for LCMV, LASV, and several other arenaviruses [4, 5], whereas the human transferrin receptor (TfR) was identified as the primary receptor used by several New World (NW) arenavirus [6]. Upon receptor binding, virions are internalized using an endocytotic pathway that is either clathrin-independent or clathrin-dependent for Old World (OW) and NW arenavirus, respectively [5]. Interestingly, cell entry of OW LCMV and LASV are independent of caveolin, dynamin, actin, or small GTPases Rab5 and Rab7 but cholesterol-dependent [7–9]. Following the release of the viral ribonucleoprotein into the cytoplasm of the infected cells, the associated polymerase directs the biosynthetic processes involved in RNA replication and gene transcription. Assembly and cell release of infectious progeny involve the association of the viral ribonucleoprotein core with the surface GP complex, a process that is required for the production of infectious virions, which bud from the plasma membrane (PM).

3. Arenavirus Z Structure and Function

Results derived from minigenome- (MG-) based assays identified NP and L as the minimal viral transacting factors required for efficient RNA synthesis mediated by the virus polymerase [10–12]. Z was not required for RNA replication or transcription, but rather Z has been shown to exhibit a dose-dependent inhibitory effect on both transcription and replication of LCMV, Tacaribe virus (TACV), and LASV MGs [10, 12–14]. The inhibitory activity of Z on RNA synthesis by the LCMV polymerase did not require the N-terminus or C-terminus of Z, whereas the RING domain was strictly required but not sufficient [13, 14]. RING domains are known to mediate protein-protein interactions, and Z protein has been documented to interact with a variety of host cellular proteins including PML [15, 16] and translation initiation factor eIF4E [15–18]. The Z-PML interaction was reported to result in disruption of PML nuclear bodies and redistribution of PML to the cytoplasm, but the biological implications of this remain to be determined. On the other hand the Z-eIF4E interaction was found to impair eIF4E-dependent translation through its RING domain [16]. Interestingly, expression of Interferon regulatory factor 7 (IRF7), a key factor in the regulation of type I interferon (IFN) production by pDCs, is highly dependent on 4E [19]. Therefore, it is plausible that Z might mediate inhibition of IRF7 expression in arenavirus-infected pDCs and, thus, contributing to the mechanisms by which arenaviruses overcome the innate immune response by the host.

The possible contribution of RING-mediated Z-host cellular protein interactions to arenavirus budding is currently unknown. Notably, arenavirus Z proteins have a strictly conserved W residue in proximity to the second conserved C residue within the RING, a feature characteristic of RING proteins with E3 ligase activity involved in ubiquitin-dependent protein degradation. However, preliminary evidence indicated that LASV Z protein lacked ubiquitin-ligating activity in the presence of a variety of E2 enzymes including Ubc4 and Cdc34/Ubc3 [16]. Whether arenavirus Z proteins may exhibit E3 ligase activity in the presence of other E2 ubiquitin-conjugating enzymes and their biological implications remain to be determined. Z has also been implicated in antagonizing the host innate immune response.

Table 1: Summary of different matrix (M) protein L domain motifs and cellular-interacting partners. Characterized viral M proteins, accessory proteins, and their L domains are shown. *1: Alix/AIP1 has been shown to connect Z and NP [45, 46]. *2: there is a discrepancy between the groups for Alix/AIP1 and Vps4 necessity for the budding [34, 35, 47].

Virus	M protein	Accessary protein	L domain	Nedd4-like Ubiquitin ligase	Tsg101	Alix/AIP1	Vps4
HIV-1	Gag		PTAP YPXnL	○	○	○	○
RSV	Gag		PPPY YPXnL	○			○
VSV	M		PTAP PPPY	○	x		x
Ebola virus	VP40		PTAP PPPY	○	○		○
Marburg virus	VP40	 NP	PPPY PSAP	○	○ ○		○
Lassa virus	Z		PTAP PPPY		○		○
LCMV	Z		PPPY		○		○
Tacaribe virus	Z		ASAP		x		○
Mopeia virus	Z	 NP	PTAP PPPY			○*1	
Sendai virus	M	 C	YLDL			○*2 ○*2	○*2
Influenza virus							x

NW, but not OW, arenavirus Z was shown to bind RIG-I and inhibits IFN-β activation [20]. The recently reported NMR structure of LASV Z [17] should facilitate future structure-function studies aimed at the elucidation of the likely several roles played by Z in the arenavirus life cycle.

4. The Z Protein Is the Driving Force of Arenavirus Budding

The arenavirus Z protein has been shown to have bona fide budding activity [21–23]. Many enveloped viruses possess a matrix (M) protein that is often the main driving force of viral budding. Accordingly, the sole expression of this M protein can produce virus-like particles (VLPs). Frequently M proteins contain short amino acid motifs, called L (late) domains that play a critical role in virus budding. To date, the sequences PT/SAP, PPXY, and YPXnL (YPXL) have been well established as L domain motifs [24–26]. In addition to these L domains, the FPDL motif and several other short amino acid motifs have also been reported to function as L domains [24–26]. These L domain motifs exert their activity in virus budding by mediating the interaction with specific host cellular factors. Thus, the PT/SAP motif binds to Tsg101, a component of ESCRT-I (endosomal sorting complex required for transport-I) and initiates the budding process [27, 28]. Vps4A/B is AAA-type ATPases involved in catalyzing the disassembly and recycling of the membrane-bound ESCRT complexes [29–31]. Evidence indicates that the M protein of many, but not all, enveloped viruses have the ability to recruit ESCRT complex to their budding sites [24–26]. In addition to M, several other viral proteins, including Sendai virus (SeV) C protein and Marburg virus (MARV) NP, have been found to bind directly to ESCRT proteins, Alix/AIP1, or both and contribute to the budding process [24, 32–35]. Interestingly, some enveloped viruses, including influenza, are able to execute very efficiently the budding process without the ESCRT machinery [24, 36]. It is worth noting that although the M protein of VSV contains both PTAP and PPPY L domain motifs that interact with Tsg101 and Nedd4; respectively, Tsg101 and Vps4A were not required for efficient budding of VSV [37]. Rous sarcoma virus (RSV) Gag has a PPPY motif whose activity has been shown to be regulated by late-domain-interacting protein (LDI-1, Nedd4 chicken homolog) [38, 39]. Recently LYPSL motif in RSV Gag was shown to serve as a second L domain motif [40]. Table 1 summaries the variety of interactions observed between L domains present in M proteins of enveloped viruses and their host cellular interacting partners.

The family Arenaviridae currently includes 23 antigenically related viruses classified into two groups: OW and NW. This classification was originally established based on serological cross-reactivity but is well supported by recent sequence-based phylogenetic studies. OW arenaviruses constitute a single lineage, while NW arenaviruses segregate into clades A, B, and C. Recently, Lujo (LUJV) and Merino Walk (MWAV) viruses were identified as newly identified members of the OW group [41, 42]. Interestingly, among different arenaviruses, there are significant differences in the type of

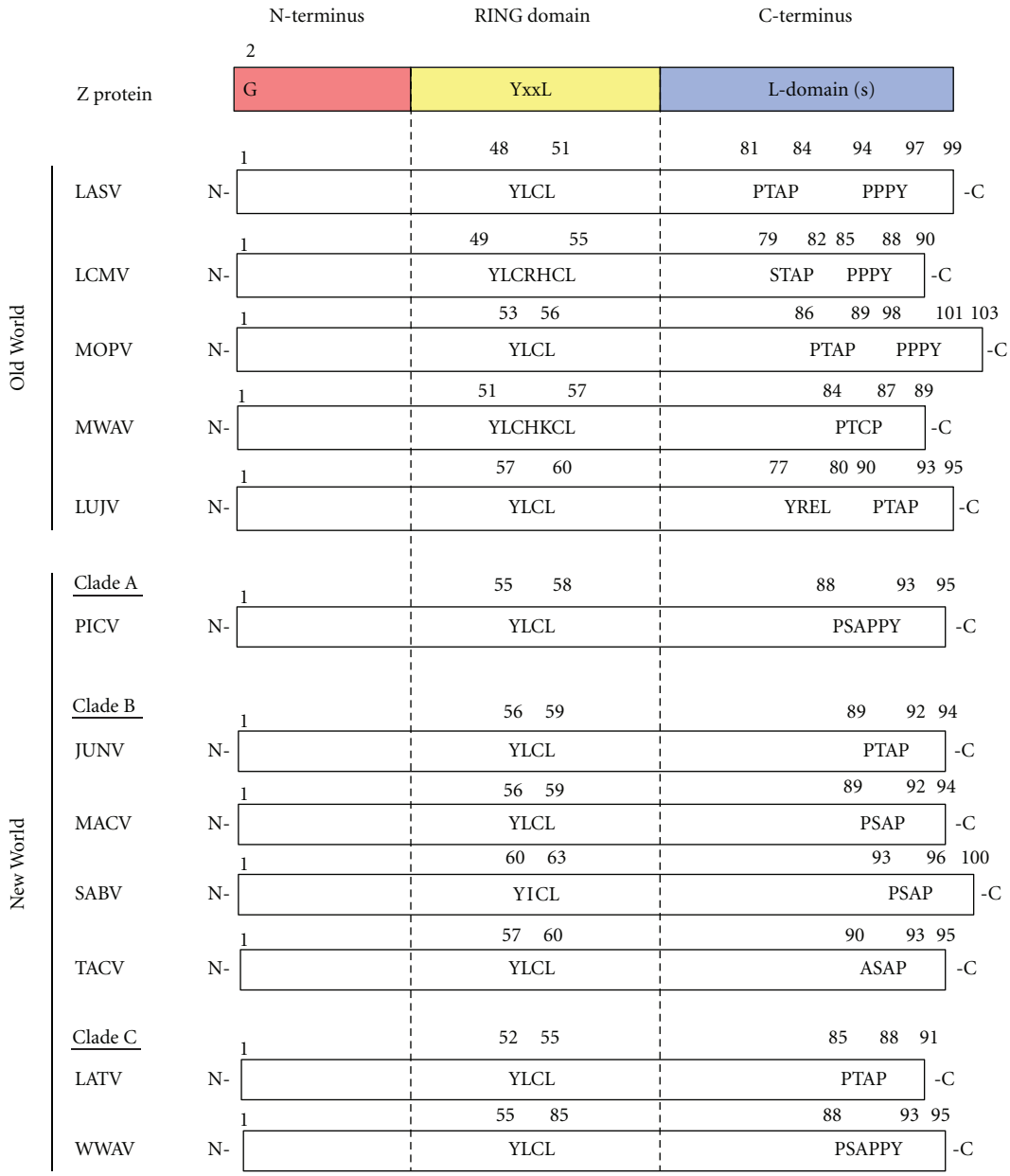

Figure 2: Organization of arenavirus Z protein. All arenavirus Z proteins have G at position 2 (G2). Within the centrally located RING domain, all known arenavirus Z proteins possess an YxxL (or YxxL-like) motif. At their C-terminus, arenavirus Z proteins have different types of L domains. Lassa virus (LASV), lymphocytic choriomeningitis virus (LCMV), Mopeia virus (MOPV), Merino Walk virus (MWAV), Lujo virus (LUJV), Pichinde virus (PICV), Junin virus (JUNV), Machupo virus (MACV), Sabia virus (SABV), Tacaribe virus (TACV), Latino virus (LATV), Whitewater Arroyo virus (WWAV).

L domain motifs present within their Z proteins (Figure 2). LCMV Z contains a canonical PPPY L domain and the PT/SAP-like domain STAP, whereas the Z of LASV and Mopeia virus (MOPV) which as LCMV are also members of the OW arenavirus group, contain, however, both PTAP and PPPY canonical L domains, but the Z of the also OW member Lujo virus contains only the PTAP L domain. On the other hand, the Z of many of the NW arenaviruses including JUNV, MACV, GATV, and Sabia (SABV) viruses contain the PT/SAP L domain. In addition Z proteins of Pichinde (PICV) and Whitewater Arroyo- (WWAV) viruses contain PTAP and APPY- (PPPY-like-) overlapping L domains, similar to those of Ebola virus (EBOV) VP40 L domain (PTAPPEY). Some arenavirus Z proteins do not contain canonical L domains but rather closely related motifs as in the case of the NW TACV and OW MWAV whose Z proteins contain ASAP and PTCP, respectively, L-like domains. In addition, all known arenavirus Z proteins contain an YxxL motif within the RING domain, but at least for TACV Z protein, it did not influence the Z budding activity [43, 44] (Figure 2).

The relative contribution of the different types of L domains to Z-mediated budding appears to be influenced by different factors including the virus species. Thus, for LASV the PPPY L domain appears to have a stronger contribution to budding than the PTAP motif [22, 23]. PPPY motif seems to have critical function compared to PTAP motif. In the case of TACV, the L-like domain ASAP was found to lack budding activity, and TACV Z-mediated budding was also Tsg101-independent but Vps4A/B-dependent [43, 44].

In addition to the critical role played by the L domain motifs in Z-mediated budding, glycine at position two (G2) was strictly required for Z-mediated budding. G2 is conserved among all known arenavirus Z proteins (Figure 2) and is required for Z myristoylation and its subsequent targeting of membranes [43, 48, 49]. Accordingly, mutation G2A abrogated Z-mediated budding. Consistent with these findings, treatment with 2-OHM (DL-2-hydroxymyristic acid), an inhibitor of protein myristoylation, caused a dramatic reduction on Z-mediated budding and production of infectious virus progeny [43, 48].

5. Novel Strategies to Identify Cellular Factors Contributing to Z-Mediated Budding and Small Molecule Inhibitors of Z-Mediated Budding

As with many other bona fide viral budding proteins, Z-mediated budding requires its interaction with specific cellular factors within the endosomal/multivesicular body pathway as we discuss below. The identification and characterization of LASV-Z-host protein interactions involved in virus budding may uncover novel anti-arenavirus targets, and facilitate the development of screening strategies to identify drugs capable of disrupting viral budding and thereby preventing virus propagation. The ability of Z to direct self-budding in the absence of other viral proteins should facilitate the development of assays amenable to both genetics and chemical High Throughput Screening (HTS) to identify host cellular proteins required for Z-mediated budding, as well as small molecule inhibitors of this process. To this end, the emergence of RNA interference as a pathway that allows the modulation of gene expression has enabled functional genetic screens in mammalian cell types. Likewise, combinatorial chemical libraries have emerged as a leading source of compounds for biological screens, and; therefore, it should be feasible to identify small molecule inhibitors of Z-mediated budding by screening chemical libraries using appropriately designed cell-based assays of Z-mediated budding. In this regard, recent findings have shown that the fusion of the smaller (185 amino acids) luciferase from *Gaussia princeps* (GLuc) to Z resulted in a chimeric protein (Z-GLuc) that retain wild-type Z budding activity that could be monitored by direct measuring of GLuc activity in tissue culture supernatant of Z-GLuc transfected cells. Initial studies have shown that this Z-GLuc-based budding assay consistently exhibits high signal-to-noise ratio (S/N) values (average 10-fold) [50], suggesting that it should be amenable for the development of both genetic and chemical HTS to identify host cellular genes contributing to Z-mediated budding and small molecule inhibitors of Z-mediated budding, respectively.

6. Contribution of the ESCRT Machinery to Arenavirus Budding

The ESCRT machinery was originally identified as the Class E subset of vacuolar protein sorting (VPS) genes required for the correct sorting of soluble hydrolases from the yeast Golgi to the vacuole [51–53]. The essential VPS-mediated sorting step occurs during MVB (multi vesicular body) formation, when ubiquitinated proteins and lipids present on the limiting endosomal membrane are recognized and sorted into endosomal membrane microdomains, which ultimately invaginate and form vesicles that bud into the lumen to create the MVB [54–56]. Vesicles of the MVB subsequently fuse with lysosome, thereby exposing the internal vesicles to the degrading lipases and proteases in this organelle. ESCRT pathway is also involved in the membrane abscission event at the conclusion of cell division [57, 58]. ESCRT-I contains Tsg101, Vps37, Vps23, and Mvb12A/B and has been shown to be recruited from the cytoplasm to the surface of maturing endosomes [29, 54–56, 59, 60]. Components of ESCRT-I, especially Tsg101, recognize ubiquitinated protein cargos and interact with ESCRT-II that participates in protein sorting and vesicle formation. It should be noted that Alix/AIP1 was found to bridge ESCRT-I and ESCRT-III using a different way to that used by ESCRT-II [61, 62]. ESCRT-III components also recruit another class E proteins, Vps4A/B, which are AAA-type ATPases involved in catalyzing the disassembly and recycling of the membrane-bound ESCRT complexes [29–31]. Notably, the abscission event during cellular cytokinesis, a process topologically similar to endosomal vesicle formation, utilizes the same ESCRT machinery [29, 58, 63].

Myristoylation of Z facilitates its attachment to the PM where Z is likely recognized by Tsg101 through the PT/SAP L domain motif present in Z (Figure 3). However, there is not direct biochemical evidence that Z binds to Tsg101 directly. Nevertheless, depletion of Tsg101 by siRNA resulted in decreased levels of both LASV and LCMV Z-mediated budding [21, 23]. Intriguingly, when the ASAP motif present on TACV-Z protein was mutated to AAAA, VLP production levels were not affected, suggesting in contrast to LCMV and LASV that TACV Z-mediated budding does not utilize Tsg101 [43, 44]. However, results of siRNA-mediated depletion and the use of dominant negative mutants indicated that Vps4A/B was necessary for both LASV and TACV Z-mediated budding activity [21, 43]. These results would suggest that the last step within the ESCRT pathway is necessary for both LASV and TACV Z-mediated budding.

The budding activity of some M proteins has been shown to be increased by the contribution of other viral proteins as illustrated in the case of the nucleoprotein (NP) and glycoprotein (GP) of the EBOV and MARV viruses [64, 65]. However, studies on LCMV and LASV Z-mediated budding failed to uncover a contribution to budding by other viral

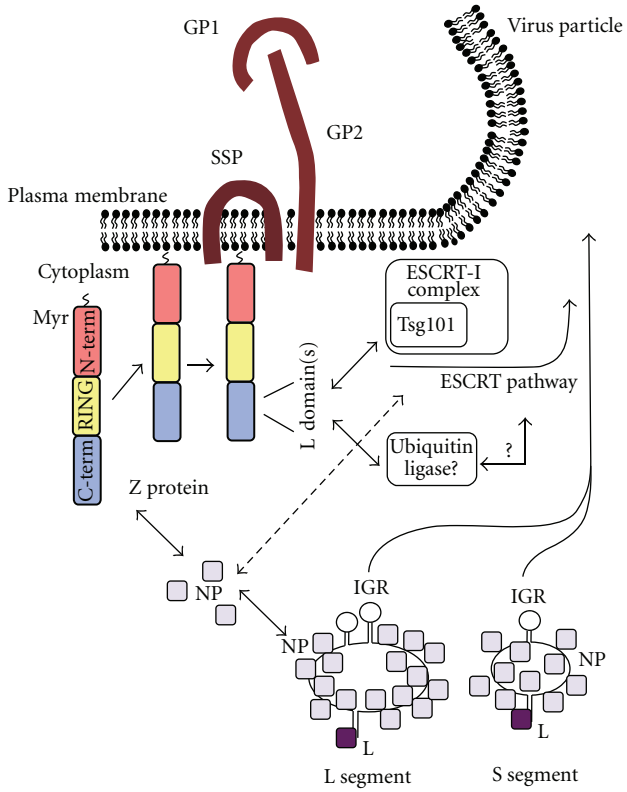

Figure 3: Model of arenavirus budding. Myristoylation of Z at G2 facilitates its interaction with the plasma membrane (PM), where Z likely forms higher-order complexes. L domains located within the C-terminus of Z facilitate its interactions with host cellular factors to allow Z to utilize the ESCRT machinery of the cell for cell egress (budding). SSP, stable signal peptide.

protein. In contrast, TACV NP was shown to enhance Z-mediated VLP production [44].

Nevertheless, recently published work has shown that Mopeia virus (MOPV) NP incorporation into VLP is mediated by AIP1/Alix via interaction with the YLCL motif present on Z [45, 46].

7. Tetherin/BST-2/CD317 as an Antagonist of Arenavirus Budding

Tetherin was identified as an IFN-inducible antiviral cellular factor that tether HIV virions at the PM [66, 67]. Subsequently studies have extended these findings to other viruses [68]. As with other host innate immune defense factors, several viruses have evolved mechanisms to counteract tetherin-mediated antiviral activity [69]. Tetherin has been shown to inhibit LASV Z-mediated budding [70]. Accordingly, 293T cells constitutively expressing tetherin resulted in decreased production levels of LASV and MACV virion particle production, whereas siRNA-mediated knockdown of endogenous tetherin in HeLa cells resulted in increased production levels of LASV and MACV virion particle production. These results would suggest that LASV does not possess any tetherin-antagonizing function as described for other viral proteins including HIV-1 Vpu, EBOV GP, and KSHV K5 [66, 71–73].

An issue that remains to be investigated relates to the contribution of tetherin to host protection and viral pathogenesis. An attractive hypothesis, but still without experimental support, would be that tetherin could do to some degree slow the process of virus propagation in vivo and thereby facilitating both the action of the host innate immune defense mechanisms and antigen presentation leading to a more robust host adaptive immune response that could control and eliminate the virus.

8. Perspectives on Arenavirus Z-Mediated Budding

Current evidence indicates that many enveloped viruses use the ESCRT machinery to exit from the cell. In the case of arenavirus budding, Z-Tsg101 interaction appears to facilitate access of Z to the ESCRT machinery. Despite significant recent progress in defining the basic aspects of arenavirus budding, there are still a large number of issues that have not been investigated including: (1) Identification and functional characterization of host cellular factors that interact with the PPXY L domain motif present in LASV, LCMV, and some other arenavirus Z to facilitate virus budding. PPXY L domain motifs present in EBOV and MARV VP40 have shown to mediate interaction with Nedd4.1 [74–76]. Likewise, for several retroviruses, the interaction of Gag PPXY L domains with ubiquitin ligases has been shown to contribute to the regulation of viral budding [24, 25, 38, 39]. How ubiquitin ligases may regulate budding remains unknown, but recent published data have shown arrestin-related proteins to connect ubiquitin ligases and the ESCRT machinery [77]. It is important to know whether specific ubiquitin ligase may regulate Z-mediated budding, and if so, what are the mechanism underlying this regulation. (2) Ubiquitin or ubiquitin-like molecules (UBLs) have been shown to modify the properties and budding activity of HIV-1 Gag and EBOV VP40 proteins [78]. It is currently unknown whether these protein modifiers may also have a role in the regulation of arenavirus budding. (3) The mechanisms by which arenavirus RNP interacts with Z and GP to form budding mature infectious progeny are largely unknown. (4) Whether the species-specific and type of cell influence arenavirus budding and the biological implications regarding the outcome of infection are issues that have not been investigated.

Detailed understanding of the virus-host cell protein interactions that direct arenavirus budding may uncover novel targets for the development of antiviral drugs to combat human pathogenic arenaviruses.

Acknowledgments

This is Publication no. 21130 from the Department of Immunology and Microbial Science, The Scripps Research Institute (TSRI), La Jolla, Calif, USA. Because space limitations, we have relied extensively in recent reviews where more

extensive detailed information, including all the original citations, can be found regarding the different topics discussed in this paper. Recognition and apologies are given in advance to the many colleagues whose original contributions have not been possible to cite. The research contributed by the authors of this paper was supported by NIH grants RO1 AI047140, RO1 AI077719 and RO1 AI079665 to J. C. de la Torre and T32-AI0735419 to S. Urata.

References

[1] M. J. Buchmeier, C. J. Peters, and J. C. de la Torre, "Arenaviridae: the virus and their replication," *Fields Virology*, vol. 2, pp. 1792–1827, 2007.

[2] M. B. Oldstone, "Biology and pathogenesis of lymphocytic choriomeningitis virus infection," *Current Topics in Microbiology and Immunology*, vol. 263, pp. 83–117, 2002.

[3] R. M. Zinkernagel, "Lymphocytic choriomeningitis virus and immunology," *Current Topics in Microbiology and Immunology*, vol. 263, pp. 1–5, 2002.

[4] W. Cao, M. D. Henry, P. Borrow et al., "Identification of α-dystroglycan as a receptor for lymphocytic choriomeningitis virus and Lassa fever virus," *Science*, vol. 282, no. 5396, pp. 2079–2081, 1998.

[5] S. Kunz, P. Borrow, and M. B. Oldstone, "Receptor structure, binding, and cell entry of arenaviruses," *Current Topics in Microbiology and Immunology*, vol. 262, pp. 111–137, 2002.

[6] S. R. Radoshitzky, J. Abraham, C. F. Spiropoulou et al., "Transferrin receptor 1 is a cellular receptor for New World haemorrhagic fever arenaviruses," *Nature*, vol. 446, no. 7131, pp. 92–96, 2007.

[7] S. Kunz, "Receptor binding and cell entry of Old World arenaviruses reveal novel aspects of virus-host interaction," *Virology*, vol. 387, no. 2, pp. 245–249, 2009.

[8] J. M. Rojek, M. Perez, and S. Kunz, "Cellular entry of lymphocytic choriomeningitis virus," *Journal of Virology*, vol. 82, no. 3, pp. 1505–1517, 2008.

[9] J. M. Rojek, A. B. Sanchez, N. T. Nguyen, J. C. de La Torre, and S. Kunz, "Different mechanisms of cell entry by human-pathogenic Old World and New World arenaviruses," *Journal of Virology*, vol. 82, no. 15, pp. 7677–7687, 2008.

[10] M. Hass, U. Gölnitz, S. Müller, B. Becker-Ziaja, and S. Günther, "Replicon system for Lassa virus," *Journal of Virology*, vol. 78, no. 24, pp. 13793–13803, 2004.

[11] K. J. Lee, I. S. Novella, M. N. Teng, M. B. Oldstone, and J. C. de La Torre, "NP and L proteins of lymphocytic choriomeningitis virus (LCMV) are sufficient for efficient transcription and replication of LCMV genomic RNA analogs," *Journal of Virology*, vol. 74, no. 8, pp. 3470–3477, 2000.

[12] N. López, R. Jácamo, and M. T. Franze-fernández, "Transcription and RNA replication of tacaribe virus genome and antigenome analogs require n and l proteins: Z protein is an inhibitor of these processes," *Journal of Virology*, vol. 75, no. 24, pp. 12241–12251, 2001.

[13] T. I. Cornu and J. C. de La Torre, "Ring finger z protein of lymphocytic choriomeningitis virus (lcmv) inhibits transcription and rna replication of an lcmv s-segment minigenome," *Journal of Virology*, vol. 75, no. 19, pp. 9415–9426, 2001.

[14] T. I. Cornu and J. C. de la Torre, "Characterization of the arenavirus RING finger Z protein regions required for Z-mediated inhibition of viral RNA synthesist," *Journal of Virology*, vol. 76, no. 13, pp. 6678–6688, 2002.

[15] K. L. Borden, E. J. Campbell Dwyer, and M. S. Salvato, "An arenavirus RING (zinc-binding) protein binds the oncoprotein promyelocyte leukemia protein (PML) and relocates PML nuclear bodies to the cytoplasm," *Journal of Virology*, vol. 72, no. 1, pp. 758–766, 1998.

[16] A. Kentsis, E. C. Dwyer, J. M. Perez et al., "The RING domains of the promyelocytic leukemia protein PML and the arenaviral protein Z repress translation by directly inhibiting translation initiation factor eIF4E," *Journal of Molecular Biology*, vol. 312, no. 4, pp. 609–623, 2001.

[17] L. Volpon, M. J. Osborne, A. A. Capul, J. C. de La Torre, and K. L. Borden, "Structural characterization of the Z RING-eIF4E complex reveals a distinct mode of control for eIF4E," *Proceedings of the National Academy of Sciences of the United States of America*, vol. 107, no. 12, pp. 5441–5446, 2010.

[18] E. J. Campbell Dwyer, H. Lai, R. C. MacDonald, M. S. Salvato, and K. L. Borden, "The lymphocytic choriomeningitis virus RING protein Z associates with eukaryotic initiation factor 4E and selectively represses translation in a RING-dependent manner," *Journal of Virology*, vol. 74, no. 7, pp. 3293–3300, 2000.

[19] R. Colina, M. Costa-Mattioli, R. J. Dowling et al., "Translational control of the innate immune response through IRF-7," *Nature*, vol. 452, no. 7185, pp. 323–328, 2008.

[20] L. Fan, T. Briese, and W. I. Lipkin, "Z proteins of new world arenaviruses bind RIG-I and interfere with type i interferon induction," *Journal of Virology*, vol. 84, no. 4, pp. 1785–1791, 2010.

[21] S. Urata, T. Noda, Y. Kawaoka, H. Yokosawa, and J. Yasuda, "Cellular factors required for Lassa virus budding," *Journal of Virology*, vol. 80, no. 8, pp. 4191–4195, 2006.

[22] T. Strecker, R. Eichler, J. Meulen et al., "Lassa virus Z protein is a matrix protein sufficient for the release of virus-like particles," *Journal of Virology*, vol. 77, no. 19, pp. 10700–10705, 2003.

[23] M. Perez, R. C. Craven, and J. C. de la Torre, "The small RING finger protein Z drives arenavirus budding: implications for antiviral strategies," *Proceedings of the National Academy of Sciences of the United States of America*, vol. 100, no. 22, pp. 12978–12983, 2003.

[24] B. J. Chen and R. A. Lamb, "Mechanisms for enveloped virus budding: can some viruses do without an ESCRT?" *Virology*, vol. 372, no. 2, pp. 221–232, 2008.

[25] P. D. Bieniasz, "Late budding domains and host proteins in enveloped virus release," *Virology*, vol. 344, no. 1, pp. 55–63, 2006.

[26] E. Morita and W. I. Sundquist, "Retrovirus budding," *Annual Review of Cell and Developmental Biology*, vol. 20, pp. 395–425, 2004.

[27] J. E. Garrus, U. K. von Schwedler, O. W. Pornillos et al., "Tsg101 and the vacuolar protein sorting pathway are essential for HIV-1 budding," *Cell*, vol. 107, no. 1, pp. 55–65, 2001.

[28] L. VerPlank, F. Bouamr, T. J. LaGrassa et al., "Tsg101, a homologue of ubiquitin-conjugating (E2) enzymes, binds the L domain in HIV type 1 Pr55Gag," *Proceedings of the National Academy of Sciences of the United States of America*, vol. 98, no. 14, pp. 7724–7729, 2001.

[29] J. H. Hurley and P. I. Hanson, "Membrane budding and scission by the ESCRT machinery: it's all in the neck," *Nature Reviews Molecular Cell Biology*, vol. 11, no. 8, pp. 556–566, 2010.

[30] M. Babst, T. K. Sato, L. M. Banta, and S. D. Emr, "Endosomal transport function in yeast requires a novel AAA-type ATPase, Vps4p," *EMBO Journal*, vol. 16, no. 8, pp. 1820–1831, 1997.

[31] M. Babst, B. Wendland, E. J. Estepa, and S. D. Emr, "The Vps4p AAA ATPase regulates membrane association of a Vps protein complex required for normal endosome function," *EMBO Journal*, vol. 17, no. 11, pp. 2982–2993, 1998.

[32] O. Dolnik, L. Kolesnikova, L. Stevermann, and S. Becker, "Tsg101 is recruited by a late domain of the nucleocapsid protein to support budding of Marburg virus-like particles," *Journal of Virology*, vol. 84, no. 15, pp. 7847–7856, 2010.

[33] T. Irie, N. Nagata, T. Yoshida, and T. Sakaguchi, "Paramyxovirus Sendai virus C proteins are essential for maintenance of negative-sense RNA genome in virus particles," *Virology*, vol. 374, no. 2, pp. 495–505, 2008.

[34] T. Sakaguchi, A. Kato, F. Sugahara et al., "AIP1/Alix is a binding partner of Sendai virus C protein and facilitates virus budding," *Journal of Virology*, vol. 79, no. 14, pp. 8933–8941, 2005.

[35] T. Irie, Y. Shimazu, T. Yoshida, and T. Sakaguchi, "The YLDL sequence within sendai virus M protein is critical for budding of virus-like particles and interacts with Alix/AIP1 independently of C protein," *Journal of Virology*, vol. 81, no. 5, pp. 2263–2273, 2007.

[36] J. S. Rossman and R. A. Lamb, "Influenza virus assembly and budding," *Virology*, vol. 411, no. 2, pp. 229–236, 2011.

[37] T. Irie, J. M. Licata, J. P. McGettigan, M. J. Schnell, and R. N. Harty, "Budding of PPxY-containing rhabdoviruses is not dependent on host proteins TGS101 and VPS4A," *Journal of Virology*, vol. 78, no. 6, pp. 2657–2665, 2004.

[38] A. Kikonyogo, F. Bouamr, M. L. Vana et al., "Proteins related to the Nedd4 family of ubiquitin protein ligases interact with the L domain of Rous sarcoma virus and are required for gag budding from cells," *Proceedings of the National Academy of Sciences of the United States of America*, vol. 98, no. 20, pp. 11199–11204, 2001.

[39] M. L. Vana, Y. Tang, A. Chen, G. Medina, C. Carter, and J. Leis, "Role of Nedd4 and ubiquitination of rous sarcoma virus Gag in budding of virus-like particles from cells," *Journal of Virology*, vol. 78, no. 24, pp. 13943–13953, 2004.

[40] K. A. Dilley, D. Gregory, M. C. Johnson, and V. M. Vogt, "An LYPSL late domain in the Gag protein contributes to the efficient release and replication of Rous sarcoma virus," *Journal of Virology*, vol. 84, no. 13, pp. 6276–6287, 2010.

[41] T. Briese, J. T. Paweska, L. K. McMullan et al., "Genetic detection and characterization of Lujo virus, a new hemorrhagic fever-associated arenavirus from southern Africa," *PLoS Pathogens*, vol. 5, no. 5, Article ID e1000455, 2009.

[42] G. Palacios, N. Savji, J. Hui et al., "Genomic and phylogenetic characterization of Merino Walk virus, a novel arenavirus isolated in South Africa," *Journal of General Virology*, vol. 91, no. 5, pp. 1315–1324, 2010.

[43] S. Urata, J. Yasuda, and J. C. de La Torre, "The Z protein of the new world arenavirus tacaribe virus has bona fide budding activity that does not depend on known late domain motifs," *Journal of Virology*, vol. 83, no. 23, pp. 12651–12655, 2009.

[44] A. Groseth, S. Wolff, T. Strecker, T. Hoenen, and S. Becker, "Efficient budding of the tacaribe virus matrix protein Z requires the nucleoprotein," *Journal of Virology*, vol. 84, no. 7, pp. 3603–3611, 2010.

[45] O. Shtanko, M. Imai, H. Goto et al., "A role for the C terminus of mopeia virus nucleoprotein in its incorporation into Z protein-induced virus-like particles," *Journal of Virology*, vol. 84, no. 10, pp. 5415–5422, 2010.

[46] O. Shtanko, S. Watanabe, L. D. Jasenosky, T. Watanabe, and Y. Kawaoka, "ALIX/AIP1 is required for NP incorporation into Mopeia virus Z-induced virus-like particles," *Journal of Virology*, vol. 85, no. 7, pp. 3631–3641, 2011.

[47] A. S. Gosselin-Grenet, J. B. Marq, L. Abrami, D. Garcin, and L. Roux, "Sendai virus budding in the course of an infection does not require Alix and VPS4A host factors," *Virology*, vol. 365, no. 1, pp. 101–112, 2007.

[48] M. Perez, D. L. Greenwald, and J. C. de La Torre, "Myristoylation of the RING finger Z protein is essential for arenavirus budding," *Journal of Virology*, vol. 78, no. 20, pp. 11443–11448, 2004.

[49] T. Strecker, A. Maisa, S. Daffis, R. Eichler, O. Lenz, and W. Garten, "The role of myristoylation in the membrane association of the Lassa virus matrix protein Z," *Virology Journal*, vol. 3, article 93, 2006.

[50] A. A. Capul and J. C. de la Torre, "A cell-based luciferase assay amenable to high-throughput screening of inhibitors of arenavirus budding," *Virology*, vol. 382, no. 1, pp. 107–114, 2008.

[51] V. A. Bankaitis, L. M. Johnson, and S. D. Emr, "Isolation of yeast mutants defective in protein targeting to the vacuole," *Proceedings of the National Academy of Sciences of the United States of America*, vol. 83, no. 23, pp. 9075–9079, 1986.

[52] J. S. Robinson, D. J. Klionsky, L. M. Banta, and S. D. Emr, "Protein sorting in Saccharomyces cerevisiae: isolation of mutants defective in the delivery and processing of multiple vacuolar hydrolases," *Molecular and Cellular Biology*, vol. 8, no. 11, pp. 4936–4948, 1988.

[53] C. K. Raymond, I. Howald-Stevenson, C. A. Vater, and T. H. Stevens, "Morphological classification of the yeast vacuolar protein sorting mutants: evidence for a prevacuolar compartment in class E vps mutants," *Molecular Biology of the Cell*, vol. 3, no. 12, pp. 1389–1402, 1992.

[54] D. J. Katzmann, M. Babst, and S. D. Emr, "Ubiquitin-dependent sorting into the multivesicular body pathway requires the function of a conserved endosomal protein sorting complex, ESCRT-I," *Cell*, vol. 106, no. 2, pp. 145–155, 2001.

[55] M. Babst, D. J. Katzmann, E. J. Estepa-Sabal, T. Meerloo, and S. D. Emr, "ESCRT-III: an endosome-associated heterooligomeric protein complex required for MVB sorting," *Developmental Cell*, vol. 3, no. 2, pp. 271–282, 2002.

[56] M. Babst, D. J. Katzmann, W. B. Snyder, B. Wendland, and S. D. Emr, "Endosome-associated complex, ESCRT-II, recruits transport machinery for protein sorting at the multivesicular body," *Developmental Cell*, vol. 3, no. 2, pp. 283–289, 2002.

[57] E. Morita, V. Sandrin, H. Y. Chung et al., "Human ESCRT and ALIX proteins interact with proteins of the midbody and function in cytokinesis," *EMBO Journal*, vol. 26, no. 19, pp. 4215–4227, 2007.

[58] J. G. Carlton and J. Martin-Serrano, "Parallels between cytokinesis and retroviral budding: a role for the ESCRT machinery," *Science*, vol. 316, no. 5833, pp. 1908–1912, 2007.

[59] T. Chu, J. Sun, S. Saksena, and S. D. Emr, "New component of ESCRT-I regulates endosomal sorting complex assembly," *Journal of Cell Biology*, vol. 175, no. 5, pp. 815–823, 2006.

[60] E. Morita, V. Sandrin, S. L. Alam, D. M. Eckert, S. P. Gygi, and W. I. Sundquist, "Identification of human MVB12 proteins as ESCRT-I subunits that function in HIV budding," *Cell Host and Microbe*, vol. 2, no. 1, pp. 41–53, 2007.

[61] B. Strack, A. Calistri, S. Craig, E. Popova, and H. G. Göttlinger, "AIP1/ALIX is a binding partner for HIV-1 p6 and EIAV p9

functioning in virus budding," *Cell*, vol. 114, no. 6, pp. 689–699, 2003.

[62] J. Martin-Serrano, A. Yarovoy, D. Perez-Caballero, and P. D. Bieniasz, "Divergent retroviral late-budding domains recruit vacuolar protein sorting factors by using alternative adaptor proteins," *Proceedings of the National Academy of Sciences of the United States of America*, vol. 100, no. 21, pp. 12414–12419, 2003.

[63] E. Morita, L. A. Colf, M. A. Karren, V. Sandrin, C. K. Rodesch, and W. I. Sundquist, "Human ESCRT-III and VPS4 proteins are required for centrosome and spindle maintenance," *Proceedings of the National Academy of Sciences of the United States of America*, vol. 107, no. 29, pp. 12889–12894, 2010.

[64] S. Urata, T. Noda, Y. Kawaoka, S. Morikawa, H. Yokosawa, and J. Yasuda, "Interaction of Tsg101 with Marburg virus VP40 depends on the PPPY motif, but not the PT/SAP motif as in the case of Ebola virus, and Tsg101 plays a critical role in the budding of Marburg virus-like particles induced by VP40, NP, and GP," *Journal of Virology*, vol. 81, no. 9, pp. 4895–4899, 2007.

[65] J. M. Licata, R. F. Johnson, Z. Han, and R. N. Harty, "Contribution of Ebola virus glycoprotein, nucleoprotein, and VP24 to budding of VP40 virus-like particles," *Journal of Virology*, vol. 78, no. 14, pp. 7344–7351, 2004.

[66] S. J. Neil, T. Zang, and P. D. Bieniasz, "Tetherin inhibits retrovirus release and is antagonized by HIV-1 Vpu," *Nature*, vol. 451, no. 7177, pp. 425–430, 2008.

[67] N. Van Damme, D. Goff, C. Katsura et al., "The interferon-induced protein BST-2 restricts HIV-1 release and is downregulated from the cell surface by the viral Vpu protein," *Cell Host and Microbe*, vol. 3, no. 4, pp. 245–252, 2008.

[68] D. T. Evans, R. Serra-Moreno, R. K. Singh, and J. C. Guatelli, "BST-2/tetherin: a new component of the innate immune response to enveloped viruses," *Trends in Microbiology*, vol. 18, no. 9, pp. 388–396, 2010.

[69] J. L. Douglas, J. K. Gustin, K. Viswanathan, M. Mansouri, A. V. Moses, and K. Früh, "The great escape: viral strategies to counter BST-2/tetherin," *PLoS Pathogens*, vol. 6, no. 5, Article ID e1000913, 2010.

[70] T. Sakuma, T. Noda, S. Urata, Y. Kawaoka, and J. Yasuda, "Inhibition of lassa and marburg virus production by tetherin," *Journal of Virology*, vol. 83, no. 5, pp. 2382–2385, 2009.

[71] R. L. Kaletsky, J. R. Francica, C. Agrawal-Gamse, and P. Bates, "Tetherin-mediated restriction of filovirus budding is antagonized by the Ebola glycoprotein," *Proceedings of the National Academy of Sciences of the United States of America*, vol. 106, no. 8, pp. 2886–2891, 2009.

[72] S. R. Radoshitzky, L. Dong, X. Chi et al., "Infectious Lassa virus, but not filoviruses, is restricted by BST-2/tetherin," *Journal of Virology*, vol. 84, no. 20, pp. 10569–10580, 2010.

[73] E. Bartee, A. McCormack, and K. Früh, "Quantitative membrane proteomics reveals new cellular targets of viral immune modulators," *PLoS Pathogens*, vol. 2, no. 10, article e107, 2006.

[74] S. Urata and J. Yasuda, "Regulation of Marburg virus (MARV) budding by Nedd4.1: a different WW domain of Nedd4.1 is critical for binding to MARV and Ebola virus VP40," *Journal of General Virology*, vol. 91, no. 1, pp. 228–234, 2010.

[75] J. Yasuda, M. Nakao, Y. Kawaoka, and H. Shida, "Nedd4 regulates egress of Ebola virus-like particles from host cells," *Journal of Virology*, vol. 77, no. 18, pp. 9987–9992, 2003.

[76] J. Timmins, G. Schoehn, S. Ricard-Blum et al., "Ebola virus matrix protein VP40 interaction with human cellular factors Tsg101 and Nedd4," *Journal of Molecular Biology*, vol. 326, no. 2, pp. 493–502, 2003.

[77] S. Rauch and J. Martin-Serrano, "Multiple interactions between the ESCRT machinery and arrestin-related proteins: implications for PPXY-dependent budding," *Journal of Virology*, vol. 85, no. 7, pp. 3546–3556, 2011.

[78] R. N. Harty, P. M. Pitha, and A. Okumura, "Antiviral activity of innate immune protein ISG15," *Journal of Innate Immunity*, vol. 1, no. 5, pp. 397–404, 2009.

Hindawi Publishing Corporation
Advances in Virology
Volume 2011, Article ID 341816, 10 pages
doi:10.1155/2011/341816

Research Article

Bimolecular Complementation to Visualize Filovirus VP40-Host Complexes in Live Mammalian Cells: Toward the Identification of Budding Inhibitors

Yuliang Liu,[1] Michael S. Lee,[2] Mark A. Olson,[2] and Ronald N. Harty[1]

[1] *Department of Pathobiology, School of Veterinary Medicine, University of Pennsylvania, 3800 Spruce Street, Philadelphia, PA 19104, USA*
[2] *Department of Cell Biology and Biochemistry, U. S. Army Medical Research Institute of Infectious Diseases, 1425 Porter Street, Frederick, MD 21702, USA*

Correspondence should be addressed to Ronald N. Harty, rharty@vet.upenn.edu

Received 8 July 2011; Accepted 9 August 2011

Academic Editor: Anthony P. Schmitt

Virus-host interactions play key roles in promoting efficient egress of many RNA viruses, including Ebola virus (EBOV or "e") and *Marburg virus* (MARV or "m"). Late- (L-) domains conserved in viral matrix proteins recruit specific host proteins, such as Tsg101 and Nedd4, to facilitate the budding process. These interactions serve as attractive targets for the development of broad-spectrum budding inhibitors. A major gap still exists in our understanding of the mechanism of filovirus budding due to the difficulty in detecting virus-host complexes and mapping their trafficking patterns in the natural environment of the cell. To address this gap, we used a bimolecular complementation (BiMC) approach to detect, localize, and follow the trafficking patterns of eVP40-Tsg101 complexes in live mammalian cells. In addition, we used the BiMC approach along with a VLP budding assay to test small molecule inhibitors identified by *in silico* screening for their ability to block eVP40 PTAP-mediated interactions with Tsg101 and subsequent budding of eVP40 VLPs. We demonstrated the potential broad spectrum activity of a lead candidate inhibitor by demonstrating its ability to block PTAP-dependent binding of HIV-1 Gag to Tsg101 and subsequent egress of HIV-1 Gag VLPs.

1. Introduction

Filoviruses are human pathogens that cause severe hemorrhagic disease and are potential agents of bioterrorism [1, 2]. EBOV and MARV are BSL-4 agents and NIAID Category A priority pathogens due to their association with high fatality rates and lack of approved vaccines or antivirals [2]. Filoviruses are enveloped, nonsegmented, negative-strand RNA viruses with an approximately 19.0-kilobase genome encoding the nucleoprotein (NP), VP35, matrix protein (VP40), attachment glycoprotein (GP), VP30, VP24, and RNA polymerase protein (L) [3]. VP40 is the major component of virions, and expression of VP40 alone in mammalian cells is sufficient to generate extracellular virus-like particles (VLPs), which resemble authentic virions in overall morphology [4–10]. Late- (L-) domain motifs conserved in the VP40 proteins are critical for efficient egress of VLPs and virions, as they function by hijacking specific host proteins involved in vacuolar protein sorting (vps) pathways to facilitate the final step of virus-cell separation [3, 6, 10–14]. EBOV VP40 (eVP40) possesses two L-domain motifs (PTAP and PPEY) at its N-terminus ($_{7}$-PTAPPEY-$_{13}$) [4, 6] whereas MARV VP40 (mVP40) and NP (mNP) contain single PPPY and PTAP L-domain motifs, respectively [12, 15]. Various approaches such as protein affinity chromatography, GST-pulldowns, and yeast two-hybrid screens have been used successfully to detect these functionally relevant L-domain mediated virus-host interactions *in vitro* [6, 12, 15]. For example, the PTAP L-domain of eVP40 recruits host Tsg101, a component of the cellular ESCRT (endosomal sorting complex required for transport) pathway involved in sorting monoubiquitinated proteins into multivesicular bodies (MVBs) [3, 6, 10, 12, 15–22] whereas the PPEY motif of eVP40 mediates an interaction with host Nedd4 ubiquitin ligase [4] leading to ubiquitination of eVP40 and enhanced VLP egress

[4, 10, 19, 23, 24]. Despite these *in vitro* studies, detection and visualization of these virus-host complexes, as well as the intracellular trafficking patterns of these complexes in the natural environment of the host cell remain elusive.

To address these gaps and to identify effective small molecule inhibitors of filovirus budding, we used a bimolecular complementation (BiMC) assay [25–28] with *Venus* enhanced yellow fluorescence protein (EYFP) to investigate filovirus VP40-host interactions in mammalian cells in real time [8]. *Venus* EYFP, a GFP variant containing a novel mutation of F46L, can be split into N- and C-terminal fragments, and reconstitution of these two EYFP fragments mediated by a protein-protein interaction results in an essentially irreversible fluorescent signal. This approach is useful for detecting and recording transient interaction events, allowing for detection of short-lived and/or weakly-associated protein-protein interactions in intact living cells [26, 28–31]. Using this approach, we were able not only to visualize an eVP40-Tsg101 interaction in live mammalian cells [8], but also were able to localize and follow the migration of eVP40-Tsg101 complexes in live cells. Lastly, we used BiMC and VLP budding assays to assess the specific inhibitory effects of small molecule compounds designed to block PTAP-mediated virus-host interactions and subsequent virus budding.

2. Materials and Methods

2.1. Cells, Plasmids, and Antisera. Human 293T cells were maintained in DMEM enriched with 10% FBS. All chimeric constructs were cloned into the pCAGGS expression vector. Plasmids eVP40-WT and eVP40-ΔPT/PY have been described previously [6]. The original MARV VP40 expression plasmid was kindly provided by Stephan Becker (Marburg, Germany). Plasmid pCS2 containing full-length *Venus* EYFP was generously provided by Roselyn J. Eisenberg, Gary Cohen, and Doina Atanasiu (University of Pennsylvania School of Dental Medicine). An HIV-1 Gag expression construct and anti-Gag antiserum were kindly provided by Paul Bates (University of Pennsylvania). NYFP and CYFP fragments were PCR-amplified and fused independently with full-length Tsg101, eVP40, mVP40, HIV Gag, or L-domain mutants of eVP40 or Gag in pCAGGS by standard cloning techniques [8]. Plasmid CYFP-mVP40 contains an in-frame FLAG epitope tag between the CYFP fragment and mVP40 ORF. Anti-eVP40 monoclonal antiserum was kindly provided by Dr. Gene Olinger (USAMRIID, Ft. Detrick, MD) [6]. Mouse monoclonal antibody against the FLAG epitope (Sigma-Aldrich) was used according to the manufacturer's instructions. Goat polyclonal antibody against pericentrin-B was purchased from Santa Cruz Biotechnology. Small-molecule compound 5539-0062 (ChemDiv, San Diego, CA) was dissolved in dimethyl sulfoxide (DMSO, FisherBiotech) at a concentration of 10 mM and stored at −20°C.

2.2. VLP Budding Assays. Human 293T cells were singly or co-transfected with the indicated plasmids using Lipofectamine (Invitrogen) in Opti-MEM (Invitrogen) according to the manufacturer's directions. VLP budding assays and western blotting were performed as described previously [8].

2.3. BiMC, Immunofluorescence, and Confocal Microscopy. Human 293T cells were grown on glass coverslips in six-well plates and cotransfected with the indicated plasmids. At 24 hours after transfection, cells were washed with PBS, fixed with cold methanol/acetone (vol/vol, 1 : 1) and stained with appropriate primary and second antibodies as indicated. Cells were washed as described above and subsequently stained with 4′,6′-diamidino-2-phenylindole (DAPI) for 10 min at room temperature. Cells were washed four times with PBS, and affixed to glass slides with Prolong Antifade (Invitrogen/Molecular Probes). Slides were viewed using an LSM-510 Meta confocal microscope (Carl Zeiss). For live cell imaging, 293T cells were seeded in glass bottom microwell dishes and transfected with the indicated plasmids. At 4 h after transfection, YFP fluorescence was observed using spinning-disk confocal microscopy in the presence of 5% CO_2 and humidity at 37°C. Cells were monitored for YFP fluorescence for a period of 20–24 hours after transfection.

2.4. siRNA Transfection. Tsg101-specific siRNA and random siRNA (used as a negative control) were purchased from Dharmacon Inc. Transfection was performed using Lipofectamine 2000 (Invitrogen) according to the manufacturer's instructions. Briefly, 293T cells were seeded in 24-well plates for 2 hours. Cells were then transfected with 20 nM of Tsg101-specific or random siRNA. At 24 h.p.t. the cells were transfected a second time with identical amounts of siRNA and the indicated plasmid(s). At 48 h.p.t. the cells were washed, fixed, and YFP fluorescence was detected as described above. Cells extracts were harvested in RIPA buffer and used in western blotting assays.

2.5. Small Molecule Inhibitors of VP40 Budding. Human 293T cells seeded in 6-well plates were pretreated with either vehicle (DMSO) alone, or compound 5539-0062 in DMSO at the indicated concentrations for 1 h at 37°C. Cells were subsequently transfected with the indicated plasmids. Viral proteins in cell extracts and VLPs were detected by western blotting as described above.

3. Results

3.1. Generation of EYFP Fusion Plasmids and Expression of EYFP Fusion Proteins. We generated a series of plasmids (some of which have been described previously, see [8]) for use in the BiMC assay that contain either the N-terminal EYFP fragment (residues 1–173, denoted NYFP), or the C-terminal EYFP fragment (residues 174–239, denoted CYFP) joined in-frame to host Tsg101, or to WT and L-domain mutants of eVP40, mVP40, and HIV-1 p55-Gag (Figure 1). All plasmids were verified by automated DNA sequencing, and expression of all YFP fusion proteins was confirmed by western blotting [8]; (Liu and Harty, data not shown). Importantly, fusion of the CYFP fragment to the N-termini of all viral proteins did not affect protein expression, nor the

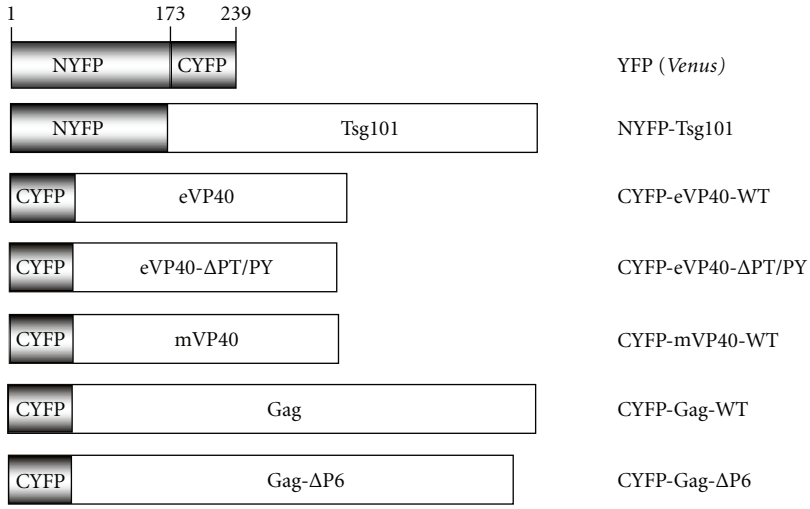

Figure 1: Schematic diagram of EYFP fusion proteins. The N-terminal half of EYFP (aa 1–173) was joined in-frame to full-length Tsg101, and the C-terminal half of EYFP (aa 174–239) was joined in-frame to the indicated WT or L-domain mutant VP40 or HIV-1 Gag proteins. A FLAG epitope tag is positioned at the N-terminus of mVP40-WT, and between the CYFP fragment and mVP40 in construct CYFP-mVP40-WT. The CYFP-Gag-ΔP6 construct was made by fusing the CYFP fragment in-frame with Gag L-domain deletion mutant (the entire p6 region containing L-domain motif PTAP is deleted).

well-characterized, L-domain-dependent budding properties of these viral matrix proteins (Liu and Harty, data not shown); [8, 32].

3.2. Detection, Localization, and Trafficking of eVP40-Host Interactions in Mammalian Cells Using BiMC. Recently, we reported that the BiMC approach could be used to detect viral protein-protein interactions in live mammalian cells [32]. Here, we used a similar approach to detect and map the intracellular localization of these filovirus-host complexes, and follow these complexes in real time as they traffic through the cell. Briefly, human 293T cells were cotransfected with plasmids expressing NYFP-Tsg101 + CYFP-eVP40-WT, or NYFP-Tsg101 + CYFP-eVP40-ΔPT/PY (L-domain deletion mutant of eVP40), and cells were examined for YFP fluorescence at 24 h.p.t. No background fluorescence was detected when fusion plasmids were transfected singly ([32], Liu et al., data not shown). YFP fluorescence was observed readily and reproducibly in 293T cells coexpressing NYFP-Tsg101 + CYFP-eVP40-WT (Figure 2(a), panel a); however, this signal was virtually absent in cells coexpressing NYFP-Tsg101 + CYFP-eVP40-ΔPT/PY (Figure 2(a), panel b) [32]. Similar results were obtained in cell lines other than human 293T cells including, Huh7, HeLa, and A549 cells (Liu and Harty, data not shown). The use of the L-domain deletion mutant of eVP40 not only validates the specificity of the observed EYFP signal (Figure 2(a), panel a), but also confirms the overall feasibility of using the BiMC approach to detect and record these transient virus-host interactions in mammalian cells [32]. It should be noted that the CYFP-eVP40-ΔPT/PY protein was shown to be functional in the BiMC assay, as it interacted with NYFP-eVP40-WT to form eVP40-WT/eVP40-ΔPT/PY complexes which resulted in YFP fluorescent cells [32].

To further prove that the observed YFP fluorescence (Figure 2(a), panel a) was due to a specific interaction between eVP40 and Tsg101, we cotransfected cells with random or Tsg101-specifc siRNAs. Briefly, human 293T cells grown on coverslips in 6-well plates were mock-transfected, or transfected with 20 nM of Tsg101-specific or random siRNA. Twenty-four hours later, cells were mock-transfected, or transfected with the same amount of siRNAs along with NYFP-Tsg101 + CYFP-eVP40 plasmids (Figure 2(a)). After an additional 24 hours, cells were examined by confocal microscopy for YFP fluorescence. A strong YFP signal was observed in cells expressing Tsg101/eVP40-WT in the presence of no siRNA (mock), or random siRNA (Figure 2(a)). In contrast, YFP fluorescence was virtually absent in cells receiving Tsg101-specific siRNA (Figure 2(a)). Importantly, the concentration of Tsg101-specfic siRNAs used above was shown by western blot to knockdown expression of Tsg101 in 293T cells by >90% (Liu and Harty, data not shown; [6]).

3.3. Trafficking and Intracellular Localization of Tsg101/eVP40 Complexes in Live Cells. Once the specificity of the NYFP-Tsg101 + CYFP-eVP40-WT interaction was confirmed, we sought to determine the kinetics of association and intracellular origin of this virus-host complex, and also follow its movement through the cell in real time. The YFP fluorescence generated at early times p.t. in cells co-expressing NYFP-Tsg101 + CYFP-eVP40-WT appeared to be punctate in nature and localized adjacent to the nucleus (Figure 2(b)). This intracellular position resembled that of the microtubule organizing center (MTOC). Therefore, we sought to determine whether the NYFP-Tsg101 + CYFP-eVP40-WT complex was initially forming at the MTOC by using an antibody to pericentrin-B: an MTOC marker protein (Figure 2(b)). Indeed, the Tsg101/eVP40-WT

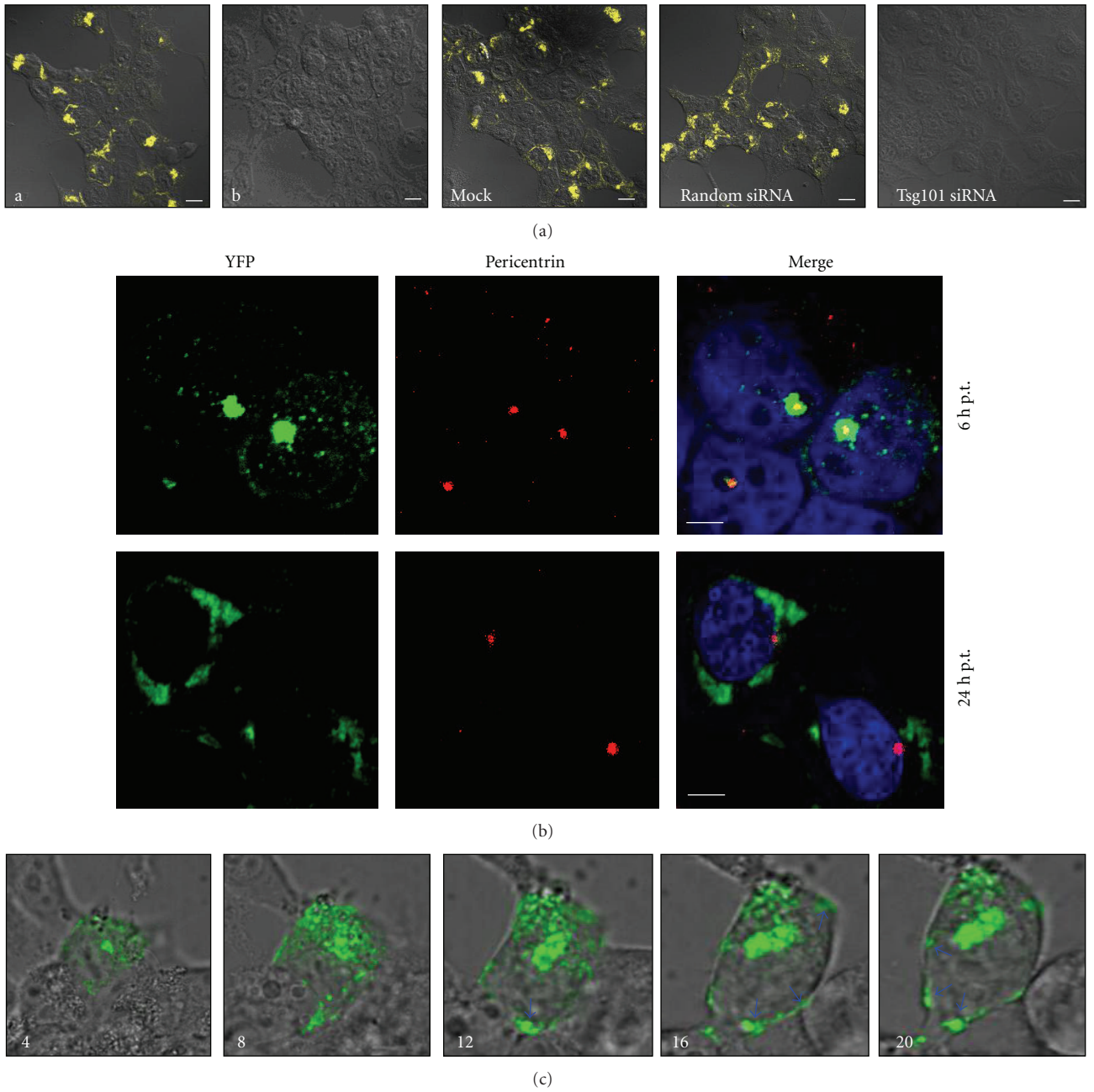

Figure 2: BiMC detecting eVP40-Tsg101 interactions and trafficking of Tsg101/eVP40 complex. (a) Human 293T cells grown on coverslips in 6-well plates were transfected with NYFP-Tsg101 + CYFP-eVP40-WT (a) or NYFP-Tsg101 + CYFP-eVP40-ΔPT/PY. (b) Cells were washed, fixed, and examined for YFP fluorescence by confocal microscopy at 24 hours p.t. Cells were mock-transfected, or transfected with 20 nM of Tsg101-specific or random siRNA. Twenty four hours later, cells were mock-transfected or transfected with the same amount of siRNA along with NYFP-Tsg101 + CYFP-eVP40. After an additional 24 hours, cells were examined for YFP fluorescence as described above. (b) Colocalization eVP40-Tsg101 complexes with pericentrin. BiMC assay showing colocalization between pericentrin-B and YFP fluorescence from 293T cells expressing NYFP-Tsg101 + CYFP-eVP40-WT at 6 hours p.t. (top panel) and 24 hours p.t. (bottom panel). (c) DIC images of a single 293T cell co-expressing NYFP-Tsg101 + CYFP-eVP40-WT at 4, 8, 12, 16, and 20 hours p.t. Blue arrows indicate Tsg101/eVP40 complex accumulation at the plasma membrane.

complex was first visible between 3–4 hours p.t., and this complex colocalized strongly with pericentrin-B at 6 hours p.t. (Figure 2(b), top row). In contrast, colocalization of the Tsg101/eVP40-WT complex with pericentrin-B was not evident at later times p.t. (12–24 hours, Figure 2(b), bottom row). These findings suggest that the Tsg101/eVP40 complex may traffic via the microtubule network to the eventual site of budding at the plasma membrane. It should be noted that additional cellular markers including calnexin (ER), Giantin (*cis*-Golgi), and EEA1 (early endosome) were used in similar

colocalization experiments; however, the Tsg101/eVP40-WT complex did not exhibit any significant level of colocalization with these host proteins (Liu and Harty, data not shown).

Further evidence supporting the movement of the Tsg101/eVP40 complex from the MTOC to the plasma membrane was obtained by continuous monitoring of the YFP signal in co-transfected cells over a 16-hour period (Figure 2(c)). Real-time images of a single cell co-expressing NYFP-Tsg101 + CYFP-eVP40-WT at the indicated times p.t. illustrates the changes in intracellular localization of Tsg101-eVP40-WT complexes from their initial formation at the MTOC between 3–4 hours after transfection, to their enhanced accumulation at distinct patches on the plasma membrane (Figure 2(c)). Taken together, the properties exhibited by Tsg101-eVP40-WT complexes in the natural environment of the cell appear to represent functional recruitment of Tsg101 by eVP40 leading to efficient budding.

3.4. Small Molecule Inhibitors of Filovirus VP40-Host Interactions and VP40 VLP Budding. Viral L-domains are attractive targets for host-oriented therapeutics which may possess broad-spectrum activity against a plethora of L-domain containing RNA viruses [33]. For example, a five amino acid cyclic peptide was reported recently to disrupt the interaction between Tsg101 and the PTAP L-domain motif of HIV-1 Gag leading to diminished egress of Gag VLPs [34, 35]. Our strategy to identify inhibitors of filovirus budding was to perform *in silico* screening of the ZINC drug-like library (2.4 million compounds) against the NMR-derived structure of human Tsg101 UEV domain (PDB id: 1M4P, conformer #1) focusing on the binding pocket of the PTAP peptide (Figure 3) [34, 36, 37]. The PTAP binding pocket is outlined roughly by residues Y63, Y68, I70, M95, F142, and S143 of Tsg101. High-throughput computational screening was performed with the AutoDock program in the DOVIS pipeline [38, 39]. The top 20,000 complexes from the initial screen were minimized in CHARMM with the MMFF force field and reranked using Accelrys Ligscore2 [40–42].

We tested the top six scoring compounds using both BiMC and VLP budding assays for their ability to disrupt either an eVP40-Tsg101, or mVP40-Tsg101 interaction and subsequent VLP egress. Of the six molecules tested, compound 5539-0062 (Figure 4(a)) exhibited PTAP-specific inhibition of eVP40 VLP egress and of eVP40-Tsg101 complex formation. Briefly, human 293T cells were first treated for 1 hour with either carrier (DMSO) alone, or increasing concentrations of compound 5539-0062, and then budding of eVP40 or mVP40 VLPs was evaluated and quantified (Figures 4(b)–4(d)). Compound 5539-0062 inhibited PTAP-dependent budding of eVP40-WT VLPs by >50% at lower concentrations, and by >90% at higher concentrations (Figures 4(b) and 4(c)). In contrast, PTAP-independent budding of mVP40-WT VLPs was reduced by <2-fold at all concentrations tested (Figures 4(b) and 4(d)). Expression controls for eVP40-WT and mVP40-WT in cells remained unaltered at all drug concentrations tested (Figures 4(b)–4(d)). It should be noted that concentrations of compound 5539-0062 used for the above experiments

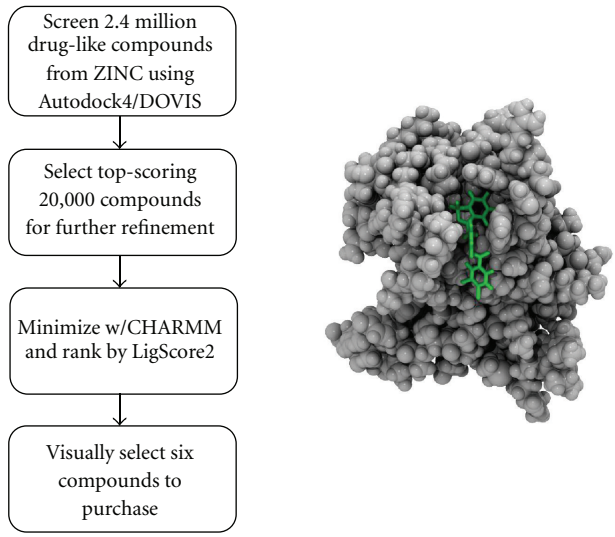

Figure 3: Strategy for computational screening of budding inhibitors. The stereo view of the PTAP motif (green) in its binding groove on the UEV domain of Tsg101.

exhibited no significant toxicity in human 293T cells in culture as determined by XTT colorimetric assay (Liu and Harty, data not shown). Consistent with the findings of our VLP budding assays (Figures 4(b)–4(d)), compound 5539-0062 blocked the interaction between NYFP-Tsg101 + CYFP-eVP40-WT as determined by BiMC (Figure 4(e)) and quantitation of YFP fluorescing cells by FACS analysis. Thus, compound 5539-0062 was capable of specifically inhibiting PTAP-dependent budding of eVP40 VLPs by disrupting the eVP40-Tsg101 interaction while having no effect on PTAP-independent budding of mVP40 VLPs.

To further prove the PTAP-specific inhibitory effect of compound 5539-0062 and assess its ability to inhibit budding of infectious virus, we infected 293T cells with either VSV-WT (containing a PPxY-type L-domain), or VSV-M40; a VSV recombinant containing the PTAP-type L-domain from eVP40 in place of the normal VSV PPxY-type L-domain [18] (Table 1). In two independent experiments, cells were infected at an MOI of 1.0 for 8 hours, and virus released into the supernatant was harvested and titered on BHK-21 cells. Equivalent titers of VSV-WT and VSV-M40 were obtained in the presence of vehicle (DMSO) alone (Table 1). While the titers of VSV-WT did decrease slightly in the presence of increasing concentrations of 5539-0062, the titers of VSV-M40 were reproducibly reduced by 3–10-fold more than those of VSV-WT in the presence of increasing concentrations of compound 5539-0062 (Table 1). These data correlate well with those shown in Figure 4, and further support the specificity of compound 5539-0062 to inhibit viral PTAP L-domain function by inhibiting budding of an infectious VSV recombinant expressing the PTAP-type L-domain from eVP40.

3.5. Compound 5539-0062 Inhibits HIV-1 Gag-Tsg101 Interaction and PTAP-Dependent Gag VLP Budding. The p6 region of HIV-1 Gag contains a well-defined PTAP L-domain motif

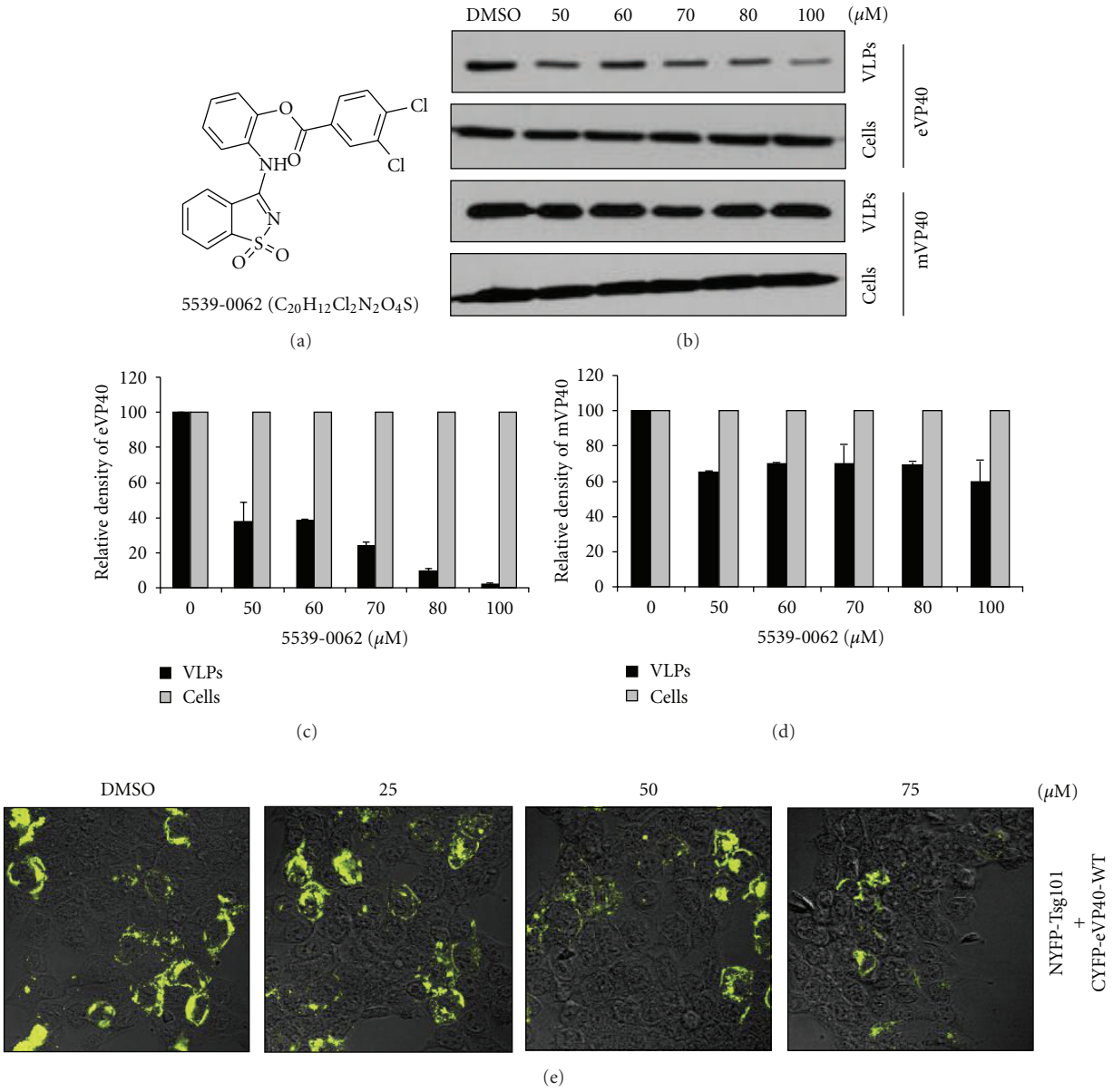

Figure 4: Inhibition of VP40-Tsg101 interactions and VLP budding. (a) Chemical structure of compound 5539-0062. (b) Budding assay and western blotting for eVP40 and mVP40 in VLPs and cell extracts from human 293T cells treated with DMSO alone, or the indicated concentrations of PTAP-inhibitor 5539-0062. (c) Bar graph of the relative amounts of eVP40-WT in cells and VLPs (part B) determined using Dot-Blot, LabWorks software (UVP). (d) Bar graph of the relative amounts of mVP40-WT in cells and VLPs (part B) determined using Dot-Blot, LabWorks software (UVP). (e) BiMC of human 293T cells expressing NYFP-Tsg101 + CYFP-eVP40-WT and treated with DMSO alone, or the indicated concentrations of PTAP-inhibitor 5539-0062. Cells were examined for YFP fluorescence at 24 hour p.t., and positive cells were quantified by FACS analysis. The average values were as follows: DMSO alone = 100%, 25 μM = 84%, 50 μM = 68%, and 75 μM = 24%.

Table 1: Viral titers in the presence of drug 5539-0062.

5539-0062 (μM)	VSV-WT		VSV-M40	
	Exp. number 1	Exp. number 2	Exp. number 1	Exp. number 2
0.0	1.2×10^5	1.2×10^5	1.2×10^5	1.1×10^5
25.0	8.2×10^4	8.0×10^4	1.4×10^4	1.0×10^4
50.0	1.5×10^4	1.6×10^4	3.6×10^3	3.8×10^3
75.0	8.6×10^3	N.D.	6.4×10^2	N.D.

N.D. = not done.

that mediates efficient budding of HIV-1 virions and Gag VLPs by recruiting Tsg101 in a manner similar to that used by eVP40 [16, 17, 20]. To determine whether PTAP inhibitor 5539-0062 has broad-spectrum antibudding activity, we employed the HIV-1 Gag protein in our VLP budding assay and generated HIV-1 Gag-YFP fusion proteins for use in BiMC. Briefly, human 293T cells were cotransfected with NYFP-Tsg101 + CYFP-Gag-WT or CYFP-Gag-ΔP6 (PTAP L-domain mutant) as a control (see Figure 1), and YFP fluorescence was detected at 24 hours p.t. (Figure 5(a)). Cells co-expressing NYFP-Tsg101 + CYFP-Gag-WT displayed a predominantly punctate YFP signal that was evident in both perinuclear patches and at the cell periphery (Figure 5(a)). As expected, the YFP signal was virtually absent in cells co-expressing NYFP-Tsg101 + CYFP-Gag-ΔP6 (Figure 5(a)). Both the CYFP-Gag-WT and CYFP-Gag-ΔP6 fusion proteins were shown to be expressed in transfected 293T cells by western blot (Liu and Harty, data not shown).

Next, we used both BiMC (Figure 5(b)) and VLP budding (Figure 5(c)) assays to determine whether compound 5539-0062 could inhibit a Gag-Tsg101 interaction and subsequent egress of HIV-1 Gag VLPs in a dose-dependent manner. Human 293T cells were treated with vehicle (DMSO) alone or the indicated concentrations of compound 5539-0062, and then co-transfected with NYFP-Tsg101 + CYFP-Gag-WT (Figure 5(b)). Cells were examined for YFP fluorescence at 24 hours p.t. by confocal microscopy (Figure 5(b)). Abundant YFP positive cells were observed in the presence of DMSO; however, the total number of YFP positive cells decreased with increasing concentrations of compound 5539-0062 (Figure 5(b)). These findings indicate that compound 5539-0062 was able to inhibit the PTAP-mediated interaction between Tsg101 and HIV-1 Gag in a dose-dependent manner.

Next, human 293T cells were first treated for 1 hour with either vehicle (DMSO) alone, or increasing concentrations of compound 5539-0062, and then transfected with HIV-1 p55-Gag expression plasmid (Figure 5(c)). p55-Gag was detected by western blot and quantified in both VLPs and cell extracts at 24 hp.t. (Figure 5(c)). Budding of p55-Gag was inhibited by compound 5539-0062 in a dose-dependent manner as shown by decreasing levels of p55-Gag in VLPs (Figure 5(c)). Equivalent levels of p55-Gag were maintained in cell extracts over the entire range of inhibitor concentrations (Figure 5(c)). Taken together, these data indicate that L-domain inhibitors such as compound 5539-0062, are likely to possess broad-spectrum antiviral activity against a wide array of RNA viruses that depend on specific L-domain/host interactions for efficient egress and spread.

4. Discussion

Filovirus-host interactions are important for efficient egress of virus particles; however, mechanistic details of the formation, dynamics, and trafficking of these virus-host complexes in the natural environment of the host cell have been elusive. In this report, we used a BiMC approach to visualize eVP40-Tsg101 complexes as they formed in the cell. The specificity of this interaction was confirmed by using an L-domain deletion mutant of eVP40 and by using Tsg101 specific siRNAs. Importantly, the NYFP-Tsg101 fusion protein was stably expressed in mammalian cells, and CYFP-VP40 fusion proteins retained their ability to bud independently from cells as VLPs in an L-domain-dependent manner. The BiMC approach is ideal for detecting weak and/or transient protein-protein interactions in living cells [27, 28]. We demonstrated that eVP40-Tsg101 complexes formed between 3–4 hours after transfection and colocalized at early times (6 hrs. p.t.) with pericentrin-B, an MTOC marker. We postulate that the initial eVP40-Tsg101 complexes may then migrate from the MTOC to the site of budding at the plasma membrane by 12–24 hours p.t. This working model correlates with previous reports which suggested that filovirus VP40 proteins may interact with and utilize the host cytoskeletal network during assembly and egress [43, 44].

Elucidation of the molecular complexities and dynamics of virus-host interactions in the natural cell environment will enhance our ability to effectively screen and validate new antivirals [29, 31, 33]. Recent studies have identified two compounds, FGI-104 and FGI-106, that showed activity against filoviruses in cell culture and in animals [45, 46]; however, the targets of FGI-104 and FGI-106 remain to be determined. In addition, small molecule inhibitors of filovirus entry have recently been identified and characterized [47–49]. Viral L-domain/host interactions remain an attractive target for the development of novel, broad-spectrum budding inhibitors [33–35, 50]. The successful development of the BiMC assay to assess filovirus-host interactions (this manuscript) and the use of our well-established VLP budding assay represent powerful tools that will allow us to screen and validate small molecule inhibitors of filovirus budding. By using the known 3D atomic structure of Tsg101 binding to the PTAP motif, we employed an *in silico* strategy to identify and rank commercially available compounds with predicted drug-like properties that could potentially block this interaction. From this screen, we identified compound 5539-0062 and used both BiMC and VLP budding assays to demonstrate that this small molecule specifically inhibited PTAP-dependent budding of eVP40 VLPs, but not PTAP-independent budding of mVP40 VLPs. Moreover, compound 5539-0062 also exhibited specific antiviral activity in cells infected with a recombinant VSV (VSV-M40) expressing the PTAP L-domain of eVP40. The reason for the low level of inhibition of PPxY-dependent budding of VSV-WT observed in the presence of compound 5539-0062 remains to be determined (Table 1), as does the potential effect of compound 5539-0062 on other stages of VSV replication. The PTAP-specific inhibitory activity exhibited by this single, first-generation compound is encouraging and serves as proof-of-principle for using this strategy and the BiMC assay to identify and validate budding inhibitors. Compound 5539-0062 could potentially be optimized to improve binding affinity by either searching for chemically similar molecules in the commercially available databases, or by using the structural interaction fingerprint method which involves selecting compounds which are predicted to have the same protein-ligand interactions as 5539-0062

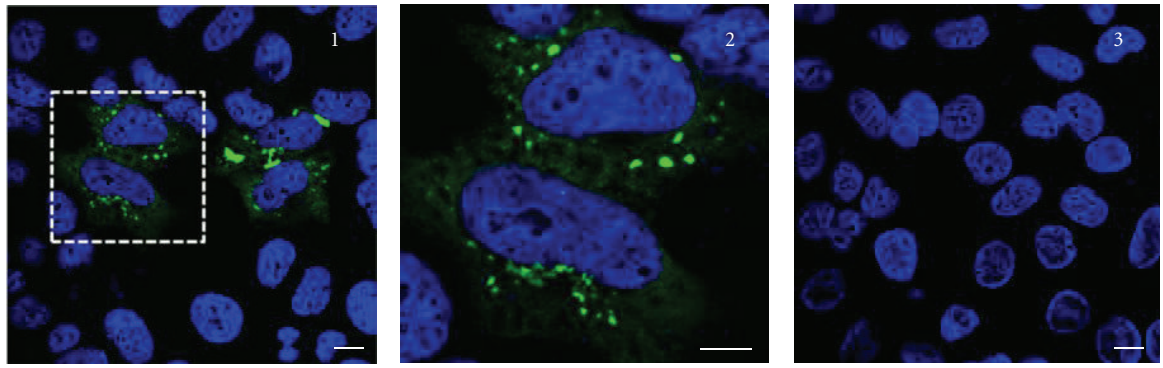

(a)

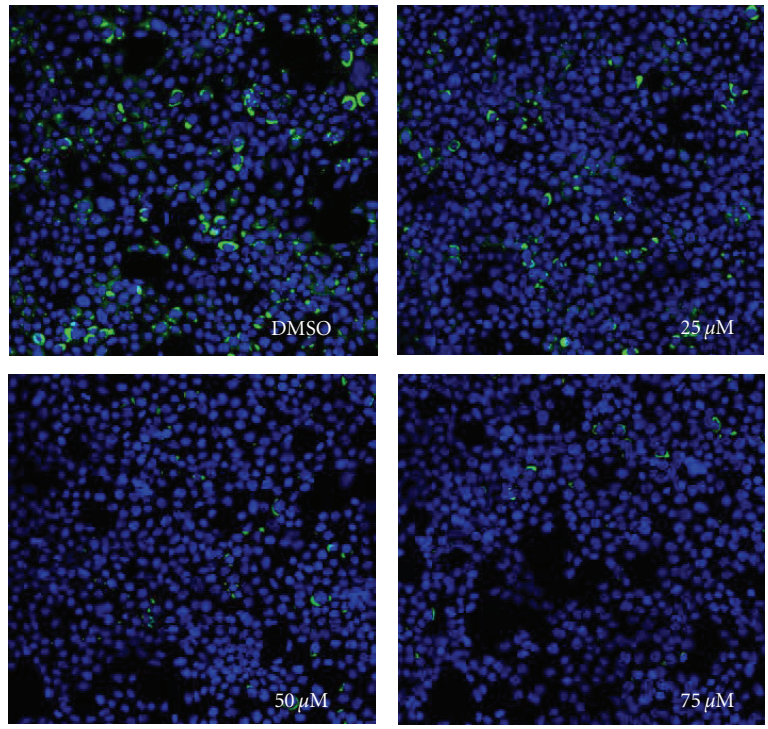

(b)

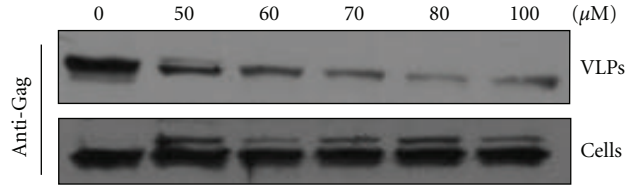

(c)

Figure 5: Inhibition of HIV-1 Gag-Tsg101 interaction and VLP budding. (a) Human 293T cells grown on coverslips in 6-well plates were transfected with NYFP-Tsg101 + CYFP-Gag-WT (panels 1 and 2) or NYFP-Tsg101 + CYFP-Gag-ΔP6 (panel 3). Cells were washed, fixed, and examined for YFP fluorescence by confocal microscopy at 24 hours p.t. The image within the dotted square in panel 1 was enlarged and shown panel 2. (b) Human 293T cells grown on coverslips in 6-well plates were transfected with NYFP-Tsg101 + CYFP-Gag-WT in the presence of DMSO alone, or 25, 50, or 75 μM of compound 5539-0062 as indicated. Cells were washed, fixed, and examined for YFP fluorescence by confocal microscopy at 24 hours p.t. (c) Standard budding assay and western blotting for Gag in VLPs and cell extracts from human 293T cells treated with DMSO alone, or the indicated concentrations of PTAP-inhibitor 5539-0062.

[51]. One advantage of L-domain inhibitors is their potential broad-spectrum activity against a wide-array of RNA viruses. Indeed, we were able to show that in addition to inhibiting budding of eVP40 VLPs, compound 5539-0062 was also able to block the PTAP-mediated interaction between Tsg101 and HIV-1 Gag, leading to inhibition of HIV-1 Gag budding.

Although the focus here was on inhibitors of PTAP-type L-domain activity, similar studies are underway to identify inhibitors of PPxY-type L-domains as well (Liu, Lee, Olson, and Harty, unpublished data). Viral PPxY-type L-domains are known to interact with host proteins such as Nedd4 E3 ubiquitin ligase [4, 24]. One could envision that the use of a cocktail of budding inhibitors containing both PTAP- and PPxY-specific compounds, for example, might be more effective at blocking virus egress than single L-domain inhibitors. Indeed, both EBOV and MARV appear to utilize both PTAP and PPxY L-domains for efficient egress [6, 12].

In addition to these virus-host interaction studies, we are investigating the contributions of viral VP40-VP40, VP40-NP, and VP40-VP35 interactions to filovirus assembly and egress [5, 7, 32, 52]. The broad applicability of the BiMC approach as well as a multicolor fluorescence strategy will enhance our understanding of the biological relevance of these complex multiprotein interactions to RNA virus egress. Extension of these studies to include live virus and/or animal models is essential and will help lead to new insights into filovirus pathogenesis and novel treatment options.

Acknowledgments

The authors would like to thank Drs. Stephan Becker, Gene Olinger, Paul Bates, Roselyn Eisenberg, Gary Cohen, and Doina Atanasiu for kindly providing them with reagents and/or discussion. They also thank Andrea Stout and Jasmine Zhao for their expert assistance with confocal microscopy. They also thank Samra Zelman for help constructing the HIV-1 YFP-Gag fusion plasmids, and all members of the Harty lab for helpful discussions. This paper was supported in part by NIH Grants AI077014, AI090284, and funding from the University of Pennsylvania Research Foundation to R. N. Harty, and DoD Defense Threat Reduction Agency Grant 4.10011_07_RD_B to M. A. Olson.

References

[1] M. Bray, "Defense against filoviruses used as biological weapons," *Antiviral Research*, vol. 57, no. 1-2, pp. 53–60, 2003.

[2] A. L. Hartman, J. S. Towner, and S. T. Nichol, "Ebola and marburg hemorrhagic fever," *Clinics in Laboratory Medicine*, vol. 30, no. 1, pp. 161–177, 2010.

[3] O. Dolnik, L. Kolesnikova, and S. Becker, "Filoviruses: interactions with the host cell," *Cellular and Molecular Life Sciences*, vol. 65, no. 5, pp. 756–776, 2008.

[4] R. N. Harty, M. E. Brown, G. Wang, J. Huibregtse, and F. P. Hayes, "A PPxY motif within the VP40 protein of Ebola virus interacts physically and functionally with a ubiquitin ligase: implications for filovirus budding," *Proceedings of the National Academy of Sciences of the United States of America*, vol. 97, no. 25, pp. 13871–13876, 2000.

[5] R. F. Johnson, P. Bell, and R. N. Harty, "Effect of Ebola virus proteins GP, NP and VP35 on VP40 VLP morphology," *Virology Journal*, vol. 3, article 31, 2006.

[6] J. M. Licata, M. Simpson-Holley, N. T. Wright, Z. Han, J. Paragas, and R. N. Harty, "Overlapping motifs (PTAP and PPEY) within the Ebola virus VP40 protein function independently as late budding domains: involvement of host proteins TSG101 and VPS-4," *The Journal of Virology*, vol. 77, no. 3, pp. 1812–1819, 2003.

[7] J. M. Licata, R. F. Johnson, Z. Han, and R. N. Harty, "Contribution of Ebola virus glycoprotein, nucleoprotein, and VP24 to budding of VP40 virus-like particles," *The Journal of Virology*, vol. 78, no. 14, pp. 7344–7351, 2004.

[8] Y. Liu, L. Cocka, A. Okumura, Y. A. Zhang, J. Oriol Sunyer, and R. N. Harty, "Conserved motifs within Ebola and Marburg virus VP40 proteins are important for stability, localization, and subsequent budding of virus-like particles," *The Journal of Virology*, vol. 84, no. 5, pp. 2294–2303, 2010.

[9] T. Noda, H. Sagara, E. Suzuki, A. Takada, H. Kida, and Y. Kawaoka, "Ebola virus VP40 drives the formation of virus-like filamentous particles along with GP," *The Journal of Virology*, vol. 76, no. 10, pp. 4855–4865, 2002.

[10] J. Timmins, G. Schoehn, S. Ricard-Blum et al., "Ebola virus matrix protein VP40 interaction with human cellular factors Tsg101 and Nedd4," *Journal of Molecular Biology*, vol. 326, no. 2, pp. 493–502, 2003.

[11] B. J. Chen and R. A. Lamb, "Mechanisms for enveloped virus budding: can some viruses do without an ESCRT?" *Virology*, vol. 372, no. 2, pp. 221–232, 2008.

[12] O. Dolnik, L. Kolesnikova, L. Stevermann, and S. Becker, "Tsg101 is recruited by a late domain of the nucleocapsid protein to support budding of Marburg virus-like particles," *The Journal of Virology*, vol. 84, no. 15, pp. 7847–7856, 2010.

[13] L. Kolesnikova, T. Strecker, E. Morita et al., "Vacuolar protein sorting pathway contributes to the release of marburg virus," *The Journal of Virology*, vol. 83, no. 5, pp. 2327–2337, 2009.

[14] S. Urata and J. Yasuda, "Regulation of Marburg virus (MARV) budding by Nedd4.1: a different WW domain of Nedd4.1 is critical for binding to MARV and Ebola virus VP40," *Journal of General Virology*, vol. 91, no. 1, pp. 228–234, 2010.

[15] S. Urata, T. Noda, Y. Kawaoka, S. Morikawa, H. Yokosawa, and J. Yasuda, "Interaction of Tsg101 with Marburg virus VP40 depends on the PPPY motif, but not the PT/SAP motif as in the case of Ebola virus, and Tsg101 plays a critical role in the budding of Marburg virus-like particles induced by VP40, NP, and GP," *The Journal of Virology*, vol. 81, no. 9, pp. 4895–4899, 2007.

[16] J. E. Garrus, U. K. Von Schwedler, O. W. Pornillos et al., "Tsg101 and the vacuolar protein sorting pathway are essential for HIV-1 budding," *Cell*, vol. 107, no. 1, pp. 55–65, 2001.

[17] A. Goff, L. S. Ehrlich, S. N. Cohen, and C. A. Carter, "Tsg101 control of human immunodeficiency virus type 1 Gag trafficking and release," *The Journal of Virology*, vol. 77, no. 17, pp. 9173–9182, 2003.

[18] T. Irie, J. M. Licata, and R. N. Harty, "Functional characterization of Ebola virus L-domains using VSV recombinants," *Virology*, vol. 336, no. 2, pp. 291–298, 2005.

[19] D. J. Katzmann, M. Babst, and S. D. Emr, "Ubiquitin-dependent sorting into the multivesicular body pathway requires the function of a conserved endosomal protein sorting complex, ESCRT-I," *Cell*, vol. 106, no. 2, pp. 145–155, 2001.

[20] J. Martin-Serrano, T. Zang, and P. D. Bieniasz, "Role of ESCRT-I in retroviral budding," *The Journal of Virology*, vol. 77, no. 8, pp. 4794–4804, 2003.

[21] J. Martin-Serrano, T. Zang, and P. D. Bieniasz, "HIV-1 and Ebola virus encode small peptide motifs that recruit Tsg101 to sites of particle assembly to facilitate egress," *Nature Medicine*, vol. 7, no. 12, pp. 1313–1319, 2001.

[22] A. Pincetic, G. Medina, C. Carter, and J. Leis, "Avian sarcoma virus and human immunodeficiency virus, type 1 use different subsets of ESCRT proteins to facilitate the budding process," *The Journal of Biological Chemistry*, vol. 283, no. 44, pp. 29822–29830, 2008.

[23] H.-Y. Chung, E. Morita, U. Von Schwedler, B. Müller, H.-G. Kräusslich, and W. I. Sundquist, "NEDD4L overexpression rescues the release and infectivity of human immunodeficiency virus type 1 constructs lacking PTAP and YPXL late domains," *The Journal of Virology*, vol. 82, no. 10, pp. 4884–4897, 2008.

[24] J. Yasuda, M. Nakao, Y. Kawaoka, and H. Shida, "Nedd4 regulates egress of Ebola virus-like particles from host cells," *The Journal of Virology*, vol. 77, no. 18, pp. 9987–9992, 2003.

[25] D. Atanasiu, J. C. Whitbeck, T. M. Cairns, B. Reilly, G. H. Cohen, and R. J. Eisenberg, "Bimolecular complementation reveals that glycoproteins gB and gH/gL of herpes simplex virus interact with each other during cell fusion," *Proceedings of the National Academy of Sciences of the United States of America*, vol. 104, no. 47, pp. 18718–18723, 2007.

[26] C. D. Hu, Y. Chinenov, and T. K. Kerppola, "Visualization of interactions among bZIP and Rel family proteins in living cells using bimolecular fluorescence complementation," *Molecular Cell*, vol. 9, no. 4, pp. 789–798, 2002.

[27] T. K. Kerppola, "Visualization of molecular interactions by fluorescence complementation," *Nature Reviews Molecular Cell Biology*, vol. 7, no. 6, pp. 449–456, 2006.

[28] T. K. Kerppola, "Bimolecular fluorescence complementation: visualization of molecular interactions in living cells," *Methods in Cell Biology*, vol. 85, pp. 431–470, 2008.

[29] M. L. MacDonald, J. Lamerdin, S. Owens et al., "Identifying off-target effects and hidden phenotypes of drugs in human cells," *Nature Chemical Biology*, vol. 2, no. 6, pp. 329–337, 2006.

[30] T. Nagai, K. Ibata, E. S. Park, M. Kubota, K. Mikoshiba, and A. Miyawaki, "A variant of yellow fluorescent protein with fast and efficient maturation for cell-biological applications," *Nature Biotechnology*, vol. 20, no. 1, pp. 87–90, 2002.

[31] H. Yu, M. West, B. H. Keon et al., "Measuring drug action in the cellular context using protein-fragment complementation assays," *Assay Drug Dev Technol*, vol. 1, no. 6, pp. 811–822, 2003.

[32] Y. Liu, S. Stone, and R. N. Harty, "Characterization of filovirus protein-protein interactions in mammalian cells using bimolecular complementation," *The Journal of Infectious Diseases*. In press.

[33] R. N. Harty, "No exit: targeting the budding process to inhibit filovirus replication," *Antiviral Research*, vol. 81, no. 3, pp. 189–197, 2009.

[34] A. Tavassoli, Q. Lu, J. Gam, H. Pan, S. J. Benkovic, and S. N. Cohen, "Inhibition of HIV budding by a genetically selected cyclic peptide targeting the Gag-TSG101 interaction," *ACS Chemical Biology*, vol. 3, no. 12, pp. 757–764, 2008.

[35] A. A. Waheed and E. O. Freed, "Peptide inhibitors of HIV-1 egress," *ACS Chemical Biology*, vol. 3, no. 12, pp. 745–747, 2008.

[36] J. J. Irwin and B. K. Shoichet, "ZINC—a free database of commercially available compounds for virtual screening," *Journal of Chemical Information and Modeling*, vol. 45, no. 1, pp. 177–182, 2005.

[37] O. Pornillos, S. L. Alam, D. R. Davis, and W. I. Sundquist, "Structure of the Tsg101 UEV domain in complex with the PTAP motif of the HIV-1 p6 protein," *Nature Structural Biology*, vol. 9, no. 11, pp. 812–817, 2002.

[38] G. M. Morris, H. Ruth, W. Lindstrom et al., "Software news and updates AutoDock4 and AutoDockTools4: automated docking with selective receptor flexibility," *Journal of Computational Chemistry*, vol. 30, no. 16, pp. 2785–2791, 2009.

[39] S. Zhang, K. Kumar, X. Jiang, A. Wallqvist, and J. Reifman, "DOVIS: an implementation for high-throughput virtual screening using AutoDock," *BMC Bioinformatics*, vol. 9, article 126, 2008.

[40] B. R. Brooks, C. L. Brooks, A. D. Mackerell et al., "CHARMM: the biomolecular simulation program," *Journal of Computational Chemistry*, vol. 30, no. 10, pp. 1545–1614, 2009.

[41] T. A. Halgren, "Merck molecular force field. I. Basis, form, scope, parameterization, and performance of MMFF94," *Journal of Computational Chemistry*, vol. 17, no. 5-6, pp. 490–519, 1996.

[42] A. Krammer, P. D. Kirchhoff, X. Jiang, C. M. Venkatachalam, and M. Waldman, "LigScore: a novel scoring function for predicting binding affinities," *Journal of Molecular Graphics and Modelling*, vol. 23, no. 5, pp. 395–407, 2005.

[43] Z. Han and R. N. Harty, "Packaging of actin into Ebola virus VLPs," *Virology Journal*, vol. 2, article 92, 2005.

[44] G. Ruthel, G. L. Demmin, G. Kallstrom et al., "Association of Ebola virus matrix protein Vp40 with microtubules," *The Journal of Virology*, vol. 79, no. 8, pp. 4709–4719, 2005.

[45] M. J. Aman, M. S. Kinch, K. Warfield et al., "Development of a broad-spectrum antiviral with activity against Ebola virus," *Antiviral Research*, vol. 83, no. 3, pp. 245–251, 2009.

[46] M. S. Kinch, A. S. Yunus, C. Lear et al., "FGI-104: a broad-spectrum small molecule inhibitor of viral infection," *American Journal of Translational Research*, vol. 1, no. 1, pp. 87–98, 2009.

[47] S. R. Radoshitzky, K. L. Warfield, X. Chi et al., "Ebolavirus Δ-peptide immunoadhesins inhibit Marburgvirus and Ebolavirus cell entry," *The Journal of Virology*, vol. 85, no. 17, pp. 8502–8513, 2011.

[48] E. H. Miller, J. S. Harrison, S. R. Radoshitzky et al., "Inhibition of Ebola virus entry by a C-peptide targeted to endosomes," *The Journal of Biological Chemistry*, vol. 286, no. 18, pp. 15854–15861, 2011.

[49] A. Basu, B. Li, D. M. Mills et al., "Identification of a small-molecule entry inhibitor for filoviruses," *The Journal of Virology*, vol. 85, no. 7, pp. 3106–3119, 2011.

[50] A. A. Capul and J. C. de la Torre, "A cell-based luciferase assay amenable to high-throughput screening of inhibitors of arenavirus budding," *Virology*, vol. 382, no. 1, pp. 107–114, 2008.

[51] Z. Deng, C. Chuaqui, and J. Singh, "Structural interaction fingerprint (SIFt): a novel method for analyzing three-dimensional protein-ligand binding interactions," *Journal of Medicinal Chemistry*, vol. 47, no. 2, pp. 337–344, 2004.

[52] T. Hoenen, N. Biedenkopf, F. Zielecki et al., "Oligomerization of ebola virus VP40 is essential for particle morphogenesis and regulation of viral transcription," *The Journal of Virology*, vol. 84, no. 14, pp. 7053–7063, 2010.

Hindawi Publishing Corporation
Advances in Virology
Volume 2011, Article ID 370606, 14 pages
doi:10.1155/2011/370606

Review Article

Association of Influenza Virus Proteins with Membrane Rafts

Michael Veit and Bastian Thaa

Department of Immunology and Molecular Biology, Veterinary Faculty, Free University Berlin, Philippstraße 13, 10115 Berlin, Germany

Correspondence should be addressed to Michael Veit, mveit@zedat.fu-berlin.de

Received 15 March 2011; Accepted 2 May 2011

Academic Editor: Carolina B. Lopez

Assembly and budding of influenza virus proceeds in the viral budozone, a domain in the plasma membrane with characteristics of cholesterol/sphingolipid-rich membrane rafts. The viral transmembrane glycoproteins hemagglutinin (HA) and neuraminidase (NA) are intrinsically targeted to these domains, while M2 is seemingly targeted to the edge of the budozone. Virus assembly is orchestrated by the matrix protein M1, binding to all viral components and the membrane. Budding progresses by protein- and lipid-mediated membrane bending and particle scission probably mediated by M2. Here, we summarize the experimental evidence for this model with emphasis on the raft-targeting features of HA, NA, and M2 and review the functional importance of raft domains for viral protein transport, assembly and budding, environmental stability, and membrane fusion.

1. Introduction

1.1. Influenza Viruses: Molecular Composition. Influenza virus particles are heterogeneous in shape, either spherical (with a diameter of roughly 100 nm) or filamentous (with a length of several micrometers). The particles contain the viral genome, which is segmented into eight entities termed viral ribonucleoprotein particles (vRNPs), each composed of a segment of viral RNA complexed to the nucleoprotein (NP) and the subunits of the viral RNA polymerase (PA, PB1, and PB2). The vRNPs are encased by a protein layer consisting of the matrix protein M1, which also lines the viral envelope from beneath and is supposed to bind to all other viral constituents. The viral envelope is a lipid bilayer derived from the apical plasma membrane of the infected cell. There are three transmembraneous viral proteins embedded in the envelope: the glycoproteins hemagglutinin (HA) and neuraminidase (NA), which protrude at the viral surface as "spikes," and—in minor quantities—the proton channel protein M2. Here, we will focus on the buildup of the viral envelope and the proteins involved (HA, NA, M2, M1), which are depicted in Figure 1.

HA (blue in Figure 1) is a type I transmembrane protein with an N-terminal signal peptide (white in Figure 1(a)), which is cleaved off after cotranslational sequestration of the nascent polypeptide chain into the endoplasmic reticulum (ER), a large ectodomain (positioned in the ER lumen and towards the extracellular milieu when located at the plasma membrane), a single transmembrane region (TMR) of approximately 27 amino acid residues located near the C-terminus of the protein, and a short cytoplasmic tail (approximately 11 residues).

HA assembles into a homotrimer in the ER and is transported *via* the secretory pathway to the plasma membrane, more specifically the apical plasma membrane in polarized (e.g., epithelial) cells, where virus assembly and budding take place [2]. In the ER and Golgi, HA is glycosylated in the ectodomain, and typically three saturated fatty acid chains are covalently attached to C-terminal cysteine residues (S-acylation). The first cysteine residue, at the border between TMR and cytoplasmic tail, is modified with stearate, while the other two cysteines in the cytoplasmic tail carry palmitates [3, 4].

The large ectodomain is processed into two subunits (HA_1 and HA_2) by a protease provided by the host organism; they remain linked by a disulfide bridge [5]. This proteolytic maturation is needed to enable *membrane fusion*, which is exerted by HA during virus entry: a hydrophobic part termed "fusion peptide" (cyan in Figure 1(a)) becomes exposed at the N-terminus of HA_2 after cleavage and is inserted

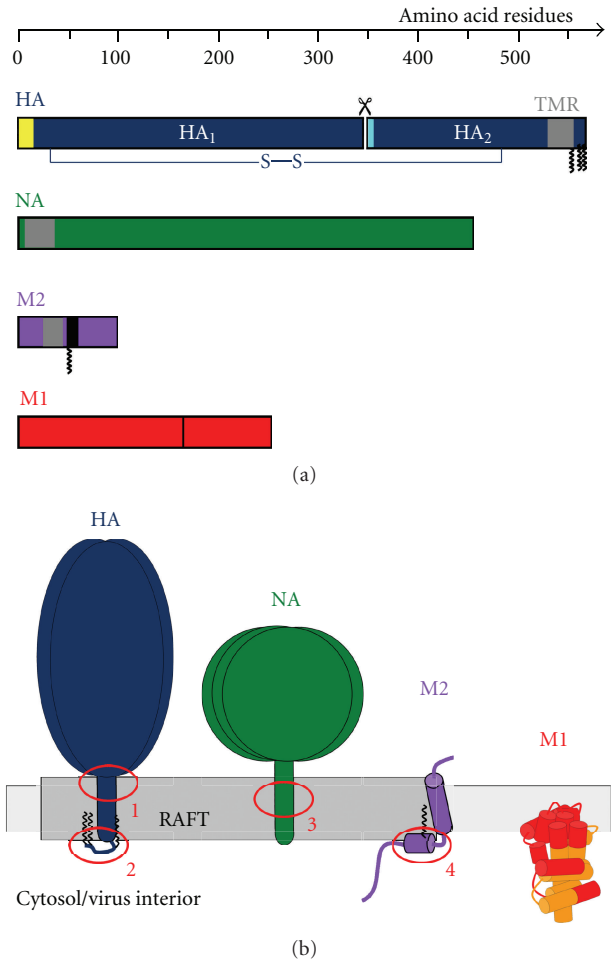

FIGURE 1: The membrane-associated proteins of influenza virus and their raft association. (a) Primary amino acid sequence of hemagglutinin (HA, processed into HA_1 and HA_2, blue), neuraminidase (NA, green), M2 (purple), and M1 (red, with amphiphilic helix in black). Transmembrane regions (TMR) in gray, S-acylations in HA and M2 indicated by zigzag line, signal peptide of HA in white, and fusion peptide in HA in cyan. (b) Topology of HA, NA, M2, and M1 in the membrane, raft localization indicated. Raft-targeting features: (1) hydrophobic amino acids in the outer part of the HA-TMR; (2) S-acylation of HA; (3) outer part of the NA-TMR; (4) S-acylation and cholesterol binding of the amphiphilic helix of M2. M1 according to the structure model of Shishkov et al. [1], membrane-interactive regions in red. Only one monomer of the trimeric HA and the tetrameric NA and M2 is shown for clarity.

into the host endosomal membrane upon activation of HA (conformational change of the ectodomain by low pH). Apart from membrane fusion, HA is also responsible for receptor recognition: a binding pocket in HA_1 recognizes sialic acid moieties in glycoproteins and glycolipids on the host cell surface [6].

NA (green in Figure 1) is a type II transmembrane protein, which assembles into a homotetramer. The first five residues from the N-terminus form the cytoplasmic tail, followed by a transmembrane anchor encompassing approximately 30 residues and the glycosylated ectodomain. NA is processed along the same intracellular route as HA (ER-Golgi-apical plasma membrane). The main function of the protein is cleavage of terminal sialic acid moieties from glycans in the mucus of the host's respiratory tract and on the viral surface, thus helping in release of newly formed viral particles from the host cell. NA is the target of the anti-influenza drug oseltamivir and other neuraminidase inhibitors [7].

M2, the third viral transmembrane protein (purple in Figure 1), is also tetrameric and forms a proton channel activated by acidic pH, the action of which is important for genome unpacking during virus entry and can be inhibited—at least in Influenza A virus strains—by the drug amantadine. In each monomer, the first 24 amino acids form the ectodomain, which is not glycosylated, the following 19 residues are the transmembrane region, and the remaining 54 residues build up the cytoplasmic tail. The sequence immediately following the TMR shapes a membrane-parallel amphiphilic helix, an α-helix with a hydrophobic face (which partially protrudes into the membrane), and a hydrophilic face (which points to the cytosol). A cysteine residue in this part of the protein is S-acylated. Similarly to HA and NA, M2 is transported along the secretory pathway to the apical plasma membrane, but the apical targeting signal in M2 has not been identified. Contrary to the other viral transmembrane proteins, however, M2 is largely excluded from virus particles [8].

The **matrix protein M1** (red in Figure 1) binds to membranes, but does not have a transmembrane span [9–11]. M1 is most likely attached to membranes by extended regions of the protein or by the cooperative action of several binding sites [12–16]. Concomitantly, a large portion of the protein was found to be membrane-associated by mass-spectrometry-based structural reconstruction [1]. M1 is central for virus morphogenesis as it is supposed to bind to all other viral components including the vRNPs and the membrane. However, M1 is not intrinsically targeted to the assembly site, the apical plasma membrane, but rather localizes to the nucleus, internal membranes, and the cytosol. Plasma membrane targeting of M1 is therefore in all likelihood mediated by at least one of the viral transmembrane proteins (HA, NA, and M2). The interaction of M1 with the cytoplasmic tails of HA (11 residues) and NA (5 residues) has only been demonstrated indirectly, for instance, by altered detergent solubility [17, 18] or increased membrane association [19] of M1 in the presence of HA/NA, an effect not seen in all studies [15]. In contrast, the interaction between M1 and the cytoplasmic tail of M2 (54 residues) is well documented, most conclusively by coimmunoprecipitation [20, 21]. M1 has the capacity to oligomerize [16], which is supposed to cluster the viral components together at the site of virus budding to organize the assembly process.

1.2. Biochemical and Biophysical Properties of Membrane Rafts. Contrary to the classical view of the plasma membrane as a homogenous lipid mixture, there is now conclusive evidence indicating the presence of specialized lipid domains

with distinct biochemical and biophysical properties. These *membrane rafts* are dynamic assemblies of cholesterol, sphingolipids, and phospholipids containing saturated fatty acids. Sphingolipids are exclusively present in the external leaflet of the plasma membrane, whereas the composition of inner leaflet rafts is not known, but it has been suggested that cholesterol plus phospholipids with saturated acyl chains is enriched [22, 23].

Membrane rafts have been characterized extensively in model membrane systems. In the cholesterol/sphingolipid-rich phase, the (mostly saturated) fatty acid chains of the membrane lipids are densely packed and restricted in mobility, but still able to diffuse and rotate, and form a "liquid-ordered" (Lo) phase segregated from the "liquid-disordered" (Ld), more fluid membrane phase. Upon phase separation of Lo and Ld domains, there is a hydrophobic mismatch and a height difference between the two membrane phases, leading to the formation of a "line tension" at their interface. This is conceptionally comparable to surface tension in a three-dimensional system, which—for instance—leads to the formation of a spherical drop of water on an oily surface to minimize the contact area with the repellent surface. Accordingly, line tension leads to the formation of a curved raft phase due to the propensity of the system to minimize its free energy [24].

However, no large-scale, long-lasting phase separation is observed in the membranes of undisturbed cells—yet, highly dynamic (millisecond range) and very small (10–200 nm) heterogeneous membrane organization dependent on the presence of cholesterol has been observed in a plethora of investigations using biophysical methodology of high temporal and spatial resolution [25].

Raft domains are best described for the plasma membrane, although cholesterol/sphingolipid-rich domains are likely to build up already in the Golgi. There are raft-targeting features in proteins for their association with rafts, most decisively glycosyl-phosphatidylinositol (GPI) anchors and S-acylation of cysteine residues [26]. Under certain conditions, for instance, upon ligand binding and receptor oligomerization, the highly dynamic "resting state" rafts can be coalesced and stabilized to fulfill a biological function [25, 27]. One example for functionalization of raft domains are signal transduction processes, for example, the formation of the immunological synapse in the activation of T cells [28]. The assembly and budding of some viruses such as influenza virus is also coupled to the formation of functionalized raft domains, here termed "budozone." In this context, rafts provide a platform to concentrate the viral components and to facilitate their interactions, while cellular proteins are excluded [24, 25].

2. Association of Influenza Virus Proteins with Rafts and Methods to Analyze Them

Influenza virus assembly and budding is linked to (coalesced) membrane rafts in the apical plasma membrane. Generally, the spike glycoproteins HA and NA are assumed to be raft-associated, while M2 is believed to be intrinsically excluded from rafts. The peripheral membrane protein M1 is considered not to have membrane subdomain specificity. In the next paragraphs, we describe the experimental evidence that had led to this model.

2.1. Hemagglutinin Is Present in Detergent-Resistant Membranes. Historically, the raft hypothesis was introduced by the observation that some parts of biological membranes (enriched in cholesterol and sphingolipids) resist solubilization by nonionic detergents such as Triton X-100 on ice and float to a low buoyant density upon density gradient centrifugation. These "detergent-resistant membranes" (DRMs) have been considered to be the biochemical correlate for rafts. They have been found to contain proteins, which were hence termed DRM-associated and regarded as raft proteins. In addition, association with DRMs should be sensitive to cholesterol extraction and inhibitors of sphingolipid synthesis [26, 27].

The hemagglutinin (HA) of influenza virus was one of the first proteins described as a component of DRMs [29] and has since been judged as paradigm for a raft-associated transmembrane protein.

The detergent extraction method was used in combination with mutagenesis to identify molecular signals in HA for raft localization. Alanine scanning of the whole transmembrane region (an exchange of three consecutive amino acids at a time by alanines) showed that hydrophobic residues located at the outer leaflet of the membrane bilayer are responsible for resistance against detergent extraction [29, 30], see label 1 in Figure 1(b). In addition, S-acylation at cytoplasmic and transmembrane cysteine residues (label 2) are required for partitioning of HA into DRMs [30]. From detergent-extraction experiments, it was concluded that palmitate bound to the cytoplasmic cysteines is more important for raft association than the stearate attached to the transmembrane cysteine [31, 32].

Presently, one can only speculate on the molecular mechanism by which the raft-targeting signals cause incorporation of HA into rafts. In principle, α-helical transmembrane regions with their protruding amino acid side chains should rather disrupt the tight packing of lipids in a raft domain as they do not readily accommodate the rigid, bulky sterol ring of cholesterol. However, direct binding of cholesterol to the protein could lead to raft targeting. In motifs such as the "cholesterol recognition/interaction amino acid consensus" (CRAC, [33]) or the "cholesterol consensus motif" (CCM, [31]), a large aliphatic residue (valine or isoleucine), a tyrosine or phenylalanine residue, and a basic amino acid (arginine or lysine) coordinate the cholesterol moiety if positioned accordingly. It is conceivable that the raft-targeting residues in the HA-TMR (valine-isoleucine-leucine/VIL), two of which (IL) are strictly conserved across all HA subtypes, form part of a cholesterol interaction pocket. However, since atomic structural information of the HA-TMR is still lacking, it is unclear whether the amino acids in question are ideally positioned. Binding to cholesterol might target HA to preexisting rafts as predicted in the "lipid shell" model for raft association

of proteins [32]. Alternatively, it has recently been shown that a peptide representing the transmembrane region of HA induces highly ordered domains in model membranes, but only if the conserved leucine residue is present [34]. Assuming a similar mode of action of the TMR in cellular membranes, this would imply that HA induces the formation of its own raft domains. Furthermore, the substitution of hydrophobic TMR residues by less hydrophobic alanines might shorten the length of the transmembrane span. A long TMR might be required for partitioning of HA into rafts, which are thicker compared to other membrane regions due to stretching of the lipids' fatty acid tails.

The presence of the second raft-targeting feature in HA, S-acylation, seems to be a common principle in many raft proteins [35]. It could be imagined that flexible acyl chains, especially if attached to the beginning of the transmembrane region, fill the voids in the irregular and rough surface of the transmembrane domain and thus "lubricate" the region for subsequent interactions with cholesterol. In addition, fatty acids attached to the cytoplasmic tail of HA might attract cholesterol, as suggested in the crystal structure of the β-adrenergic receptor, in which cholesterol is visible in the vicinity of covalently bound palmitate. However, it should be noted that S-acylation *per se*, irrespective of whether palmitate or stearate is attached, is not sufficient to cause raft localization of viral transmembrane proteins [36]. An example is the HEF glycoprotein of influenza C virus, which does not associate with DRMs, but is stearoylated at a transmembrane cysteine [3, 12].

It has been questioned repeatedly whether association with DRMs reflects raft association of a protein in living cells. Components might be enriched in DRMs simply because they possess common biophysical properties. Furthermore, partitioning of proteins into detergent-soluble and -insoluble fractions is seldom absolute; sometimes, only very few percent of a protein population are present in DRMs. Extraction conditions are not standardized, and therefore results obtained by using different protocols can hardly be compared [37]. Thus, more sophisticated methods have subsequently been used to confirm and characterize the raft localization of HA.

2.2. Analysis of the Distribution of HA with High-Resolution Methods. Fluorescence microscopy in living cells has failed to reveal laterally segregated clusters of HA or other raft-associated proteins and lipids, indicating that rafts in undisturbed cells must be smaller than the resolution of the light microscope (<200 nm). However, when antibodies against both HA and a glycolipid-anchored protein were applied, HA was found to cocluster with the established raft component. It was assumed that cross-linking of HA trimers by antibodies stabilizes small raft structures, which subsequently coalesce with other raft domains to form large, visible patches [38]. However, this study could not establish potential clustering of HA in unperturbed cells. Since then, methods with a higher lateral resolution than the conventional light microscope have been used.

Immunoelectron microscopy combined with rigorous statistical analysis showed that in transfected cells HA neither is randomly distributed in the plasma membrane nor accumulates only in very small domains with the size of a small, dynamic raft. Instead, clustering of HA molecules on different length scales from 20 nm up to 900 nm was found. In the course of virus infection, the HA clusters were observed to increase in size, indicating increasing coalescence of HA-containing domains. Since the nanodomains contained the ganglioside GM1, they are likely derived from rafts. However, only HA clusters at the nanometer length scale, that is, with the size of uninduced rafts, could be disintegrated by extraction of cholesterol [39, 40]. Fluorescence-photoactivation-localization microscopy (FPALM), a recently developed nanoscopic method with very high spatial resolution (40 nm), essentially confirmed HA clustering for unfixed, living cells [41].

Thus, HA somehow accumulates in microdomains of the membrane or even induces their formation, which leads to its separation from most cellular proteins. Since the area of the HA cluster is large enough to cover the surface of a spherical virus particle, these structures were termed the viral preenvelope or the viral budozone to indicate that they might be a precursor of budding virus particles [39, 42]. The large size of the HA clusters suggests that they are composed of several small rafts. In addition, the HA clusters do not possess round (perimeter minimized), but irregular domain boundaries with long and narrow extensions. This suggests that not only partitioning of HA into rafts, but also other mechanisms for formation of membrane subdomains may be responsible for clustering of HA [39, 43]. One candidate for such a function is cortical actin, which generates a meshwork of microfilaments at the inner leaflet of the plasma membrane that might transiently entrap HA [44]. Furthermore, cortical actin might organize and maintain the formation of rafts [45]. This effect might be mediated by the lipid phosphatidylinositol-(4,5)-phosphate ($PtdIns(4,5)P_2$), a key regulator of assembly and disassembly of microfilaments [46]. The actin cytoskeleton has also been shown to be functionally linked to rafts in the context of virus infection: the disruption of the actin meshwork leads to a redistribution of HA and to reduced budding, most relevantly in the case of filamentous virus particles, maybe because their surface area is higher than in spherical particles [38].

Förster's (or fluorescence) resonance energy transfer (FRET) is exceptionally well suited to demonstrate very close association between two molecules, for example, if they populate the same small raft domain, even for a very short time period. FRET relies on the transfer of energy from an excited donor fluorophore, such as the cyan-fluorescent protein (CFP), to an acceptor fluorophore, for example, the yellow-fluorescent protein (YFP), if they are in very close vicinity to each other (<10 nm). Association of two proteins can be assessed in cells by fusing them to CFP and YFP, respectively, and conducting FRET measurements. To exclude that a FRET signal is due to random collision of two molecules, as it may occur frequently if both diffuse in the plane of a membrane, the FRET data obtained must

be correlated with the expression level of the probes. If the FRET efficiency increases with the concentration of the FRET acceptor protein at the membrane, FRET is caused by random collision. In contrast, if FRET is due to clustering of the two proteins under study, the FRET efficiency is largely independent of the concentration of the acceptor protein and saturated even at relatively low FRET acceptor concentrations [39, 40]. To evaluate the data, a hyperbolic function is fitted to the data, which yields a "dissociation constant" K_D as a parameter to assess the associative properties of donor and acceptor [43]. Influenza virus HA, fused at its cytoplasmic tail to CFP [42], clusters with an established marker for inner leaflet rafts, myristoylated and palmitoylated YFP [43]. Furthermore, an artificial HA-derived FRET probe, consisting of a signal peptide, a fluorescent protein, and the transmembrane as well as cytoplasmic domain of HA [44], clusters with a glycolipid-anchored protein, an established marker for rafts of the outer leaflet. In this construct, tagging of the cytoplasmic tail was circumvented to avoid interference with its role in lateral organization. For both HA constructs, clustering was significantly reduced when rafts were disintegrated by cholesterol extraction and when the two described raft-targeting signals of HA were removed. Both signals had a similar effect on raft-targeting of HA and did not work synergistically with each other.

One disadvantage of the FRET technique is that neither K_D values nor FRET-efficiencies can be compared between different protein pairs, even if they are attached to the same donor and acceptor fluorophore. The FRET efficiency depends on the distance between the donor and the acceptor and their relative orientation, parameters which cannot be measured within cells. It is thus not possible to determine the percentage of molecules that interact with a raft marker or quantitatively compare the raft association of different viral proteins.

2.3. Diffusional Mobility of HA at the Plasma Membrane. It has been hypothesized that the embedding of a protein in raft domains leads to a slower diffusion compared to non-raft proteins, which diffuse as single entities [47]. Accordingly, fluorescence recovery after photobleaching (FRAP), where the speed of replenishment of a previously bleached spot within the membrane is measured, was employed for HA. More than 80% of all HA molecules proved to be mobile, indicating that the HA clusters are not static in the timeframe of FRAP experiments (several minutes). Wild-type HA diffused somewhat slower compared to HA with deleted raft-targeting signals, but its diffusion rate was elevated to non-raft HA values after disruption of rafts by depletion of cholesterol [48]. However, HA (with or without raft-targeting signals) diffused much slower compared to the marker of inner leaflet rafts indicating that they do not diffuse together in a stable raft complex [42].

Yet, the diffusional mobility as measured by FRAP is determined by the type of transmembrane anchorage rather than raft localization: proteins anchored by lipid moieties (prenylation, S-acylation) diffuse quicker than transmembrane proteins regardless of whether they associate with rafts; the raft protein HA shows similar diffusion behavior as the non-raft protein G from vesicular stomatitis virus (VSV-G) [49].

FRAP is only suitable to determine the overall mobility of HA over a large area of the plasma membrane (several μm^2), which contains both raft and non-raft domains. To dissect the diffusional behavior of HA on the very small spatial and temporal scale of (undisturbed) rafts, methodology of very high resolution needs to be employed [50]. Indeed, the nanoscopic method FPALM showed that HA is mobile when observed at high spatial resolution (<200 nm), that is, at the dimension of the HA cluster. It was concluded that the membrane enwrapping the HA cluster is not composed of a solid phase and thus allows HA molecules to diffuse and eventually leave the boundary of the cluster [41].

No studies have been done on the clustering behavior of HA in its natural habitat, the apical membrane of polarized cells, which is particularly rich in raft lipids and possibly mostly raft-like; that is, the raft domain might be the dominant, percolating phase [51]. In other membranes, rafts are believed to be minor domains which float like a ship in a sea of non-raft lipids, a property to which the name "raft" refers. It might well be that the different properties of apical membranes might affect clustering and diffusion of HA.

In summary, these results are consistent with a model of dynamic partitioning of HA into and out of pre-existing raft domains, which permits the protein to transiently populate raft domains, as well as to undergo diffusion outside of rafts. Alternatively, HA might transiently induce the formation of rafts, which rapidly dissipate if no further stimulus is delivered. Recent real time studies on the biogenesis of individual human immunodeficiency virus (HIV) particles have shown that five to ten minutes are required for particle assembly and additional 20 minutes for budding and release [52, 53]. Assuming that a similar time frame applies for assembly and budding of influenza virus particles, it is unclear how such unstable HA clusters can support the whole assembly process. However, it is reasonable to assume that in the context of virus infection, binding of HA to M1 and the subsequent oligomerization of the latter might further stabilize the HA clusters and serve as a nucleation site for the recruitment of viral RNPs.

2.4. Model Membranes to Analyze Raft Localization of HA. Raft association of HA has also been analyzed *in vitro* using model membranes, which have the advantage that their chemical composition can be accurately controlled. One suitable system is giant unilamellar vesicles (GUVs), spherically closed free-standing bilayers with a size in the range of tens of micrometers, thus having a cell-like curvature. When prepared from phospholipids, sphingomyelin (SM), and cholesterol at a molar ratio of 1 : 1 : 1, the "canonical raft mixture," separation of the lipids into two phases occurs. The phases can be visualized by fluorescence microscopy using fluorescent lipid probes, which favor either the liquid-disordered (Ld) or the liquid-ordered (Lo), raft-like phase. Membrane proteins, chemically labeled with a fluorophore, can be reconstituted into GUVs which allows direct testing

of the phase preference of a protein [54]. Surprisingly, HA, either the authentic protein purified from virus particles or a peptide representing its transmembrane region, is exclusively present in the liquid-disordered, non-raft domain [55]. However, only a few proteins considered as raft components in living cells, for example, GPI-anchored proteins, associate with the raft domains in GUVs.

Using swelling procedures, artificial membranes can also be prepared from the plasma membrane of a cell that expresses a fluorescent construct of the protein of interest. Similarly to GUVs, these giant plasma membrane vesicles (GPMVs) show long-lasting, large-scale separation into raft and non-raft phase upon cooling, but contain the lipid and protein diversity of natural membranes. Using such membranes, partitioning of HA (fused to a fluorescent protein) was more variable; that is, a minor, but significant amount was also present in the raft-like phase [55, 56].

The differences in raft localization of HA in cellular membranes, GPMVs, and GUVs might be explained by differences in the packaging order of their lipids. Using fluorescent lipid probes, it was shown that the raft phase is most densely packed in GUVs, a property which might prevent access especially of transmembrane proteins [55, 57]. In addition, GUVs and GPMVs lack cortical actin which probably helps in organization and maintenance of raft domains in cells. Furthermore, lipid asymmetry of the bilayer, characteristic for the plasma membrane of cells, is not preserved in GUVs and GPMVs. Finally, in some procedures to prepare HA or GPMVs, the reducing agent dithiothreitol (DTT) is used, which is known to cleave off thioester-bound fatty acids. In the mentioned studies, this might have removed the raft-targeting feature and concomitantly have led to non-raft localization of HA. An alternative procedure for GPMV formation which avoids the usage of DTT showed that many proteins predicted to be raft-localized in cells partition into the ordered phase [35]. The study also showed that a large fraction of raft-associated transmembrane proteins is palmitoylated and that this hydrophobic modification is required for raft partitioning. It will be interesting to see how HA behaves in that artificial membrane system.

In principle, faithful reconstitution of viral proteins into model membranes might be the first step towards an *in vitro* system for virus assembly and budding that would allow to decipher all the required components, that is, individual viral proteins and lipids.

2.5. Raft Localization of Other Influenza Virus Membrane Proteins. Much less is known about the raft localization of the second glycoprotein of influenza virus, the **neuraminidase NA**, which is also DRM-associated and apically transported. The signals for apical transport and raft localization are both situated in the transmembrane region of NA, but overlap only partly. Raft targeting was mapped to the TMR half situated in the outer membrane leaflet (label 3 in Figure 1(b)), but the molecular cause for this has not been determined [58, 59]. Immunoelectron microscopy showed that NA localizes to the same microdomains as HA in virus-infected cells [60]. No functional fluorescent construct of NA has been described so far that would allow to study raft association in living cells similarly to the experiments conducted with HA, for example, by FRET.

The **matrix protein M1** does not contain a transmembrane domain and is anchored to cellular membranes by a variety of interactions [14]. M1 expressed alone is not associated with DRMs, but coexpression of HA and/or NA increases detergent resistance of M1 [17, 18]. It was therefore proposed that M1 is drawn to rafts of the plasma membrane by interactions with the cytoplasmic tails of HA and NA, but such an interaction has not been directly demonstrated so far. However, viruses lacking the cytoplasmic tails of HA and NA were found to have severe assembly defects, show irregular morphology, and are defective in vRNP packaging [61]. Those defects were much less pronounced when only one cytoplasmic tail was missing indicating redundant functions of both tails [62].

The second splice product of the M gene, the **ion-channel protein M2**, is not associated with DRMs [18]. However, M2 possess two possible raft targeting features, S-acylation [63] and an affinity for the raft-lipid cholesterol [64]. Several overlapping CRAC motifs, which are thought to mediate the interaction with cholesterol, and the single acylation site are both located within an amphiphilic helix in the cytoplasmic tail of M2 (label 4 in Figure 1(b)). It was therefore proposed that acylation and cholesterol binding target the amphiphilic helix to the raft domain but the relatively short transmembrane region of M2 prevents complete immersion of the protein in the more ordered, hence thicker raft domains. As a consequence, M2 was hypothesized to localize to the edge of the viral budozone, to be involved in raft coalescence and to mediate pinching off of virus particles from the plasma membrane by the induction of curvature through wedge-like insertion of the amphiphilic helix into the membrane [64].

Testing possible raft localization of M2 with FRET showed that the molecule (fused to a fluorescent protein) does not interact with the double-acylated marker for inner leaflet rafts [65]. However, in GPMVs prepared in the absence of DTT, M2 (partly) partitioned into the raft domain, a property which was dependent on acylation, but not on intact CRAC motifs. Thus, in principle, M2 can interact with raft domains but an enrichment at the interface between the liquid-ordered and -disordered phase was not observed in this system [66].

Surprisingly, the results from FRET experiments point to an interaction (or very close colocalization) of M2 with HA [65]. The FRET signal between M2 and HA (fused to fluorescent proteins) depends on the raft-targeting signals of HA and on an intact actin cytoskeleton, reinforcing the notion that cortical actin is involved in the organization of the viral budozone. How can it be reconciled that M2 clusters with raft-associated HA, but not with the double-acylated raft marker? The raft marker, when expressed in the absence of HA, is probably present in small, unstimulated rafts, to which M2 has no access. HA organizes the larger viral budozone, into which the raft marker can partition; M2 apparently interacts with this functionalized domain. Thus, M2 must have an intrinsic signal that targets the protein to

the viral budozone; this signal might be identical or similar to the (unidentified) signal for apical targeting of the protein. In the course of virus infection, M2 shows increasing DRM and cholesterol-rich membrane association [67]. This is most likely mediated by the matrix protein M1, which bridges the viral components in the budozone.

There are two reports describing that the **nucleoprotein NP**, the major vRNP component, localizes to apical membranes and associates with DRMs, even when expressed in the absence of other viral proteins [68, 69]. This observation implies that NP contains intrinsic signals for apical transport and raft association, although the protein is hydrophilic and is not modified by lipid moieties. However, others have not seen polarized localization of NP in transfected cells [16].

3. Function of Rafts for Influenza Virus Replication

It is assumed that rafts play a decisive role at several steps during virus replication and are hence vital for virus viability. These steps include intracellular transport of viral proteins (most notably HA) to the assembly site, assembly and budding of progeny virus particles at the plasma membrane, environmental stability of the virus particles, and fusion of viral and host cell endosomal membrane upon virus entry.

3.1. Intracellular Transport of HA. HA is transported to the apical plasma membrane *via* the secretory pathway. Deletion of the raft-targeting sequence in the outer leaflet of its transmembrane region severely retards Golgi-localized processing of HA, such as acquisition of Endo-H resistant carbohydrates and proteolytic cleavage. In contrast, trimerization of the molecule in the ER was not affected demonstrating that the transport delay is localized to the Golgi apparatus (Engel, de Vries, Herrmann, Veit, submitted). This is in line with a recent model on the organization of vesicular transport through the Golgi, which predicts that each cisterna of this organelle contains two lipid phases, a "processing domain" enriched in glycerophospholipids and an "export domain" enriched in cholesterol and sphingolipids. Processing enzymes, such as glycosyl transferases, are mostly excluded from export domains and therefore remain trapped in the Golgi, whereas transmembrane cargo proteins preferentially partition into the export domain [70]. Thus, decreasing the access to raft-like export domains should decelerate transport of transmembrane proteins through the Golgi. Since the second signal for targeting of HA to rafts of the plasma membrane, S-acylation at cytoplasmic cysteines, had no effect on transport, the putative export domain in the Golgi differs from conventional rafts of the plasma membrane.

Membrane rafts might also be involved in further steps of HA transport. It was postulated early on that cholesterol-sphingolipid clusters form vesicles in the trans-Golgi network (TGN), which serve as carriers for these lipids and entrapped proteins to the apical plasma membrane in epithelial cells [71, 72]. This model suggests that association with raft-like membranes is a prerequisite for apical transport of HA. Indeed, HA acquires detergent resistance at a late stage during its transport to the cell surface, probably in the TGN [73], and lowering cholesterol levels blocks transport of HA from the TGN to the cell surface [74]. However, several mutations in the transmembrane region of HA have been described which block association with DRMs, but not apical transport [75]. The lipid content of plasma membrane rafts could differ from that of transport vesicles. This could be determined experimentally by purification of HA-containing transport vesicles and analysis of their lipidome [76]. In short, there is evidence that raft domains are involved in forward transport of raft-associated cargo proteins such as HA through Golgi and TGN. This is accompanied by an increasing cholesterol content along the secretory route (ER<Golgi<plasma membrane, [77]).

3.2. Budding of Virus Particles. The two glycoproteins of the virus, hemagglutinin (HA) and neuraminidase (NA), accumulate in rafts of the plasma membrane. M1 is then supposed to weakly bind to the cytoplasmic tails of HA and NA. Oligomerization of M1 strengthens the weak interactions with HA and NA and draws M1 to the viral budozone. M2, which is abundantly expressed at the plasma membrane, but largely excluded from virus particles, assumingly accumulates at the edge of the budozone. Finally, interactions between vRNPs and M1 initiate budding and release of virus particles [69, 78–81]. During that process, it must be ensured that most newly formed virus particles contain a complete set of vRNPs. Since cryoelectron tomography has shown that each virus particle contains a specific pattern of exactly eight, individually discernible vRNPs, a highly selective mechanism of genome packaging is currently the favoured model [82]. Short nucleotide sequences identical in every RNA segment, which are situated at the 5′- and 3′-termini of each RNA, form a terminal panhandle structure that is required for packaging into RNPs, but the individual packaging signals present in each vRNP still need to be identified [83, 84].

Budding is a membrane-remodeling process which entails membrane bending (induction of curvature), that leads to the formation of an Ω-shaped bud, followed by constriction of the bud's neck, and, ultimately, the disconnection of the particle (scission) owing to very close apposition and fusion of the neck membranes [85]. During the whole budding process, a part of the (almost) planar plasma membrane is converted into a spherical (highly curved) vesicle. Since the plasma membrane tends to stay flat, this shape change is an energetically unfavorable process and the required energy must be provided by interaction with proteins [86]. Principally, there are two ways how proteins can induce curvature in cellular membranes. Intrinsically curved proteins or protein oligomers can provide "scaffolding" that leads to membrane bending; partially membrane-inserted proteins or protein domains can act as a "wedge" by displacing membrane lipids in only one bilayer leaflet [86–88]. The lipids themselves can intrinsically favor curvature if they are "cone-shaped" (if they exhibit a difference in the cross-section area of the hydrophilic head group and the hydrophobic region).

In addition, since a small spherical virus contains roughly 10% more lipid molecules in the outer bilayer compared to the inner bilayer [86], enrichment of outer leaflet lipids (or partial depletion of inner leaflet lipids) at the budding site will aid in membrane deformation. Finally, formation of raft domains could also aid in the process of budding. In that case, the hydrophobic mismatch and the height difference between the domains leads to a "line tension" at the domain interface. To minimize the free energy of the system, curvature is induced in the bilayer of the budozone, which may initiate or support protein-based budding [89, 90].

In contrast to many other enveloped viruses, it is still not unambiguously defined which of the influenza virus proteins provide the energy for membrane deformation. To experimentally determine the driving force for budding, that is, the "minimal set" of required viral proteins, the proteins in question are expressed in cells and the shedding of "virus-like particles" (VLPs)—vesicles containing the expressed viral proteins and having the same density as actual virus particles—is detected biochemically. At first, M1 was found to be sufficient for VLP production [91, 92], consistent with a budding model based on scaffold formation by the matrix protein. This might, however, have been an artifact of the expression system; in chemically transfected cells, HA and NA [93–95] rather than M1 were found to be sufficient for VLP formation. Remarkably, it was found that M1 artificially tagged with lipid anchors is targeted to the plasma membrane and is then sufficient for VLP formation [96]. In the context of virus infection, M1 can fulfill this function by being transported to the plasma membrane by the other viral membrane proteins (see above). Of these, HA and NA are also capable of triggering VLP formation on their own, albeit with increased efficiency if M1 is coexpressed [93]. When HA and NA cytoplasmic tail mutants were included in the VLPs, M1 failed to be efficiently incorporated into VLPs, consistent with a model in which the glycoproteins control virus budding by sorting to lipid raft microdomains and recruiting the internal viral core components. It has to be kept in mind, however, that VLP formation is prone to artifacts as cells tend to continuously shed vesicles that might unspecifically incorporate the overexpressed viral protein [97].

The role of rafts for virus budding has also been analyzed in the context of virus infection. Removal of the raft-targeting signal in the transmembrane region of HA decreased virus production, and there was less HA incorporated in the produced particles. This HA mutant was randomly distributed over the plasma membrane, contrary to wild-type HA. Thus, clustering of HA in rafts, as described above for wild-type HA, ensures its inclusion in particles and/or is required for efficient budding [98].

Likewise, the interferon-induced cellular protein viperin increases the lateral mobility of HA by decreasing its raft association and severely inhibits the release of virus particles [99]. Many of the virions on the surface of viperin-expressing cells displayed a "daisy-chain" structure in which two or more viral particles appeared to be linked by a connecting membrane. Similar (or other) abnormal virus structures have been observed for viruses with deletions of the cytoplasmic tails of HA and NA [61]. Viruses containing HA without the two palmitoylated cytoplasmic cysteines incorporated reduced amounts of the internal components NP and M1 and also revealed defects in virus release. Surprisingly, exchange of the M1 protein by that of a different influenza virus strain restored assembly of viruses with nonpalmitoylated HA [100]. This observation links palmitoylation of HA to the matrix protein. However, similar experiments with H7-subtype HA did not reveal a defect in virus budding, but in virus entry by membrane fusion (see below, [101]). Nevertheless, the cumulative evidence just described clearly indicates that HA (and especially its S-acylated cytoplasmic tail) plays an important role in virus budding.

The ultimate step in virus budding is the scission of the virus particle from the plasma membrane. Recent evidence indicates that this is mediated by the amphiphilic helix of M2, probably acting as a "wedge." Peptides representing the helix induced the formation of vesicles from GUVs [67]. Mutation of five hydrophobic residues in the amphiphilic helix of the M2-CT affected virus shape and virus budding [67, 102]. However, neither the CRAC motifs implied in cholesterol binding nor acylation are absolutely essential for the production of virus particles: there are virus strains in which the acylation site or intact CRAC motifs are lacking, and recombinant viruses in which the acylated cysteine [103] or parts of the CRAC motifs [104] were replaced grew similarly well as the corresponding wild-type virus, and deletion of both the CRAC motif and the acylation site simultaneously also did not affect virus production, at least in cell culture (Thaa, Wolff, Herrmann, Veit, to be published). However, attenuation of virus infectivity was observed in mice both for virus with nonacylated [105] and CRAC-disrupted [104] M2.

In addition, it is likely that cellular proteins contribute to budding. The endosomal sorting complex required for transport (ESCRT), parts of which are involved in budding of other viruses such as HIV, seems to be dispensable for influenza virus budding [93, 106]. There is however some evidence that actin is involved especially in the formation of filamentous virus particles [38, 107]. Polymerisation of actin could provide a pushing force to extend the growing bud. Additionally, the endocytic recycling GTPase Rab11 was recently identified as a budding cofactor [108]. It was subsequently shown that Rab11 (and the underlying vesicular transport pathway) is involved in cytoplasmic transport of vRNPs to the plasma membrane [109]. It will be interesting to decipher its exact mode of action as well as to identify possible other cellular budding factors.

To summarize, efficient budding of influenza virus seems to come about by the combined action of scaffold-based, wedge-mediated, and domain-induced processes (see Figure 2). M1 oligomerization could provide a scaffold, the amphiphilic helix of M2 might act as a wedge, and both work in concert with the HA-induced formation of a large-scale, intrinsically bent raft domain. However, it is surprising that mutations in several protein domains suggested to be essential for virus budding, such as the cytoplasmic tails of HA and NA and large parts of M2 including its amphiphilic

helix, sometimes have no or only a moderate effect on virus replication [61, 62, 103, 104, 110–113]. Thus, budding can be considered to be a particularly robust process, relatively insensitive to disturbing effects or the failure of one of the many functionalities. The precision of the assembly process, that is, how faithfully all viral elements are included into one particle, is not known. The overwhelming majority of released particles (90–99%) are noninfectious, indicating that not all viral elements have been incorporated in a functionally active form. However, other causes for the failure to initiate infection, such as successful interference by a cellular factor, binding to an inappropriate receptor, or defects in membrane fusion, certainly contribute to the high proportion of non infectious virus particles. Furthermore, highly purified virus particles contain various cellular proteins demonstrating that they were incompletely excluded from the budding site [114]. The probably high error rate of virus budding distinguishes it from budding of cellular transport vesicles, which otherwise follow similar principles [115].

3.3. Stability of the Viral Envelope. It has been observed early on that the influenza virus envelope contains detergent-insoluble and ordered lipid assemblies [116]. Recently, a detailed comparison of all the lipid species present in virus particles and in the apical membrane of epithelial host cells revealed that cholesterol and sphingolipids are enriched in the viral membrane providing conclusive evidence that viruses bud through raft domains (Mathias J. Gerl and Kai Simons, personal communication). The question arises whether the raft lipids in the envelope are just a nonfunctional by-product of virus budding through rafts or whether they serve a specific function during subsequent steps of the viral life cycle.

A recent NMR study on the mobility of lipids in the viral envelope suggests that the raft lipids might be important for airborne transmission of viruses between individuals [117]. The lipids form both ordered (raft-like or solid) as well as disordered phases, but their relative proportion is strongly dependent on the temperature. At 4°C, the envelope is almost entirely in the ordered phase, which, however, is only a significant, but minor fraction at 41°C. The occurrence of two phases, probably caused by different lipid assemblies, might explain why HA and NA spikes are not randomly distributed in the viral envelope—rather, local clusters of NA spikes, surrounded by the more abundant HA, are observed by cryoelectron tomography [69, 118].

Thus, inclusion of raft lipids into the viral envelope equips the particle with a versatile system that autonomously regulates the rigidity of the membrane to fit the respective physiological needs. After discharge of a virus particle from the lungs of an infected person, the virus is exposed to lower temperatures. This leads to solidification of the viral envelope to protect the viral genome against environmental damage. In accordance with this, cold conditions favour transmission of influenza virus explaining its predominant winter spread [119]. After uptake in the body of the next individual, the particle is exposed to increasing temperatures which "melt"

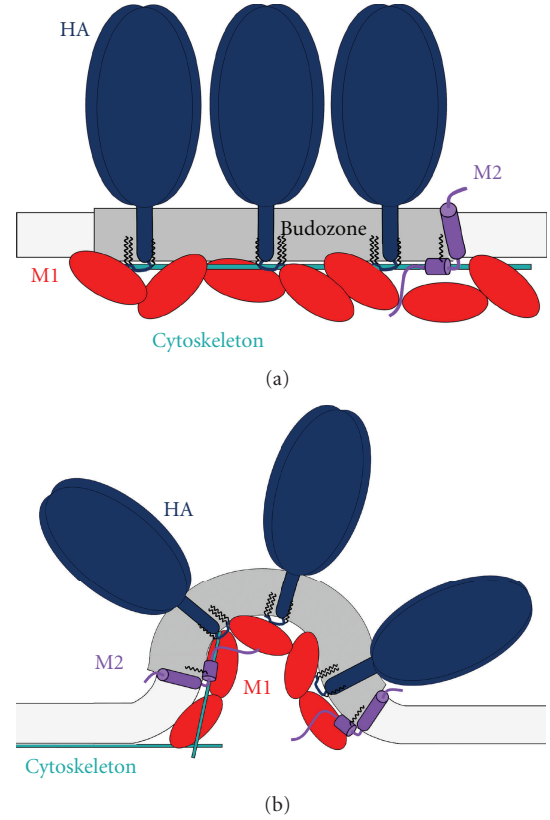

Figure 2: Schematic representation of influenza virus budding. (a) Formation of the budozone, a coalesced raft domain, in the plasma membrane. HA (blue) and NA (not shown) are targeted to rafts; M2 (purple) might be positioned at the edge of the budozone. M1 (red) binds to membranes and all the viral proteins including the viral RNPs (not shown) and clusters the viral components. The cytoskeleton (cyan) is involved in establishment of the budozone. (b) Formation of curvature for budding. Interactions involved: M1 acts as a scaffold from beneath, the cytoskeleton provides outward pushing, the line tension at the domain boundary leads to bending, and the amphiphilic helix of M2 acts as a wedge. See text for details.

the viral envelope. A liquid membrane is required to allow the fusion of virus particles with cellular membranes.

3.4. Membrane Fusion Activity of HA. Membrane fusion is divided into several stages: lipid-mixing (hemifusion) and reversible formation of a fusion pore precedes the final merger of viral and cellular membranes. These events can be measured separately by loading erythrocyte ghosts with fluorescent dyes, either the membrane with lipid dyes or the interior with aqueous dyes, and following their transfer into HA-expressing cells with fluorescence microscopy [6, 120–122].

To analyze a possible effect of rafts on membrane fusion, HA without raft-targeting signals was expressed in eukaryotic cells and the fusion activity was recorded as syncytium formation (i.e., fused cells with more than one nucleus) between HA-expressing and neighboring cells. Cells expressing HA with a deleted raft-targeting signal at the

beginning of the TMR were capable to induce both hemifusion and full fusion, but the number of fusion events was reduced. Virus particles containing non-raft HA were less infectious and exhibited reduced fusion activity. However, since these particles contained less HA, it was concluded that not the fusion activity *per se* was compromised but that rafts concentrate HA for efficient fusion activity [98].

Confusing and partly inconsistent data on the effect of removal of acylation sites on the fusion activity of HA have been published. It was reported that nonacylated H1- and H7-subtype HA and HA of influenza B virus show restricted fusion pore formation [101, 123, 124] and that nonpalmitoylated HA of the H2 subtype revealed impaired syncytium formation [125]. In contrast, HA deacylation mutants from the same H2 subtype, but also from H3, and H7 subtypes mediated cell-cell fusion [126–128]. Likewise, unperturbed transfer of aqueous dyes into HA-expressing cells was observed for avian H7-subtype HA in other studies [129] and also for human H3-subtype HA [100]. However, in all cases where an effect of acylation on the membrane fusion activity of HA was reported, a late event in this process, namely, the opening, flickering, and/or dilation of the fusion pore was affected.

Membrane fusion is believed to proceed *via* a fusion stalk, where lipids with a certain structure connect the viral envelope with the cellular membrane such that lipid exchange occurs between the outer leaflets of both membranes [120]. It is conceivable that HA-bound fatty acids might perturb the organization of the membrane lipids at this stage of the fusion process, which would then accelerate opening and/or dilation of the fusion pore and allow membrane fusion to proceed to completion. Alternatively, HA-bound fatty acids might not work directly during fusion, but attract cholesterol to the viral envelope, which could serve a specific function during membrane fusion.

A direct role of cholesterol during membrane fusion was addressed in several studies. Extraction of cholesterol from virus particles reduced their infectivity, most likely due to an inhibition of membrane fusion [130]. In a more comprehensive analysis, HA-expressing insect cells, which naturally contain low cholesterol levels, were loaded with cholesterol and fusion with erythrocytes (labeled with fluorescent dyes) was measured. Cholesterol enhanced the rate of lipid mixing (a marker for hemifusion) and the amount and extent of aqueous dye transfer (a marker for fusion pore expansion). It was concluded that cholesterol acts both at an early stage of fusion, that is, prior to fusion pore opening, and at an late stage during fusion pore expansion [131]. In principle, the fusion-promoting effect of cholesterol might be due to three, not mutually exclusive, modes of action. First, cholesterol might bind to the transmembrane region of HA thereby directing the conformational changes required for fusion. Secondly, the negative membrane curvature spontaneously induced by the sterol might promote the local bilayer bending that takes place during membrane fusion. Finally, cholesterol might increase the mobility of HA in the membrane that is required for fusion pore expansion by increasing the fraction of lipids in the fluid state.

The confusing and partly inconsistent variety of published data on the effect of acylation site removal on the fusion activity of HA suggests that the methods used are not ideally suited for this purpose. It is questionable whether syncytium formation and fusion of HA-expressing cells with erythrocytes accurately reflect entry of influenza virus into target cells. Furthermore, these methods are only semiquantitative and kinetic measurements are barely possible. In addition, the fusion activity of HA depends on its density on the cell surface [132], which can hardly be measured accurately and cannot be controlled in conventional expression systems. It would be helpful to establish an experimental fusion system composed of closely controlled amounts of purified HA (with and without raft-targeting signals) reconstituted into lipid vesicles with the authentic composition of the viral envelope and fluorescently labeled liposomes as the target membrane to quantitatively analyze the contribution of HA-linked fatty acids to fusion pore formation and its widening.

4. Conclusion

In summary, HA might pass through a functional "raft cycle" during replication of influenza virus. In the Golgi, HA associates with membrane rafts, which might form vesicles to facilitate transport of entrapped proteins to the apical membrane. At the plasma membrane, HA induces the formation of the viral budozone, a membrane nanodomain where assembly of viral components and exclusion of cellular proteins occur. Upon assembly of all virus components, HA might cause bending of the membrane and M2, which is supposedly attracted to the edge of the viral budozone, might mediate pinching off of virus particles. Budding of virus particles through rafts equips the particle with an appropriate lipid mixture that protects particles from environmental damage and, in the case of cholesterol, might promote membrane fusion upon virus entry. Thus, rafts are functionally indispensable for the replication cycle of influenza virus and hence perhaps a possible target for anti-influenza drugs to be developed.

Acknowledgments

The work done in the authors' laboratory is funded by the German Research Foundation (DFG), projects SPP 1175, SFB 740, and Ve 141/10, and by 7th Framework Programme of the European Commission, Marie Curie Initial Training Network "Virus-Entry."

References

[1] A. V. Shishkov, E. N. Bogacheva, A. A. Dolgov et al., "The in situ structural characterization of the influenza A virus matrix M1 protein within a virion," *Protein and Peptide Letters*, vol. 16, no. 11, pp. 1407–1413, 2009.

[2] G. R. Whittaker, "Intracellular trafficking of influenza virus: clinical implications for molecular medicine," *Expert Reviews in Molecular Medicine*, vol. 2001, pp. 1–13, 2001.

[3] L. V. Kordyukova, M. V. Serebryakova, L. A. Baratova, and M. Veit, "S acylation of the hemagglutinin of influenza viruses: mass spectrometry reveals site-specific attachment of stearic acid to a transmembrane cysteine," *Journal of Virology*, vol. 82, no. 18, pp. 9288–9292, 2008.

[4] M. Veit and M. F. G. Schmidt, "Palmitoylation of influenza virus proteins," *Berliner und Münchener Tierärztliche Wochenschrift*, vol. 119, no. 3-4, pp. 112–122, 2006.

[5] W. Garten and H. D. Klenk, "Understanding influenza virus pathogenicity," *Trends in Microbiology*, vol. 7, no. 3, pp. 99–100, 1999.

[6] J. J. Skehel and D. C. Wiley, "Receptor binding and membrane fusion in virus entry: the influenza hemagglutinin," *Annual Review of Biochemistry*, vol. 69, pp. 531–569, 2000.

[7] G. M. Air, A. A. Ghate, and S. J. Stray, "Influenza neuraminidase as target for antivirals," *Advances in Virus Research*, vol. 54, pp. 375–402, 1999.

[8] L. H. Pinto and R. A. Lamb, "The M2 proton channels of influenza A and B viruses," *Journal of Biological Chemistry*, vol. 281, no. 14, pp. 8997–9000, 2006.

[9] F. Baudin, I. Petit, W. Weissenhorn, and R. W. H. Ruigrok, "In vitro dissection of the membrane and RNP binding activities of influenza virus M1 protein," *Virology*, vol. 281, no. 1, pp. 102–108, 2001.

[10] H. D. Klenk, W. Wollert, R. Rott, and C. Scholtissek, "Association of influenza virus proteins with cytoplasmic fractions," *Virology*, vol. 57, no. 1, pp. 28–41, 1974.

[11] R. W. Ruigrok, A. Barge, P. Durrer, J. Brunner, K. Ma, and G. R. Whittaker, "Membrane interaction of influenza virus M1 protein," *Virology*, vol. 267, no. 2, pp. 289–298, 2000.

[12] A. Gregoriades and B. Frangione, "Insertion of influenza M protein into the viral lipid bilayer and localization of site of insertion," *Journal of Virology*, vol. 40, no. 1, pp. 323–328, 1981.

[13] E. Kretzschmar, M. Bui, and J. K. Rose, "Membrane association of influenza virus matrix protein does not require specific hydrophobic domains or the viral glycoproteins," *Virology*, vol. 220, no. 1, pp. 37–45, 1996.

[14] B. Thaa, A. Herrmann, and M. Veit, "The polybasic region is not essential for membrane binding of the matrix protein M1 of influenza virus," *Virology*, vol. 383, no. 1, pp. 150–155, 2009.

[15] J. Zhang and R. A. Lamb, "Characterization of the membrane association of the influenza virus matrix protein in living cells," *Virology*, vol. 225, no. 2, pp. 255–266, 1996.

[16] H. Zhao, M. Ekström, and H. Garoff, "The M1 and NP proteins of influenza A virus form homo- but not heterooligomeric complexes when coexpressed in BHK-21 cells," *Journal of General Virology*, vol. 79, no. 10, pp. 2435–2446, 1998.

[17] S. Barman, A. Ali, E. K. Hui, L. Adhikary, and D. P. Nayak, "Transport of viral proteins to the apical membranes and interaction of matrix protein with glycoproteins in the assembly of influenza viruses," *Virus Research*, vol. 77, no. 1, pp. 61–69, 2001.

[18] J. Zhang, A. Pekosz, and R. A. Lamb, "Influenza virus assembly and lipid raft microdomains: a role for the cytoplasmic tails of the spike glycoproteins," *Journal of Virology*, vol. 74, no. 10, pp. 4634–4644, 2000.

[19] M. Enami and K. Enami, "Influenza virus hemagglutinin and neuraminidase glycoproteins stimulate the membrane association of the matrix protein," *Journal of Virology*, vol. 70, no. 10, pp. 6653–6657, 1996.

[20] B. J. Chen, G. P. Leser, D. Jackson, and R. A. Lamb, "The influenza virus M2 protein cytoplasmic tail interacts with the M1 protein and influences virus assembly at the site of virus budding," *Journal of Virology*, vol. 82, no. 20, pp. 10059–10070, 2008.

[21] M. F. McCown and A. Pekosz, "Distinct domains of the influenza A virus M2 protein cytoplasmic tail mediate binding to the M1 protein and facilitate infectious virus production," *Journal of Virology*, vol. 80, no. 16, pp. 8178–8189, 2006.

[22] L. J. Pike, "Rafts defined: a report on the Keystone symposium on lipid rafts and cell function," *Journal of Lipid Research*, vol. 47, no. 7, pp. 1597–1598, 2006.

[23] K. Simons and E. Ikonen, "Functional rafts in cell membranes," *Nature*, vol. 387, no. 6633, pp. 569–572, 1997.

[24] K. Simons and W. L. C. Vaz, "Model systems, lipid rafts, and cell membranes," *Annual Review of Biophysics and Biomolecular Structure*, vol. 33, pp. 269–295, 2004.

[25] D. Lingwood and K. Simons, "Lipid rafts as a membrane-organizing principle," *Science*, vol. 327, no. 5961, pp. 46–50, 2010.

[26] I. Levental, M. Grzybek, and K. Simons, "Greasing their way: lipid modifications determine protein association with membrane rafts," *Biochemistry*, vol. 49, no. 30, pp. 6305–6316, 2010.

[27] K. Simons and M. J. Gerl, "Revitalizing membrane rafts: new tools and insights," *Nature Reviews Molecular Cell Biology*, vol. 11, pp. 688–699, 2010.

[28] K. Simons and D. Toomre, "Lipid rafts and signal transduction," *Nature Reviews Molecular Cell Biology*, vol. 1, no. 1, pp. 31–39, 2000.

[29] K. Fiedler, T. Kobayashi, T. V. Kurzchalia, and K. Simons, "Glycosphingolipid-enriched, detergent-insoluble complexes in protein sorting in epithelial cells," *Biochemistry*, vol. 32, no. 25, pp. 6365–6373, 1993.

[30] K. A. Melkonian, A. G. Ostermeyer, J. Z. Chen, M. G. Roth, and D. A. Brown, "Role of lipid modifications in targeting proteins to detergent-resistant membrane rafts. Many raft proteins are acylated, while few are prenylated," *Journal of Biological Chemistry*, vol. 274, no. 6, pp. 3910–3917, 1999.

[31] M. A. Hanson, V. Cherezov, M. T. Griffith et al., "A specific cholesterol binding site is established by the 2.8 Å structure of the human beta2-adrenergic receptor," *Structure*, vol. 16, no. 6, pp. 897–905, 2008.

[32] R. G. Anderson and K. Jacobson, "A role for lipid shells in targeting proteins to caveolae, rafts, and other lipid domains," *Science*, vol. 296, no. 5574, pp. 1821–1825, 2002.

[33] H. Li and V. Papadopoulos, "Peripheral-type benzodiazepine receptor function in cholesterol transport. Identification of a putative cholesterol recognition/interaction amino acid sequence and consensus pattern," *Endocrinology*, vol. 139, no. 12, pp. 4991–4997, 1998.

[34] M. Ge and J. H. Freed, "Two conserved residues are important for inducing highly ordered membrane domains by the transmembrane domain of influenza hemagglutinin," *Biophysical Journal*, vol. 100, no. 1, pp. 90–97, 2011.

[35] I. Levental, D. Lingwood, M. Grzybek, Ü. Coskun, and K. Simons, "Palmitoylation regulates raft affinity for the majority of integral raft proteins," *Proceedings of the National Academy of Science of the United States of America*, vol. 107, no. 51, pp. 22050–22054, 2010.

[36] L. V. Kordyukova, M. V. Serebryakova, L. A. Baratova, and M. Veit, "Site-specific attachment of palmitate or stearate to

cytoplasmic versus transmembrane cysteines is a common feature of viral spike proteins," *Virology*, vol. 398, no. 1, pp. 49–56, 2010.

[37] S. Munro, "Lipid rafts: elusive or illusive?" *Cell*, vol. 115, no. 4, pp. 377–388, 2003.

[38] M. Simpson-Holley, D. Ellis, D. Fisher, D. Elton, J. McCauley, and P. Digard, "A functional link between the actin cytoskeleton and lipid rafts during budding of filamentous influenza virions," *Virology*, vol. 301, no. 2, pp. 212–225, 2002.

[39] A. K. Kenworthy and M. Edidin, "Distribution of a glycosylphosphatidylinositol-anchored protein at the apical surface of MDCK cells examined at a resolution of < 100 Å using imaging fluorescence resonance energy transfer," *Journal of Cell Biology*, vol. 142, no. 1, pp. 69–84, 1998.

[40] M. Rao and S. Mayor, "Use of Förster's resonance energy transfer microscopy to study lipid rafts," *Biochimica et Biophysica Acta*, vol. 1746, no. 3, pp. 221–233, 2005.

[41] S. T. Hess, T. J. Gould, M. V. Gudheti, S. A. Maas, K. D. Mills, and J. Zimmerberg, "Dynamic clustered distribution of hemagglutinin resolved at 40 nm in living cell membranes discriminates between raft theories," *Proceedings of the National Academy of Sciences of the United States of America*, vol. 104, no. 44, pp. 17370–17375, 2007.

[42] S. Engel, S. Scolari, B. Thaa et al., "FLIM-FRET and FRAP reveal association of influenza virus haemagglutinin with membrane rafts," *Biochemical Journal*, vol. 425, no. 3, pp. 567–573, 2010.

[43] D. A. Zacharias, J. D. Violin, A. C. Newton, and R. Y. Tsien, "Partitioning of lipid-modified monomeric GFPs into membrane microdomains of live cells," *Science*, vol. 296, no. 5569, pp. 913–916, 2002.

[44] S. Scolari, S. Engel, N. Krebs et al., "Lateral distribution of the transmembrane domain of influenza virus hemagglutinin revealed by time-resolved fluorescence imaging," *Journal of Biological Chemistry*, vol. 284, no. 23, pp. 15708–15716, 2009.

[45] D. Goswami, K. Gowrishankar, S. Bilgrami et al., "Nanoclusters of GPI-anchored proteins are formed by cortical actin-driven activity," *Cell*, vol. 135, no. 6, pp. 1085–1097, 2008.

[46] M. Edidin, "Switching sides: the actin/membrane lipid connection," *Biophysical Journal*, vol. 91, no. 11, p. 3963, 2006.

[47] J. Lippincott-Schwartz, E. Snapp, and A. Kemvorthy, "Studying protein dynamics in living cells," *Nature Reviews Molecular Cell Biology*, vol. 2, no. 6, pp. 444–456, 2001.

[48] D. E. Shvartsman, M. Kotler, R. D. Tall, M. G. Roth, and Y. I. Henis, "Differently anchored influenza hemagglutinin mutants display distinct interaction dynamics with mutual rafts," *Journal of Cell Biology*, vol. 163, no. 4, pp. 879–888, 2003.

[49] A. K. Kenworthy, B. J. Nichols, C. L. Remmert et al., "Dynamics of putative raft-associated proteins at the cell surface," *Journal of Cell Biology*, vol. 165, no. 5, pp. 735–746, 2004.

[50] A. Kusumi, Y. M. Shirai, I. Koyama-Honda, K. G. N. Suzuki, and T. K. Fujiwara, "Hierarchical organization of the plasma membrane: investigations by single-molecule tracking vs. fluorescence correlation spectroscopy," *FEBS Letters*, vol. 584, no. 9, pp. 1814–1823, 2010.

[51] D. Meder, M. J. Moreno, P. Verkade, W. L. C. Vaz, and K. Simons, "Phase coexistence and connectivity in the apical membrane of polarized epithelial cells," *Proceedings of the National Academy of Sciences of the United States of America*, vol. 103, no. 2, pp. 329–334, 2006.

[52] S. Ivanchenko, W. J. Godinez, M. Lampe et al., "Dynamics of HIV-1 assembly and release," *PLoS Pathogens*, vol. 5, no. 11, Article ID e1000652, 2009.

[53] N. Jouvenet, P. D. Bieniasz, and S. M. Simon, "Imaging the biogenesis of individual HIV-1 virions in live cells," *Nature*, vol. 454, no. 7201, pp. 236–240, 2008.

[54] K. Bacia, C. G. Schuette, N. Kahya, R. Jahn, and P. Schwille, "SNAREs prefer liquid-disordered over "raft" (liquid-ordered) domains when reconstituted into giant unilamellar vesicles," *Journal of Biological Chemistry*, vol. 279, no. 36, pp. 37951–37955, 2004.

[55] J. Nikolaus, S. Scolari, E. Bayraktarov et al., "Hemagglutinin of influenza virus partitions into the nonraft domain of model membranes," *Biophysical Journal*, vol. 99, no. 2, pp. 489–498, 2010.

[56] S. A. Johnson, B. M. Stinson, M. S. Go et al., "Temperature-dependent phase behavior and protein partitioning in giant plasma membrane vesicles," *Biochimica et Biophysica Acta*, vol. 1798, no. 7, pp. 1427–1435, 2010.

[57] M. T. Stockl and A. Herrmann, "Detection of lipid domains in model and cell membranes by fluorescence lifetime imaging microscopy," *Biochimica et Biophysica Acta*, vol. 1798, no. 7, pp. 1444–1456, 2010.

[58] S. Barman, L. Adhikary, A. K. Chakrabarti, C. Bernas, Y. Kawaoka, and D. P. Nayak, "Role of transmembrane domain and cytoplasmic tail amino acid sequences of influenza A virus neuraminidase in raft association and virus budding," *Journal of Virology*, vol. 78, no. 10, pp. 5258–5269, 2004.

[59] S. Barman and D. P. Nayak, "Analysis of the transmembrane domain of influenza virus neuraminidase, a type II transmembrane glycoprotein, for apical sorting and raft association," *Journal of Virology*, vol. 74, no. 14, pp. 6538–6545, 2000.

[60] G. P. Leser and R. A. Lamb, "Influenza virus assembly and budding in raft-derived microdomains: a quantitative analysis of the surface distribution of HA, NA and M2 proteins," *Virology*, vol. 342, no. 2, pp. 215–227, 2005.

[61] H. Jin, G. P. Leser, J. Zhang, and R. A. Lamb, "Influenza virus hemagglutinin and neuraminidase cytoplasmic tails control particle shape," *European Molecular Biology Laboratory Journal*, vol. 16, no. 6, pp. 1236–1247, 1997.

[62] H. Jin, G. P. Leser, and R. A. Lamb, "The influenza virus hemagglutinin cytoplasmic tail is not essential for virus assembly or infectivity," *European Molecular Biology Laboratory Journal*, vol. 13, no. 22, pp. 5504–5515, 1994.

[63] M. Veit, H. D. Klenk, A. Kendal, and R. Rott, "The M2 protein of influenza A virus is acetylated," *Journal of General Virology*, vol. 72, no. 6, pp. 1461–1465, 1991.

[64] C. Schroeder, H. Heider, E. Möncke-Buchner, and T. I. Lin, "The influenza virus ion channel and maturation cofactor M2 is a cholesterol-binding protein," *European Biophysics Journal*, vol. 34, no. 1, pp. 52–66, 2005.

[65] B. Thaa, A. Herrmann, and M. Veit, "Intrinsic cytoskeleton-dependent clustering of influenza virus M2 protein with hemagglutinin assessed by FLIM-FRET," *Journal of Virology*, vol. 84, pp. 12445–12449, 2010.

[66] B. Thaa, I. Levental, A. Herrmann, and M. Veit, "Intrinsic membrane association of the cytoplasmic tail of influenza virus M2 protein and lateral membrane sorting regulated by cholesterol binding and palmitoylation," *Biochemical Journal*, vol. 437, no. 3, pp. 389–397, 2011.

[67] J. S. Rossman, X. Jing, G. P. Leser, and R. A. Lamb, "Influenza virus M2 protein mediates ESCRT-independent membrane scission," *Cell*, vol. 142, no. 6, pp. 902–913, 2010.

[68] M. Carrasco, M. J. Amorim, and P. Digard, "Lipid raft-dependent targeting of the influenza A virus nucleoprotein to the apical plasma membrane," *Traffic*, vol. 5, no. 12, pp. 979–992, 2004.

[69] D. P. Nayak, R. A. Balogun, H. Yamada, Z. H. Zhou, and S. Barman, "Influenza virus morphogenesis and budding," *Virus Research*, vol. 143, no. 2, pp. 147–161, 2009.

[70] G. H. Patterson, K. Hirschberg, R. S. Polishchuk, D. Gerlich, R. D. Phair, and J. Lippincott-Schwartz, "Transport through the Golgi apparatus by rapid partitioning within a two-phase membrane system," *Cell*, vol. 133, no. 6, pp. 1055–1067, 2008.

[71] S. Schuck and K. Simons, "Polarized sorting in epithelial cells: raft clustering and the biogenesis of the apical membrane," *Journal of Cell Science*, vol. 117, no. 25, pp. 5955–5964, 2004.

[72] K. Simons and G. Van Meer, "Lipid sorting in epithelial cells," *Biochemistry*, vol. 27, no. 17, pp. 6197–6202, 1988.

[73] J. E. Skibbens, M. G. Roth, and K. S. Matlin, "Differential extractability of influenza virus hemagglutinin during intracellular transport in polarized epithelial cells and nonpolar fibroblasts," *Journal of Cell Biology*, vol. 108, no. 3, pp. 821–832, 1989.

[74] P. Keller and K. Simons, "Cholesterol is required for surface transport of influenza virus hemagglutinin," *Journal of Cell Biology*, vol. 140, no. 6, pp. 1357–1367, 1998.

[75] R. D. Tall, M. A. Alonso, and M. G. Roth, "Features of influenza HA required for apical sorting differ from those required for association with DRMS or MAL," *Traffic*, vol. 4, no. 12, pp. 838–849, 2003.

[76] R. W. Klemm, C. S. Ejsing, M. A. Surma et al., "Segregation of sphingolipids and sterols during formation of secretory vesicles at the trans-Golgi network," *Journal of Cell Biology*, vol. 185, no. 4, pp. 601–612, 2009.

[77] G. van Meer, D. R. Voelker, and G. W. Feigenson, "Membrane lipids: where they are and how they behave," *Nature Reviews Molecular Cell Biology*, vol. 9, no. 2, pp. 112–124, 2008.

[78] B. J. Chen and R. A. Lamb, "Mechanisms for enveloped virus budding: can some viruses do without an ESCRT?" *Virology*, vol. 372, no. 2, pp. 221–232, 2008.

[79] D. P. Nayak, E. K. W. Hui, and S. Barman, "Assembly and budding of influenza virus," *Virus Research*, vol. 106, no. 2, pp. 147–165, 2004.

[80] J. S. Rossman and R. A. Lamb, "Influenza virus assembly and budding," *Virology*, vol. 411, pp. 229–236, 2011.

[81] A. P. Schmitt and R. A. Lamb, "Escaping from the cell: assembly and budding of negative-strand RNA viruses," *Current Topics in Microbiology and Immunology*, vol. 283, pp. 145–196, 2004.

[82] T. Noda, H. Sagara, A. Yen et al., "Architecture of ribonucleoprotein complexes in influenza A virus particles," *Nature*, vol. 439, no. 7075, pp. 490–492, 2006.

[83] E. C. Hutchinson, J. C. von Kirchbach, J. R. Gog, and P. Digard, "Genome packaging in influenza A virus," *Journal of General Virology*, vol. 91, no. 2, pp. 313–328, 2010.

[84] T. Noda and Y. Kawaoka, "Structure of influenza virus ribonucleoprotein complexes and their packaging into virions," *Reviews in Medical Virology*, vol. 20, no. 6, pp. 380–391, 2011.

[85] M. M. Kozlov, H. T. McMahon, and L. V. Chernomordik, "Protein-driven membrane stresses in fusion and fission," *Trends in Biochemical Sciences*, vol. 35, no. 12, pp. 699–706, 2010.

[86] J. Zimmerberg and M. M. Kozlov, "How proteins produce cellular membrane curvature," *Nature Reviews Molecular Cell Biology*, vol. 7, no. 1, pp. 9–19, 2006.

[87] H. T. McMahon and J. L. Gallop, "Membrane curvature and mechanisms of dynamic cell membrane remodelling," *Nature*, vol. 438, no. 7068, pp. 590–596, 2005.

[88] W. A. Prinz and J. E. Hinshaw, "Membrane-bending proteins," *Critical Reviews in Biochemistry and Molecular Biology*, vol. 44, no. 5, pp. 278–291, 2009.

[89] R. Lipowsky, "Domain-induced budding of fluid membranes," *Biophysical Journal*, vol. 64, no. 4, pp. 1133–1138, 1993.

[90] B. J. Reynwar, G. Illya, V. A. Harmandaris, M. M. Müller, K. Kremer, and M. Deserno, "Aggregation and vesiculation of membrane proteins by curvature-mediated interactions," *Nature*, vol. 447, no. 7143, pp. 461–464, 2007.

[91] P. Gómez-Puertas, C. Albo, E. Pérez-Pastrana, A. Vivo, and A. Portela, "Influenza virus matrix protein is the major driving force in virus budding," *Journal of Virology*, vol. 74, no. 24, pp. 11538–11547, 2000.

[92] T. Latham and J. M. Galarza, "Formation of wild-type and chimeric influenza virus-like particles following simultaneous expression of only four structural proteins," *Journal of Virology*, vol. 75, no. 13, pp. 6154–6165, 2001.

[93] B. J. Chen, G. P. Leser, E. Morita, and R. A. Lamb, "Influenza virus hemagglutinin and neuraminidase, but not the matrix protein, are required for assembly and budding of plasmid-derived virus-like particles," *Journal of Virology*, vol. 81, no. 13, pp. 7111–7123, 2007.

[94] J. C. Lai, W. W. Chan, F. Kien, J. M. Nicholls, J. S. Peiris, and J. M. Garcia, "Formation of virus-like particles from human cell lines exclusively expressing influenza neuraminidase," *The Journal of General Virology*, vol. 91, no. 9, pp. 2322–2330, 2010.

[95] M. A. Yondola, F. Fernandes, A. Belicha-Villanueva et al., "Budding capability of the influenza virus neuraminidase can be modulated by tetherin," *Journal of Virology*, vol. 85, no. 6, pp. 2480–2491, 2011.

[96] D. Wang, A. Harmon, J. Jin et al., "The lack of an inherent membrane targeting signal is responsible for the failure of the matrix (M1) protein of influenza A virus to bud into virus-like particles," *Journal of Virology*, vol. 84, no. 9, pp. 4673–4681, 2010.

[97] V. Muralidharan-Chari, J. W. Clancy, A. Sedgwick, and C. D'Souza-Schorey, "Microvesicles: mediators of extracellular communication during cancer progression," *Journal of Cell Science*, vol. 123, no. 10, pp. 1603–1611, 2010.

[98] M. Takeda, G. P. Leser, C. J. Russell, and R. A. Lamb, "Influenza virus hemagglutinin concentrates in lipid raft microdomains for efficient viral fusion," *Proceedings of the National Academy of Sciences of the United States of America*, vol. 100, no. 25, pp. 14610–14617, 2003.

[99] X. Wang, E. R. Hinson, and P. Cresswell, "The interferon-inducible protein viperin inhibits influenza virus release by perturbing lipid rafts," *Cell Host and Microbe*, vol. 2, no. 2, pp. 96–105, 2007.

[100] B. J. Chen, M. Takeda, and R. A. Lamb, "Influenza virus hemagglutinin (H3 subtype) requires palmitoylation of its cytoplasmic tail for assembly: M1 proteins of two subtypes differ in their ability to support assembly," *Journal of Virology*, vol. 79, no. 21, pp. 13673–13684, 2005.

[101] R. Wagner, A. Herwig, N. Azzouz, and H. D. Klenk, 'Acylation-mediated membrane anchoring of avian influenza virus

hemagglutinin is essential for fusion pore formation and virus infectivity," *Journal of Virology*, vol. 79, no. 10, pp. 6449–6458, 2005.

[102] J. S. Rossman, X. Jing, G. P. Leser, V. Balannik, L. H. Pinto, and R. A. Lamb, "Influenza virus m2 ion channel protein is necessary for filamentous virion formation," *Journal of Virology*, vol. 84, no. 10, pp. 5078–5088, 2010.

[103] M. R. Castrucci, M. Hughes, L. Calzoletti et al., "The cysteine residues of the M2 protein are not required for influenza A virus replication," *Virology*, vol. 238, no. 1, pp. 128–134, 1997.

[104] S. M. Stewart, W. H. Wu, E. N. Lalime et al., "The cholesterol recognition/interaction amino acid consensus motif of the influenza A virus M2 protein is not required for virus replication but contributes to virulence," *Virology*, vol. 405, no. 2, pp. 530–538, 2010.

[105] M. L. Grantham, W. H. Wu, E. N. Lalime, M. E. Lorenzo, S. L. Klein, and A. Pekosz, "Palmitoylation of the influenza A virus M2 protein is not required for virus replication in vitro but contributes to virus virulence," *Journal of Virology*, vol. 83, no. 17, pp. 8655–8661, 2009.

[106] E. A. Bruce, L. Medcalf, C. M. Crump et al., "Budding of filamentous and non-filamentous influenza A virus occurs via a VPS4 and VPS28-independent pathway," *Virology*, vol. 390, no. 2, pp. 268–278, 2009.

[107] P. C. Roberts and R. W. Compans, "Host cell dependence of viral morphology," *Proceedings of the National Academy of Sciences of the United States of America*, vol. 95, no. 10, pp. 5746–5751, 1998.

[108] E. A. Bruce, P. Digard, and A. D. Stuart, "The Rab11 pathway is required for influenza A virus budding and filament formation," *Journal of Virology*, vol. 84, no. 12, pp. 5848–5859, 2010.

[109] M. J. Amorim, E. A. Bruce, E. K. Read et al., "A rab11- and microtubule-dependent mechanism for cytoplasmic transport of influenza a virus viral RNA," *Journal of Virology*, vol. 85, no. 9, pp. 4143–1456, 2011.

[110] A. García-Sastre and P. Palese, "The cytoplasmic tail of the neuraminidase protein of influenza A virus does not play an important role in the packaging of this protein into viral envelopes," *Virus Research*, vol. 37, no. 1, pp. 37–47, 1995.

[111] E. C. Hutchinson, M. D. Curran, E. K. Read, J. R. Gog, and P. Digard, "Mutational analysis of cis-acting RNA signals in segment 7 of influenza a virus," *Journal of Virology*, vol. 82, no. 23, pp. 11869–11879, 2008.

[112] M. Takeda, A. Pekosz, K. Shuck, L. H. Pinto, and R. A. Lamb, "Influenza A virus M ion channel activity is essential for efficient replication in tissue culture," *Journal of Virology*, vol. 76, no. 3, pp. 1391–1399, 2002.

[113] T. Watanabe, S. Watanabe, H. Ito, H. Kida, and Y. Kawaoka, "Influenza A virus can undergo multiple cycles of replication without M2 Ion channel activity," *Journal of Virology*, vol. 75, no. 12, pp. 5656–5662, 2001.

[114] M. L. Shaw, K. L. Stone, C. M. Colangelo, E. E. Gulcicek, and P. Palese, "Cellular proteins in influenza virus particles," *PLoS Pathogens*, vol. 4, no. 6, Article ID e1000085, 2008.

[115] B. Thaa, K. P. Hofmann, and M. Veit, "Viruses as vesicular carriers of the viral genome: a functional module perspective," *Biochimica et Biophysica Acta*, vol. 1803, no. 4, pp. 507–519, 2010.

[116] P. Scheiffele, A. Rietveld, T. Wilk, and K. Simons, "Influenza viruses select ordered lipid domains during budding from the plasma membrane," *Journal of Biological Chemistry*, vol. 274, no. 4, pp. 2038–2044, 1999.

[117] I. V. Polozov, L. Bezrukov, K. Gawrisch, and J. Zimmerberg, "Progressive ordering with decreasing temperature of the phospholipids of influenza virus," *Nature Chemical Biology*, vol. 4, no. 4, pp. 248–255, 2008.

[118] A. Harris, G. Cardone, D. C. Winkler et al., "Influenza virus pleiomorphy characterized by cryoelectron tomography," *Proceedings of the National Academy of Sciences of the United States of America*, vol. 103, no. 50, pp. 19123–19127, 2006.

[119] A. C. Lowen, S. Mubareka, J. Steel, and P. Palese, "Influenza virus transmission is dependent on relative humidity and temperature," *PLoS Pathogens*, vol. 3, no. 10, pp. 1470–1476, 2007.

[120] L. V. Chernomordik and M. M. Kozlov, "Membrane hemifusion: crossing a chasm in two leaps," *Cell*, vol. 123, no. 3, pp. 375–382, 2005.

[121] L. J. Earp, S. E. Delos, H. E. Park, and J. M. White, "The many mechanisms of viral membrane fusion proteins," *Current topics in Microbiology and Immunology*, vol. 285, pp. 25–66, 2005.

[122] G. W. Kemble, T. Danieli, and J. M. White, "Lipid-anchored influenza hemagglutinin promotes hemifusion, not complete fusion," *Cell*, vol. 76, no. 2, pp. 383–391, 1994.

[123] T. Sakai, R. Ohuchi, and M. Ohuchi, "Fatty acids on the A/USSR/77 influenza virus hemagglutinin facilitate the transition from hemifusion to fusion pore formation," *Journal of Virology*, vol. 76, no. 9, pp. 4603–4611, 2002.

[124] M. Ujike, K. Nakajima, and E. Nobusawa, "Influence of acylation sites of influenza B virus hemagglutinin on fusion pore formation and dilation," *Journal of Virology*, vol. 78, no. 21, pp. 11536–11543, 2004.

[125] C. W. Naeve and D. Williams, "Fatty acids on the A/Japan/305/57 influenza virus hemagglutinin have a role in membrane fusion," *European Molecular Biology Laboratory Journal*, vol. 9, no. 12, pp. 3857–3866, 1990.

[126] H. Y. Naim, B. Amarneh, N. T. Ktistakis, and M. G. Roth, "Effects of altering palmitylation sites on biosynthesis and function of the influenza virus hemagglutinin," *Journal of Virology*, vol. 66, no. 12, pp. 7585–7588, 1992.

[127] D. A. Steinhauer, S. A. Wharton, D. C. Wiley, and J. J. Skehel, "Deacylation of the hemagglutinin of influenza A/Aichi/2/68 has no effect on membrane fusion properties," *Virology*, vol. 184, no. 1, pp. 445–448, 1991.

[128] M. Veit, E. Kretzschmar, K. Kuroda et al., "Site-specific mutagenesis identifies three cysteine residues in the cytoplasmic tail as acylation sites of influenza virus hemagglutinin," *Journal of Virology*, vol. 65, no. 5, pp. 2491–2500, 1991.

[129] C. Fischer, B. Schroth-Diez, A. Herrmann, W. Garten, and H. D. Klenk, "Acylation of the influenza hemagglutinin modulates fusion activity," *Virology*, vol. 248, no. 2, pp. 284–294, 1998.

[130] X. Sun and G. R. Whittaker, "Role for influenza virus envelope cholesterol in virus entry and infection," *Journal of Virology*, vol. 77, no. 23, pp. 12543–12551, 2003.

[131] S. Biswas, S. R. Yin, P. S. Blank, and J. Zimmerberg, "Cholesterol promotes hemifusion and pore widening in membrane fusion induced by influenza hemagglutinin," *Journal of General Physiology*, vol. 131, no. 5, pp. 503–513, 2008.

[132] J. Bentz and A. Mittal, "Architecture of the influenza hemagglutinin membrane fusion site," *Biochimica et Biophysica Acta*, vol. 1614, no. 1, pp. 24–35, 2003.

Hindawi Publishing Corporation
Advances in Virology
Volume 2011, Article ID 343408, 11 pages
doi:10.1155/2011/343408

Research Article

Requirements for Human Respiratory Syncytial Virus Glycoproteins in Assembly and Egress from Infected Cells

Melissa Batonick and Gail W. Wertz

Department of Pathology, University of Virginia, MR5 Building, P.O. Box 800904, Charlottesville, VA 22908-0904, USA

Correspondence should be addressed to Gail W. Wertz, gww4f@virginia.edu

Received 27 March 2011; Accepted 16 May 2011

Academic Editor: Anthony P. Schmitt

Human respiratory syncytial virus (HRSV) is an enveloped RNA virus that assembles and buds from the plasma membrane of infected cells. The ribonucleoprotein complex (RNP) must associate with the viral matrix protein and glycoproteins to form newly infectious particles prior to budding. The viral proteins involved in HRSV assembly and egress are mostly unexplored. We investigated whether the glycoproteins of HRSV were involved in the late stages of viral replication by utilizing recombinant viruses where each individual glycoprotein gene was deleted and replaced with a reporter gene to maintain wild-type levels of gene expression. These engineered viruses allowed us to study the roles of the glycoproteins in assembly and budding in the context of infectious virus. Microscopy data showed that the F glycoprotein was involved in the localization of the glycoproteins with the other viral proteins at the plasma membrane. Biochemical analyses showed that deletion of the F and G proteins affected incorporation of the other viral proteins into budded virions. However, efficient viral release was unaffected by the deletion of any of the glycoproteins individually or in concert. These studies attribute a novel role to the F and G proteins in viral protein localization and assembly.

1. Introduction

Human respiratory syncytial virus (HRSV) is the leading viral cause of serious pediatric respiratory tract disease worldwide and a common cause of morbidity in the elderly [1, 2]. Currently there is no vaccine available and the only treatment is a monoclonal antibody given to high-risk infants [3]. Research into vaccine development and therapeutic design is ongoing but an obvious hurdle is the lack of a complete understanding of the replication cycle. The role of the individual viral gene products in each step of virus replication, particularly in the assembly and release of viral particles, is unclear.

HRSV, a member of the *Paramyxoviridae* family, has a negative-sense, single-stranded RNA genome of 15,222 nucleotides. The genome contains ten genes encoding eleven known gene products. The viral ribonucleoprotein (RNP) consists of the RNA genome encapsidated by the nucleoprotein (N), having associated the phosphoprotein (P) and RNA-dependent RNA polymerase (L) [4, 5] as well as the M2-1 protein, which is involved in transcription processivity [6]. The viral genome also encodes the structural matrix protein (M) [7] and three transmembrane glycoproteins that are presented on the surface of the viral particle, the small hydrophobic glycoprotein (SH) [8], the attachment glycoprotein (G) [9], and the fusion glycoprotein (F) [10]. The major identified function for the glycoproteins is in viral entry. The F protein is required for fusion between the cellular and viral membranes [11], thus allowing the viral genome to enter the host cell cytoplasm. The G protein is involved in host cell attachment [12] and is necessary for infectivity *in vivo* and in some cultured cell types while in others its deletion has no effect on infectivity [13]. The role of the SH protein is still unclear, although it has recently been found to inhibit apoptosis [14, 15]. The viral glycoproteins along with the M, N, P, L, and M2 proteins are essential structural and enzymatic components of HRSV. How these viral components assemble to form a newly infectious virion and how the release of the virus from the host cell is coordinated is largely unknown.

HRSV assembles at and buds from the plasma membrane of the infected cell to gain its envelope [16–18]. For many paramyxoviruses, it has been shown that the M protein is sufficient for particle release, and in some cases the F glycoprotein has been shown to enhance the process [19–24]. In other instances, such as for SV5, viral budding requires the M protein, one of its two viral glycoproteins, and the N protein [25]. These studies used transient transfection systems to additively express individual viral proteins and analyzed their effects on the amount of released virus-like particles (VLPs). A similar study done with HRSV found the M, P, N, and F proteins to be the minimal requirements for formation and passage of VLPs containing minigenomes [26]. However, this study did not look specifically at the release of the VLPs; therefore it is still unclear whether the F protein is needed only for viral entry or for entry and subsequent steps leading to VLP passage.

Previously, we examined the effect of HRSV glycoprotein deletions on the directional targeting of the virus in polarized epithelial cells [27]. This earlier study was a qualitative investigation which demonstrated that HRSV particles are able to bud directionally in the absence of all three glycoproteins. However, a quantitative analysis of the contribution of these viral proteins to the late stages of viral protein trafficking, assembly, and release was not done. In the present study, the role of the three viral glycoproteins in viral assembly and egress from infected cells was examined. First, the contribution of each glycoprotein to viral assembly was analyzed by investigating the localization of the remaining viral structural proteins at the plasma membrane by confocal microscopy. Next, the protein composition of particles released from cells infected with WT or glycoprotein deleted HRSV was biochemically quantitated to determine if one or more glycoproteins are involved in the incorporation of viral proteins into newly formed viral particles. Finally, the effect of each glycoprotein on the efficiency of virus particle budding from infected cells was analyzed.

2. Results

2.1. Engineered Viruses. To examine the involvement of each glycoprotein in the assembly and release of HRSV, we used viruses previously engineered to have each glycoprotein gene deleted individually from the HRSV genome and its ORF replaced with that of a reporter gene (Figure 1) [27]. We also utilized an engineered virus with all three glycoprotein genes deleted [27]. Since HRSV transcription is obligatorily sequential and due to attenuation at each gene junction, the replacement of any deleted genes was necessary to maintain authentic levels of viral gene expression. Briefly, in the case of individual deletions, GFP was used to replace the deleted gene. When three genes, SH, G, and F, were deleted they were replaced respectively with the GFP, CAT, and GUS, reporter genes (Figure 1). All of the viruses described above not only maintained the same number of genes as in WT HRSV but also had the genuine intergenic junctions to preserve authentic transcription levels.

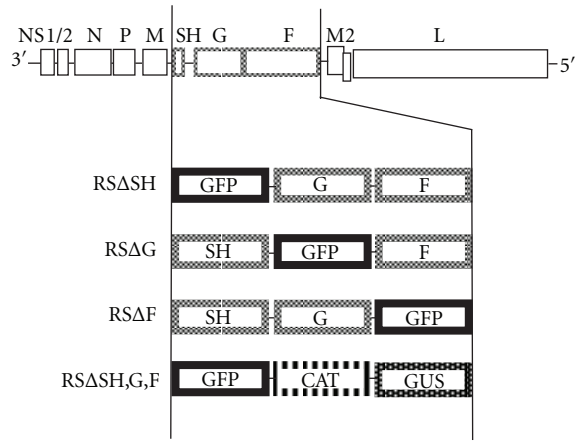

Figure 1: Schematic of the gene content of engineered viruses. All engineered viruses were generated from a cDNA of the A2 strain of HRSV. Viruses RSΔSH, RSΔG, and RSΔF are missing the ORFs of the SH, G, and F genes, respectively, which have been substituted with that of GFP. Virus RSΔSH,G,F has the ORFs encoding each of the three HSRV glycoproteins replaced with those of reporter genes GFP, CAT, and GUS, respectively.

2.2. Effect of Single Glycoprotein Deletions on the Intracellular Localization of HRSV Proteins at the Site of Viral Assembly. The HRSV proteins must assemble at the plasma membrane to initiate budding of the RNP to form newly enveloped and infectious viral particles upon release from the cell. In polarized epithelial cells, this process takes place on the apical membrane [18]. We previously demonstrated that the glycoproteins are not involved in the directional targeting of the viral proteins for viral release from the apical membrane to occur [27]. However, the techniques used in this prior study did not analyze the effects of individual glycoprotein gene deletions on intracellular assembly with other viral proteins. To address this question, the level of colocalization at the plasma membrane of each of the three glycoproteins with the N protein, which was used as a marker for ribonucleocapsids, was analyzed by microscopy.

A549 cells were infected with WT or individual glycoprotein deleted viruses at a MOI of 0.2. Twenty-four hours after infection the cells were fixed, permeabilized, and incubated with primary antibodies against N, and SH, or G, or F proteins in turn and followed by secondary antibodies conjugated to AlexaFluor 647 and 594 fluorescent dyes. A confocal microscope was used to take multiple z plane images (z-stacks) through the cell as described in Section 4. Since viral assembly takes place at the plasma membrane we focused on the z-stack containing that section of the infected cell, which is shown in all images and is depicted in the diagram in Figure 2(a). In Figures 2(b), 2(c), and 2(d) the N protein is shown in green with the three glycoproteins, in individual panels, shown in red (F and N staining is shown in Figure 2(b), G and N staining is shown in Figure 2(c), and SH and N staining is shown in Figure 2(d)). A merge panel of the two stained proteins is also shown along with a magnification of the merge to further demonstrate the colocalization in each image. Also shown within each merge

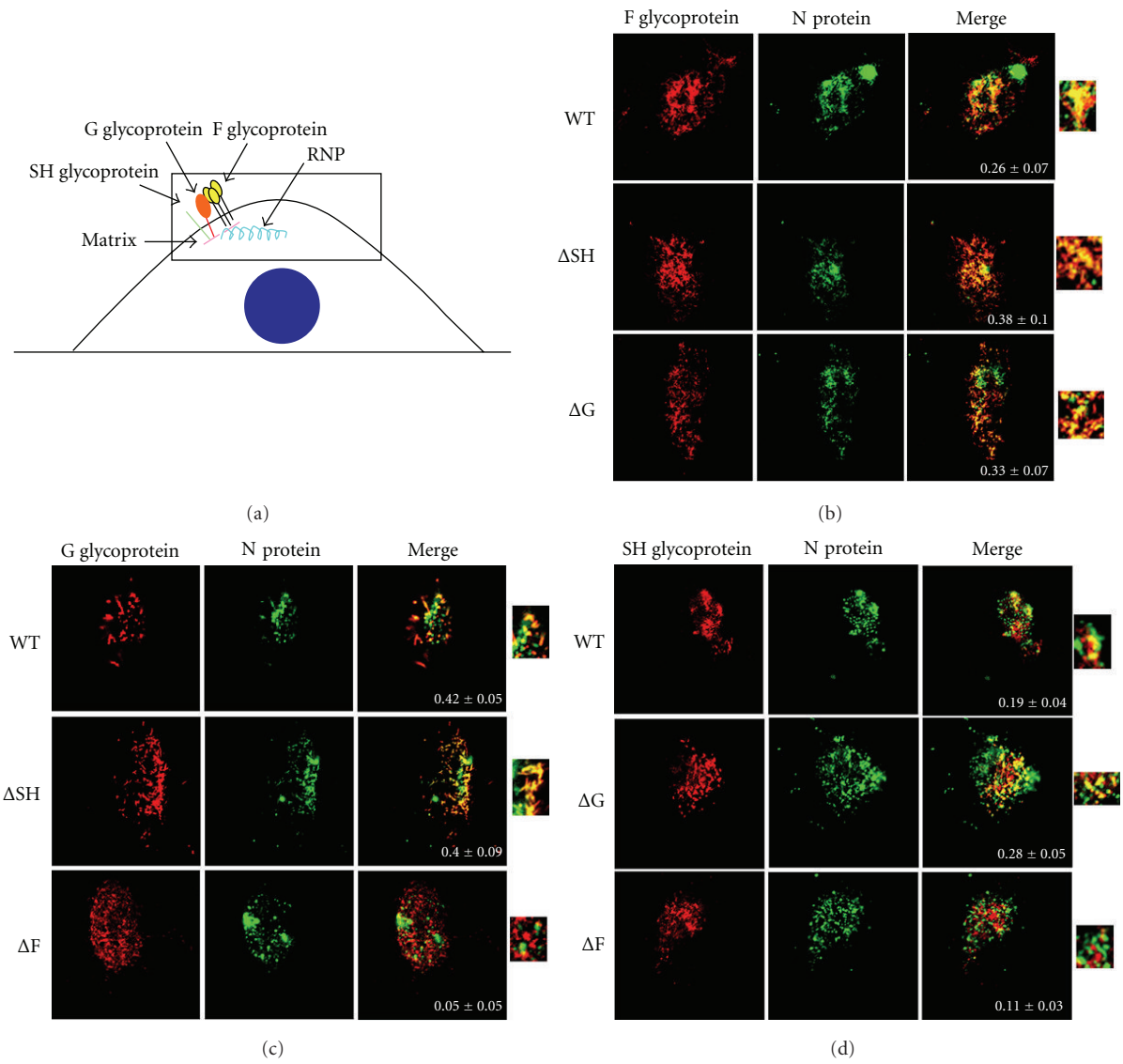

Figure 2: Effect of the deletion of individual glycoprotein genes on colocalization of the HRSV nucleocapsid protein with each glycoprotein at the plasma membrane. (a) A diagram of an infected cell depicting HRSV assembly at the plasma membrane. The boxed area represents the 1 μm z-stack shown in subsequent confocal microscope images. The nucleus is depicted as a blue circle. A549 cells infected with WT or glycoprotein deleted HRSV at a MOI of 0.2 were fixed, permeabilized, and incubated with an anti-N antibody and an anti-F antibody (b), an anti-G antibody (c), or an anti-SH antibody (d). The glycoprotein stains are shown in the left row (red), the N protein stains in the middle row (green), and a merge of the two stains in the right row. A blowup of the merge is also shown. Images were taken on a Zeiss confocal microscope. An average of fourteen cells were imaged per staining, and colocalization was measured using ImageJ JACoP plugin. Pearson's coefficient ± standard error of mean is shown within the merge panels.

panel is the amount of colocalization quantitated by NIH ImageJ software [28] and is depicted as Pearson's coefficient [29], where a number near +1 suggests perfect correlation between two biomolecules, a number near 0 indicates no correlation, and a number near −1 suggests an inverse correlation or exclusion of the biomolecules.

An average of fourteen cells were imaged per staining, and their average Pearson's coefficient was quantitated along with the standard error of the mean (SEM). As shown in Figure 2(b), similar levels of colocalization were observed between the N and F proteins in cells infected with WT, ΔSH, and ΔG viruses (Pearson's coefficients of 0.26, 0.38, and 0.33, resp.) suggesting that the SH and G proteins are not necessary for the assembly of the remaining glycoproteins and the RNPs at the cell surface. In Figure 2(c) similar amounts of colocalization between the N and G proteins were observed in cells infected with WT and ΔSH viruses (Pearson's coefficient of 0.42 and 0.40, resp.) whereas a ninefold decrease in colocalization between the N and G proteins was observed in cells infected with ΔF virus (Pearson's coefficient of 0.05). This indicated that F is involved in the colocalization of the N and G proteins at the cell surface. In addition,

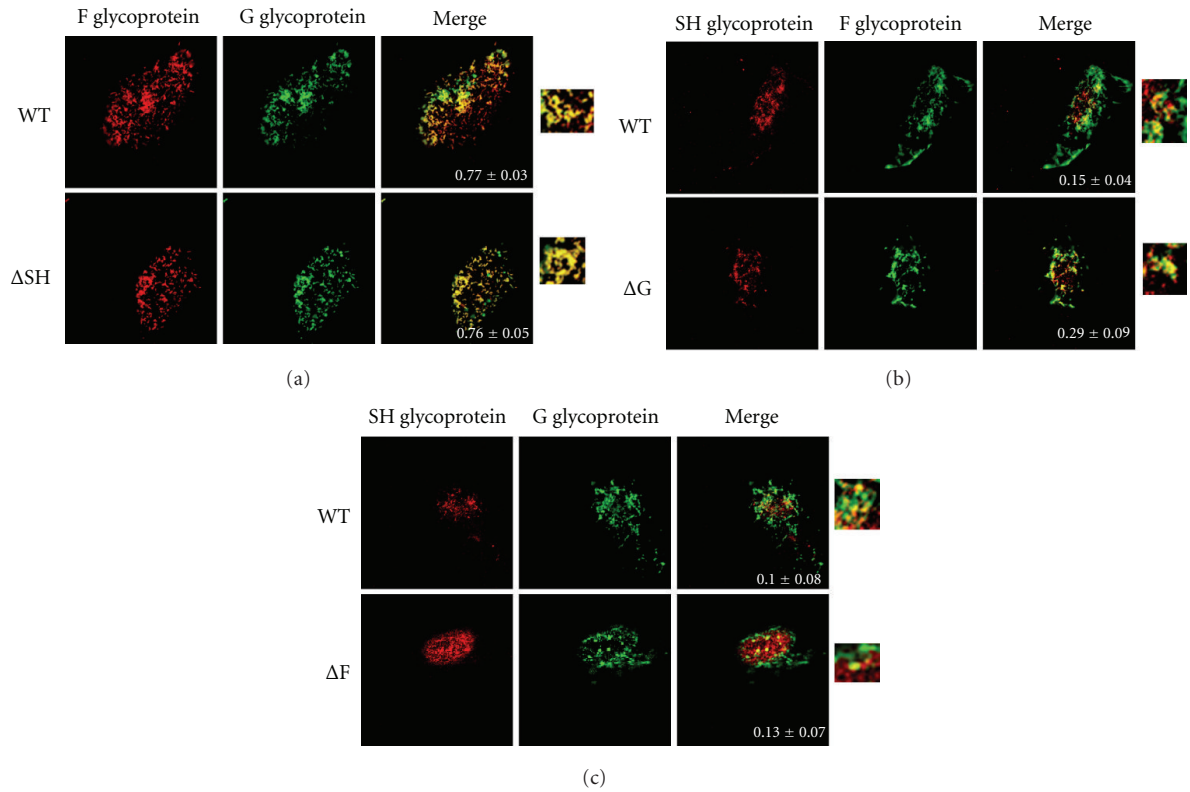

Figure 3: Effect of the deletion of individual glycoprotein genes on the colocalization of pairs of HRSV glycoproteins at the plasma membrane. Localization of HRSV glycoproteins at the site of viral assembly by confocal microscopy. A549 cells infected with WT or glycoprotein deleted HRSV as indicated at a MOI 0.2 were fixed, permeabilized, and incubated with primary antibodies against two different glycoproteins. (a) Staining of F and G glycoproteins where F is shown in red and G in green. (b) Staining of SH and F where SH is shown in red and F in green. (c) Staining of SH and G where SH is shown in red and G in green. A merge of the two stains is shown in the right row. A blowup of the merge is also shown. Images were taken on a Zeiss confocal microscope. An average of twelve cells were imaged per staining, and colocalization was measured using ImageJ and JACoP plugin. Pearson's coefficient ± standard error of mean is shown within the merge panels.

the distribution of the G protein at the plasma membrane differed in cells infected with ΔF virus as compared to cells infected with WT or ΔSH viruses. In the absence of the F glycoprotein, G protein had a more monodisperse distribution rather than the filamentous forms seen in WT-infected cells (cf. Figure 2(c), cells infected with WT virus and ΔF virus). Colocalization was observed between the N and SH proteins in cells infected with WT virus, albeit at a relatively low level (Figure 2(d); Pearson's coefficient of 0.19). A slightly increased but similarly low level of colocalization between the N and SH proteins was seen in cells infected with ΔG virus (Pearson's coefficient of 0.28). In cells infected with the ΔF virus, however, colocalization was seen at approximately half of WT levels (Pearson's coefficient of 0.11). Thus, the above results show that the absence of the F protein affects the colocalization of the G protein with the N protein at the plasma membrane and, to a lesser extent, that the absence of the F protein affects the colocalization of the SH protein with the N protein at the plasma membrane.

Next, we examined the effect of deletions of individual glycoproteins on the levels of colocalization between the remaining two glycoproteins at the plasma membrane by microscopy. A549 cells infected with WT or engineered viruses were fixed and permeabilized and then incubated with primary antibodies against two of the glycoproteins. In Figure 3(a), the F glycoprotein is shown in red and the G protein is shown in green. In Figures 3(b) and 3(c), the SH glycoprotein is shown in red while the F and G proteins are shown in green, respectively. In each case a merge panel of the two proteins is also shown along with a magnification of the merge to further illustrate the extent of colocalization in each image. Also shown within the merge panel is the amount of colocalization depicted as Pearson's coefficient as described for Figure 2. An average of twelve cells were imaged per staining, and their colocalization is shown along with the standard error of the mean (SEM).

High levels of colocalization were observed between the F and G glycoproteins in cells infected with WT virus (Figure 3(a); Pearson's coefficient of 0.77), and deletion of the SH gene did not affect F and G protein colocalization (Figure 3(a); Pearson's coefficient of 0.76). Colocalization between the SH and F proteins in WT- or ΔG-infected cells was observed at relatively low levels (Pearson's coefficient of

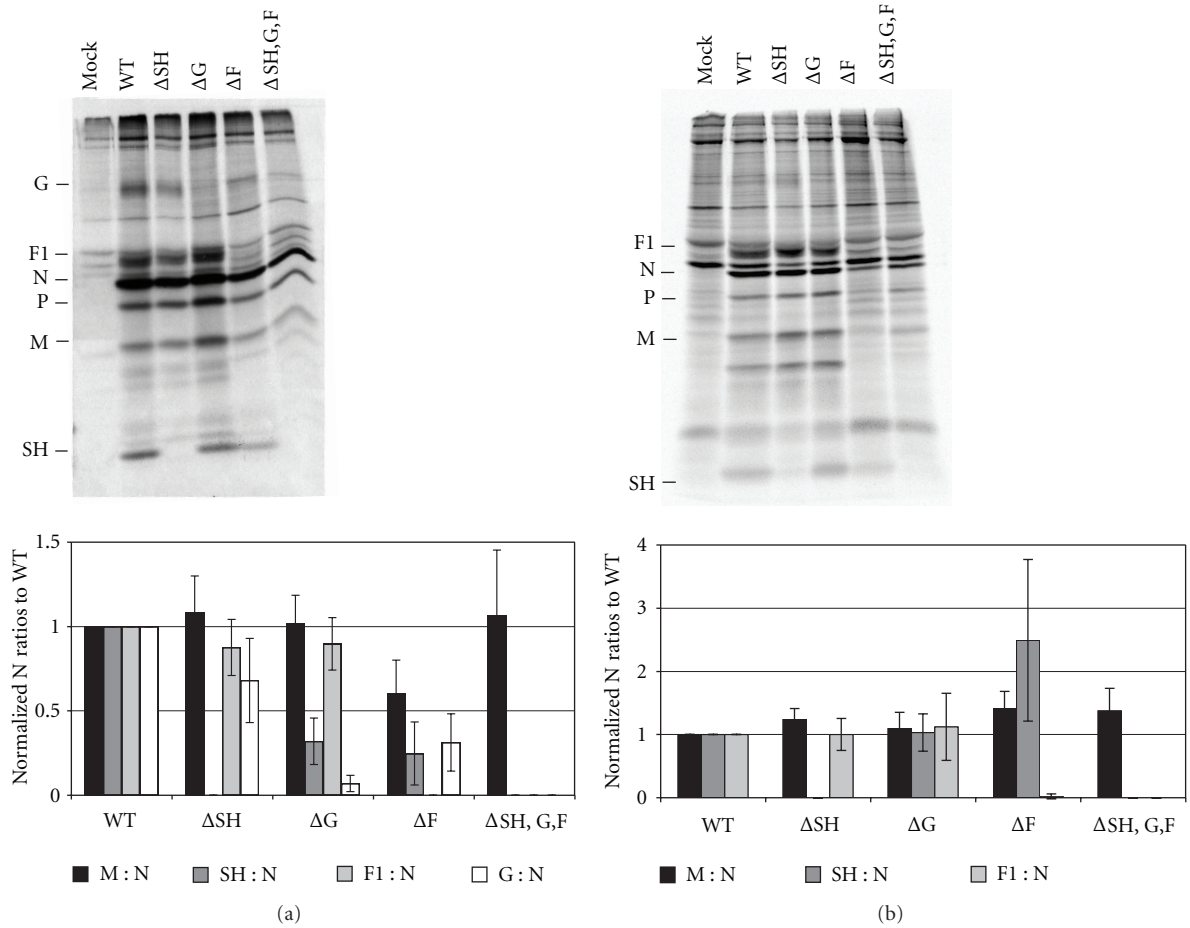

Figure 4: Effect of deletion of glycoprotein genes on the incorporation of HRSV proteins into released viral particles. Twenty-four hours after infection, A549 cells infected with WT or glycoprotein deleted HRSV at a MOI of 1.0 were radiolabeled with ^{35}S Cys/Met for 16 h. The supernatant containing the released viral particles was collected, cleared of cell debris, and concentrated by centrifugation. (a) The viral pellet was resuspended, and viral proteins were immunoprecipitated with a polyclonal anti-HRSV antibody along with monoclonal antibodies against G and SH. Proteins were analyzed by electrophoresis on a 12% SDS polyacrylamide gel. A representative gel is shown. The bar graph depicts ratios of each HRSV structural protein to N protein, normalized to the ratios found in WT viral particles. (b) Infected cells were lysed and viral proteins were immunoprecipitated with a polyclonal anti-HRSV antibody along with antibodies against G and SH. Proteins were analyzed on a 12% SDS-PAGE. A representative gel is shown. The bar graph depicts ratios of each HRSV structural protein to N protein, normalized to the ratios found in WT-infected lysate. Proteins were quantitated on a phosphorImager. Error bars represent standard deviation from at least three experiments.

0.15 and 0.29, resp.; Figure 3(b)). Low amounts of colocalization were also observed between the SH and G proteins in WT- and in ΔF-infected cells (Pearson's coefficient of 0.10 and 0.13, resp.; Figure 3(c)). Taken together these data indicate that deletion of any single glycoprotein did not affect the localization of the other two glycoproteins. Further, these data show the F and G glycoproteins colocalize substantially; however, SH does not colocalize with either F or G proteins to a high degree.

2.3. Effect of HRSV Glycoprotein Deletions on the Incorporation of Viral Proteins into Newly Budded Virions. To further scrutinize a potential role for HRSV glycoproteins in the late stages of the viral replication cycle, released particles were biochemically analyzed for their viral protein composition. A549 cells were infected with WT or glycoprotein deleted HRSV at a MOI of 1.0. Twenty-four hours after infection the cells were radiolabeled with ^{35}S Cys/Met for 16 h. The supernatant containing the released virions was collected and concentrated by centrifugation. The viral proteins present in the pelleted virions were analyzed by immunoprecipitation followed by SDS polyacrylamide gel electrophoresis as described in Section 4. The ratio of the HRSV structural proteins, M, F, G, and SH relative to the N protein was determined. The ratios found in glycoprotein deleted viral particles were compared to those found in WT viral particles (Figure 4(a)). The F glycoprotein is translated as the precursor protein F0 and then cleaved into F1 and F2. The cleaved product F1 was labeled most efficiently by ^{35}S Cys/Met, and so we quantified this protein to represent F. As shown in Figure 4(a) when cells were infected with the ΔSH virus no substantial differences in the incorporation of

the M, G, or F proteins into viral particles were observed when compared to WT particles. Cells infected with the ΔG virus had WT-like levels of the M and F proteins in released virions; however, the amount of SH protein incorporation was decreased to approximately 40% of that found in WT viral particles. Virus released from ΔF-infected A549 cells had slightly decreased levels of the M protein, at 70% of that found in WT virus. The most dramatic differences in particles released from ΔF-infected cells were observed in the amounts of incorporated SH and G proteins, which were reduced to 25% and 30% of WT levels, respectively. Cells infected with the ΔSH,G,F virus had WT-like amounts of M protein incorporation.

Although all engineered viruses containing glycoprotein deletions had replacement reporter genes to ensure WT levels of transcription of the downstream genes [30], viral protein levels in cells infected with the engineered viruses were also analyzed to determine whether the levels of protein synthesis were affected by the deletion of the glycoproteins. To confirm that the protein incorporation defects observed in budded viral particles were not due to decreased amounts of those viral proteins in infected cells, the HRSV structural proteins in infected cell lysates were also quantitated and reported as a ratio to the N protein. As shown in Figure 4(b), the ratios of the M, SH, and F proteins to the N protein in cell lysates infected with glycoprotein deleted viruses were equivalent to or greater than those found in WT-virus-infected cell lysate. These data indicated that the effect of G and F glycoprotein deletions on decreased SH incorporation into particles was not due to overall reduction in SH protein synthesis.

We used A549 cells in these studies because infectivity experiments performed in different cell types showed that the ΔF virus, which utilizes GP64 for viral entry [31] did not give a productive infection in HEp2 cells (see supplementary Figure 1(a) in Supplementary Material available online at doi: 10.1155/2011/343408). We found that A549 cells allowed for more robust infection of ΔF viruses than HEp2 and Vbac cells [32] (supplementary Figure 1(a)). In contrast, the ΔSH virus had equivalent levels of infection in all cell types tested (supplementary Figure 1(b)). However, in A549 cells the quantitative detection of a discrete band of a mature 84 kD G protein even in WT-infected cell lysates was difficult. We suspect, in A549 cells, that the heterodisperse nature of the extensive O-linked glycosylation and the low methionine content of G protein prevent detection of a discrete band. However, previous work showed that gene transcription levels were not altered in the glycoprotein deleted viruses [30], and we know from the microscopy data in this study that the amount of the G protein stainings in WT- and in ΔF-infected A549 cells were comparable (Figures 2(c) and 3(c)). As such, although we were unable to confirm equivalent G-to-N-protein ratios in cell lysates infected with glycoprotein deleted viruses as compared to WT-infected cell lysates (Figure 4(b)), data strongly suggests that the G protein synthesis was unaffected by the deletion of the F glycoprotein.

2.4. Involvement of HRSV Glycoproteins in Viral Release. Since we observed a role for the glycoproteins in viral assembly, we asked if they were also involved in the other late stage of the replication cycle, viral release. We knew from our previous work that the glycoproteins were not required for viral release [27], but those studies had not quantitatively examined the effect of glycoprotein deletions on the efficiency of viral budding. To address this question, we infected A549 cells with either WT or glycoprotein deleted virus and quantified the amount of particles released as a percent of total virus produced in cells. In infected cells the N protein will either associate with the viral genome to form RNPs and localize to the plasma membrane for viral assembly or remain in the cytoplasm as a soluble protein. To quantify HRSV production and viral release, we only considered the N protein bound to RNPs since this is the form that assembles into viral particles and buds from the plasma membrane. Therefore our first step was to separate N protein in RNPs from free soluble N protein in infected cell lysates as a measure of virus inside the cell. Infected A549 cells were radiolabeled with ^{35}S Cys/Met and lysed as described in Section 4. The lysate was layered on top of a 40% glycerol cushion and ultracentrifuged as described in Section 4. Fractions were taken from the top of the tube (fraction 1) to the bottom of the tube (fraction 4), and the pellet was resuspended in lysis buffer. HRSV proteins in each fraction were identified by immunoprecipitation followed by analysis on 12% SDS polyacrylamide gel as described in Section 4. As shown in Figure 5(a), soluble proteins such as G, F1, N, P, M, and SH were found in fractions 1–4 whereas predominantly proteins bound to the viral genome, L, N, P, and M2-1, were found in the pellet.

To quantify the amount of virus released from infected cells, A549 cells were infected with WT or glycoprotein deleted viruses at a MOI of 1.0. Twenty-four hours after infection the cells were radiolabeled with ^{35}S Cys/Met. Supernatants containing released virions were collected and concentrated by centrifugation, as described previously in [27] and in Section 4. Pelleted virions were disrupted and HRSV proteins were identified by immunoprecipitation followed by analysis by polyacrylamide gel electrophoresis. The infected cells were also lysed and RNPs separated by glycerol sedimentation as described above. The RNP bound N protein present in pelleted virions and in infected cell lysates was analyzed on SDS gels and quantitated. The amount of N protein present in released virus is shown as a percent of total N protein in RNPs quantified from both lysate and virus (Figures 5(b) and 5(c)). Cells infected with ΔSH, ΔG, ΔF viruses, or the triple deletion virus ΔSH,G,F, did not show any decrease in the levels of released viral particles compared with cells infected with WT virus. These findings show that the viral glycoproteins do not negatively affect the efficiency of viral egress.

3. Discussion

The major HRSV structural proteins are the nucleocapsid protein (N), the matrix (M) protein, and the F, G, and SH glycoproteins, all of which associate at the plasma membrane for viral assembly and release. Little is known about the protein requirements of HRSV during the late

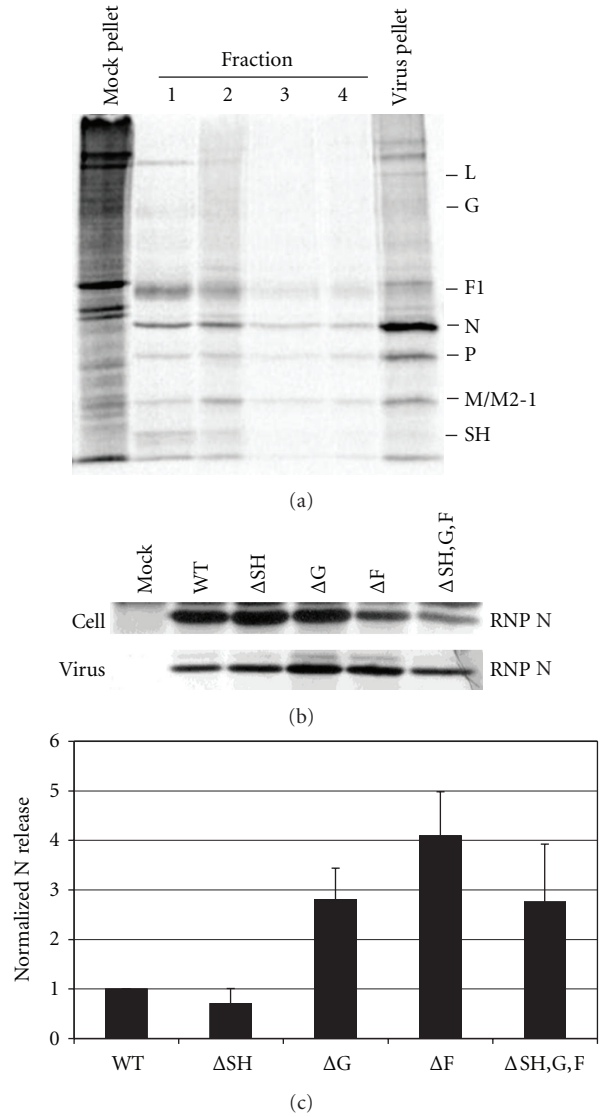

Figure 5: Effect of glycoprotein deletions on the release of virions from infected A549 cells. A549 cells were infected with WT or glycoprotein deleted virus and particles released into the supernatant were quantified as a percent of total virus produced. The N protein in isolated RNPs was used to quantitate the virus in cell lysates and in virions. (a) Separation of RNPs containing the viral genome and associated proteins from soluble proteins in infected cell lysates. Infected cell lysates were ultracentrifuged through a 40% glycerol cushion. Fractions were taken from the top of the tube (fraction 1) to the bottom of the tube (fraction 4) in 0.5 mL volumes. The pellet was resuspended in 0.1 mL lysis buffer. Viral proteins in each fraction and the pellet were immunoprecipitated and analyzed on a 12% SDS polyacrylamide gel. A representative gel is shown. HRSV proteins are indicated on the right of the gel. (b) Ribonucleoprotein (RNP) associated N protein in infected cell lysates was harvested as described above and in Section 4, and viral proteins were analyzed by immunoprecipitation and electrophoresis on 12% SDS gels. Released virions were recovered from supernatant fluids by centrifugation and viral proteins were analyzed by immunoprecipitation and electrophoresis on 12% SDS gels. A representative gel is shown. (c) Bar graph depicts the percent of N protein quantified in released virus from total RNP-associated N protein quantified in infected cell lysate and in released virus. The N protein was quantitated by phosphoimage analysis. Error bars represent standard deviation from at least three experiments.

stage of virus replication. It has been established for many paramyxoviruses that the M protein is necessary for the formation of viral particles [19–25], but the involvement of the glycoproteins varies depending upon the virus. The HRSV glycoproteins have defined roles in attachment and entry, but delineating their potential roles in the downstream steps of the replication cycle is difficult due to the necessity of the F protein for viral entry into cells.

In this study we utilized genetically engineered HRSV in which one or more of the glycoprotein genes were deleted and replaced with reporter genes (Figure 1). Recombinant viruses lacking the F protein were used in conjunction with a cell line that expresses GP64 to overcome the inherent viral entry deficit of a F deleted virus [32]. In a previous study using these engineered viruses we showed that HRSV with all three glycoprotein genes deleted released viral particles

specifically from the apical membrane of polarized epithelial cells [27], which confirmed that the glycoproteins were not essential for directional targeting or for viral release. However, we did not address whether the glycoproteins affected the quantitative efficiency of viral egress or whether the glycoproteins were involved in the assembly of the other viral proteins at the plasma membrane to form newly infectious viral particles.

Prior to viral budding from infected cells, the three HRSV glycoproteins must assemble with the RNPs at the plasma membrane. To determine if the individual glycoproteins are involved in the assembly of the other structural proteins, we studied cells infected with viruses having individual glycoprotein genes deleted and examined the colocalization of the remaining glycoproteins at the plasma membrane by confocal microscopy. We observed that the deletion of any individual glycoprotein did not affect the colocalization of the remaining glycoproteins at the cell surface (Figure 3). Using the N protein as a marker for RNPs, we also investigated whether deletion of the individual glycoproteins affected the assembly of the remaining glycoproteins and the N protein at the plasma membrane. We found that deletion of the F glycoprotein substantially reduced the colocalization of the G protein with the N protein at the plasma membrane. Deletion of the F protein also reduced colocalization between the SH and N proteins at the cell surface (Figures 2(c) and 2(d), resp.). These data indicate that F protein plays a previously unidentified role in localizing virus structural proteins during HRSV assembly. Interestingly, we also observed in ΔF-virus-infected cells that the staining pattern of G protein on the plasma membrane was altered as compared to WT-virus-infected cells (Figure 2(c), compare G staining in WT-infected cell with that in ΔF-infected cell). These findings are consistent with results from a previous study which showed that the G glycoprotein localized to viral filaments at the plasma membrane in cells infected with WT virus, but not in cells infected with an engineered HRSV with the cytoplasmic tail of F protein deleted (FΔCT) [33], further suggesting that the F protein is involved in protein sorting at the cell surface.

Once the viral proteins have assembled at the cell surface, they are incorporated into newly formed virus particles as RNPs bud from the plasma membrane. We analyzed whether deletion of each individual glycoprotein affected the ability of the remaining structural proteins to incorporate into budded virions. We found that cells infected with viruses lacking the F glycoprotein incorporated decreased amounts of the G and SH proteins relative to the N protein in released virus (Figure 4(a)). These findings are in agreement with the previous observation that the deletion of the F protein resulted in decreased amounts of colocalization between RNPs and both the G and SH proteins at the cell surface (Figures 2(c) and 2(d), resp.). Cells infected with viruses lacking the G protein also incorporated lower amounts of the SH protein into released virions (Figure 4(a)). These results indicate that the F and G glycoproteins are involved in HRSV particle assembly.

We used two approaches, microscopy and protein biochemistry, to investigate the effect of the glycoprotein deletions on viral assembly. These two methods further dissected the assembly process into two separate steps: the accumulation of viral proteins at the plasma membrane, which is the site of viral assembly, and the incorporation of the accumulating proteins into budding viral particles. Both experiments concluded that SH is not involved in either stage of viral assembly as WT-like levels of colocalization were observed between the remaining structural proteins at the plasma membrane of ΔSH-infected cells, and WT-like levels of HRSV proteins were found in released particles. Both the microscopy and the biochemical data indicated that F glycoprotein is involved in both steps of the assembly process as colocalization between the N and SH proteins and between the N and G proteins in ΔF-infected cells was decreased as compared to WT-infected cells. Cells infected with ΔF virus also had decreased amounts of the G and SH proteins incorporated into budded virions as compared to WT particles. The G glycoprotein does not appear to be implicated in the accumulation of viral proteins at the plasma membrane since WT and elevated levels of colocalization were observed between the N, SH, and F proteins in cells infected with ΔG virus. However, the G protein was involved in the incorporation of the SH protein into the budding virion as shown by a decrease in the SH-to-N-protein ratio in particles released from ΔG-infected cells as compared to WT virions. The reasons for this dichotomy are unknown. The SH protein exists in several modified and unmodified forms including its modification by polylactosaminoglycans, and these forms as well as the unmodified form are found in virions [34]. It would be of interest to determine whether there may be interactions between one or more of the modified forms of SH and the highly O glycosylated G protein. The M protein was incorporated at near WT-like levels in all glycoprotein deleted viruses, including the triple deleted virus, indicating that the M protein assembles into budding virus independently of the glycoproteins.

The final step to produce new viral particles after the viral proteins have assembled at the plasma membrane is egress from infected cells. To determine if the viral glycoproteins were involved in the budding process, we analyzed whether deletion of the glycoproteins affected the efficiency of viral release. We found that the absence of any or all of the three glycoproteins did not have a deleterious effect on the amount of virus released from infected cells (Figure 5). Indeed, ΔF- and ΔG-infected cells released slightly increased amounts of viral particles into the supernatant as compared to WT infected cells. We speculate that fewer glycosylated proteins in the virus led to less reattachment of viral particles to the cell. This resulted in fewer cell-associated virions and hence an increase in released viral particles in the supernatant.

Previous studies have shown an interaction between the SH and G proteins in cells infected with WT HRSV [35] which may explain the requirement for the G protein in the incorporation of the SH protein into budding virus. Interactions have also been shown for the G and M proteins [36] and for the G and F proteins [37]. An oligomeric complex was also reported in infected cell lysates between the F, G, and SH proteins [38]. It has been hypothesized that the F glycoprotein interacts with other viral proteins via its cytoplasmic tail (CT), based on a study which showed

that the ability of the F protein to interact with lipid rafts at the plasma membrane was disrupted and the localization of the F and the G proteins at the plasma membrane was altered when cells were infected with FΔCT virus [33]. These previous studies along with the data presented here indicate that the three HRSV glycoproteins interact with other viral structural proteins in infected cells, and, importantly, this study attributes a novel role to the F and G glycoproteins in the late stages of viral replication.

4. Materials and Methods

4.1. Cells and Antibodies. A549, Vero, and HEp2 cells were acquired from the American Type Culture Collection (ATCC). A549 cells were grown in Ham's F12K medium (Sigma Aldrich, St. Louis, Mo) containing 10% fetal bovine serum, and Vero and HEp2 cells were grown in Dulbecco's minimal essential medium (DMEM; Invitrogen, Carlsbad, Calif) containing 5% fetal bovine serum. Vbac cells (Vero cells expressing the baculovirus GP64 protein carrying the HRSV F protein COOH-terminal residues 563 to 573) were described previously in [32]. Monoclonal antibodies (MAbs) 19 and 29 were provided by Geraldine Taylor (Institute for Animal Health, Compton, UK), as was the bovine polyclonal antibody against all HRSV proteins, R45. The monoclonal antibody, mAb15, was provided by James Stott (Institute for Animal Health, Compton, UK). Rabbit anti-SH antibody was provided by Biao He (University of Georgia). AlexaFluor-conjugated secondary antibodies were from Molecular Probes (Carlsbad, Calif).

4.2. Construction of cDNAs and Recovery of Infectious HRSVs. All cDNAs were constructed from the HRSV A2 strain. cDNAs engineered to contain glycoprotein gene deletions for these studies were constructed as described previously in [27, 30, 33]. Briefly, using standard cloning techniques, vectors were constructed lacking the G or F transmembrane glycoprotein open reading frame (ORF) and containing the EGFP ORF instead, as shown in Figure 1. All HRSV ORFs were maintained in their original genome positions to maintain expression profiles similar to that of a wild-type virus. For generation of the recombinant wild-type (WT) virus, the vector contained the authentic SH, G, and F ORFs and no marker protein ORF. The ORFs contained in each of the vectors were separated by authentic HRSV intergenic junctions and flanked by unique restriction sites *Fse*I and *Asc*I. Using matching *Fse*I and *Asc*I restriction sites, the vectors were then cloned into an SH/G/F-deleted cDNA backbone. The engineered cDNAs were screened by restriction enzyme analysis, and all modified areas were verified by nucleotide sequencing prior to virus recovery.

Infectious viruses were recovered from cDNA as described previously in [31]. Notably, to relieve selection pressure that might result from the effect of gene replacements, a plasmid encoding a chimeric VSV G protein was included in the initial transfection, and Vbac cells were used for virus amplification. Viral RNAs were harvested from cells infected with the engineered viruses at passage 3, amplified by RT-PCR, and the sequence of selected areas was verified by bulk nucleotide sequence analysis. No changes were found. Virus stocks at passages 3 to 5 were used for the experiments described.

4.3. Virus Infections. Infections of cells by HRSV were carried out by adsorbing virus to cells for 1.5 h at 33°C, followed by removing the inoculum and washing the cells once with growth media and then continuing incubation at 33°C for 24 h or 48 h, depending on the assay.

4.4. Immunofluorescence Staining and Confocal Microscopy. A549 cells were plated on sterile coverslips in 6-well plates (BD biosciences, San Jose, Calif). Cells were then infected with engineered viruses at a MOI of 0.2 and further incubated at 33°C. Twenty-four hours after infection, cells were washed twice with PBS and fixed with 3.7% paraformaldehyde (PFA) in phosphate-buffered saline (PBS) for 15 min at room temperature (RT). Cells were washed twice with PBS, permeabilized with 0.02% triton X-100, blocked in 1% BSA for 10 min, and stained with the following primary antibodies diluted in 0.1% BSA: F mAb19 at 1 : 5000; G mAb29 at 1 : 2000; N mAb15 at 1 : 15000; rabbit anti-SH at 1 : 200 for 1 h at RT. Cells were washed twice with PBS, blocked with 1% BSA, and incubated with secondary antimouse or antirabbit antibodies conjugated to AlexaFluor 594 or 647 (Invitrogen) at a dilution of 1 : 1000 for 30 min at RT. When costaining with primary antibodies from the same host, the Apex labeling kit was used (Invitrogen) to directly conjugate the primary antibody with AlexaFluor 647. Cells were washed twice with PBS and stained with Hoechst stain (Molecular Probes) at 0.05 mg/mL in PBS. Cells were washed three times with PBS, mounted on slides, and stored at 4°C in the dark. Images were taken on a Zeiss LSM 510-UV confocal microscope using the 40x or the 100x objective. 1 μm z-stacks were taken through each cell, and the top plasma membrane stack was taken to visualize the site of HRSV assembly. The plasma membrane containing section was identified as the most apical stack containing in-focus staining and without visible nuclear staining.

The fluorescence in the top plasma membrane stack was quantitated to determine the levels of colocalization between N and each glycoprotein or between two glycoproteins. Quantitation of pixels was done using ImageJ with JACoP plugin [39]. Thresholds for each wavelength were determined on JACop using Costes automatic thresholding [40], and the amount of colocalization of pixels above the threshold was determined and reported as Pearson's coefficient (R) ± standard error of the mean (SEM).

4.5. Viral Assembly and Release Assays. A549 cells were plated in 60 mm dishes (BD biosciences) and incubated at 37°C. Approximately 6 h later, the cells were infected with engineered viruses at a MOI of 1.0 and incubated at 33°C. 24 h later the cells were radiolabeled using ^{35}S Cys/Met trans mix (Promega, Madison, Wis) and incubated at 33°C. 16 h later the supernatants containing the released virions were carefully removed from the cell monolayer and put into

2 mL tubes. The supernatants were centrifuged at 750 ×g for 4 min to pellet any cell debris. The supernatants containing the viral particles were transferred to a new 1.5 mL tube and centrifuged at 1500 ×g for 30 min, a speed that allows for the fragile HRSV particles to be concentrated and still maintain infectivity [27]. We confirmed that this pelleting method concentrated virions with one glycoprotein or two glycoproteins deleted to ensure that particles with decreased density still pelleted at the low speed (data not shown). The viral pellets were resuspended in 0.1 mL lysis buffer consisting of 1% NP40, 0.4% deoxycholic acid, 66 mM EDTA, and 10 mM Tris-HCl, pH 7.4. The entire volume was incubated with the bovine polyclonal antibody R45 at 1 : 100 dilution + rabbit anti-SH antibody at 1 : 25 + anti-G mAb29 at 1 : 100 overnight at 4°C. Meanwhile, the infected cell monolayers were washed once with PBS and then lysed in lysis buffer (described above). The lysates were harvested into 1.5 mL tubes, incubated on ice for 7 min, and vortexed for 30 sec. The cell nuclei were removed by centrifugation at 14,000 rpm for 1 min. The RNP-associated proteins were then pelleted by ultracentrifugation through a 40% glycerol cushion at 190,000 ×g for 2 h at 4°C. The pellets were resuspended in 0.1 mL lysis buffer and incubated with R45 antibody at 1 : 100 dilution overnight at 4°C. The next day 25 μL of Protein G sepharose (GE Healthcare, Piscataway, NJ) was added to each lysate + antibody and released virus + antibody and incubated for at least 1 h at 4°C. The immunoprecipitations were washed 3x with wash buffer consisting of 1% NP-40, 0.5% DOC, 0.1% SDS, 150 mM NaCl, and 10 mM Tris-HCl, pH 7.4, and then boiled for 3 min in 25 μL of 2x reducing Laemmli buffer. All samples were electrophoresed on 12% polyacrylamide gels. The gels were fixed, dried, and exposed to both film and a phosphorImage screen. Protein amounts were quantified from phosphorImage scans on a model 860 STORM scanner and the ImageQuant software (Molecular Dynamics).

Acknowledgments

The authors thank the members of the Wertz laboratory for helpful discussions during the preparation of the paper. Specifically, they thank Deena Jacob for technical assistance in the laboratory and Djamila Harouaka for critical reading of the paper. This work was supported by Public Health Service Grant AI20181 to G. W. Wertz from the NIAID of the National Institutes of Health.

References

[1] A. R. Falsey, "Respiratory syncytial virus infection in older persons," *Vaccine*, vol. 16, no. 18, pp. 1775–1778, 1998.

[2] C. B. Hall, A. E. Kopelman, R. G. Douglas Jr., J. M. Geiman, and M. P. Meagher, "Neonatal respiratory syncytial virus infection," *New England Journal of Medicine*, vol. 300, no. 8, pp. 393–396, 1979.

[3] S. Johnson, C. Oliver, G. A. Prince et al., "Development of a humanized monoclonal antibody (MEDI-493) with potent in vitro and in vivo activity against respiratory syncytial virus," *Journal of Infectious Diseases*, vol. 176, no. 5, pp. 1215–1224, 1997.

[4] H. Grosfeld, M. G. Hill, and P. L. Collins, "RNA replication by respiratory syncytial virus (RSV) is directed by the N, P, and L proteins; transcription also occurs under these conditions but requires RSV superinfection for efficient synthesis of full-length mRNA," *Journal of Virology*, vol. 69, no. 9, pp. 5677–5686, 1995.

[5] Q. Yu, R. W. Hardy, and G. W. Wertz, "Functional cDNA clones of the human respiratory syncytial (RS) virus N, P, and L proteins support replication of RS virus genomic RNA analogs and define minimal trans-acting requirements for RNA replication," *Journal of Virology*, vol. 69, no. 4, pp. 2412–2419, 1995.

[6] P. L. Collins, M. G. Hill, J. Cristina, and H. Grosfeld, "Transcription elongation factor of respiratory syncytial virus, a nonsegmented negative-strand RNA virus," *Proceedings of the National Academy of Sciences of the United States of America*, vol. 93, no. 1, pp. 81–85, 1996.

[7] M. Satake and S. Venkatesan, "Nucleotide sequence of the gene encoding respiratory syncytial virus matrix protein," *Journal of Virology*, vol. 50, no. 1, pp. 92–99, 1984.

[8] P. L. Collins and G. W. Wertz, "The 1A protein gene of human respiratory syncytial virus: nucleotide sequence of the mRNA and a related polycistronic transcript," *Virology*, vol. 141, no. 2, pp. 283–291, 1985.

[9] G. W. Wertz, P. L. Collins, Y. Huang, C. Gruber, S. Levine, and L. A. Ball, "Nucleotide sequence of the G protein gene of human respiratory syncytial virus reveals an unusual type of viral membrane protein," *Proceedings of the National Academy of Sciences of the United States of America*, vol. 82, no. 12, pp. 4075–4079, 1985.

[10] P. L. Collins, Y. T. Huang, and G. W. Wertz, "Nucleotide sequence of the gene encoding the fusion (F) glycoprotein of human respiratory syncytial virus," *Proceedings of the National Academy of Sciences of the United States of America*, vol. 81, no. 24 I, pp. 7683–7687, 1984.

[11] E. E. Walsh and J. Hruska, "Monoclonal antibodies to respiratory syncytial virus proteins: identification of the fusion protein," *Journal of Virology*, vol. 47, no. 1, pp. 171–177, 1983.

[12] S. Levine, R. Kaliaber-Franco, and P. R. Paradiso, "Demonstration that glycoprotein G is the attachment protein of respiratory syncytial virus," *Journal of General Virology*, vol. 68, no. 9, pp. 2521–2524, 1987.

[13] M. N. Teng, S. S. Whitehead, and P. L. Collins, "Contribution of the respiratory syncytial virus G glycoprotein and its secreted and membrane-bound forms to virus replication in vitro and in vivo," *Virology*, vol. 289, no. 2, pp. 283–296, 2001.

[14] S. D. Carter, K. C. Dent, E. Atkins et al., "Direct visualization of the small hydrophobic protein of human respiratory syncytial virus reveals the structural basis for membrane permeability," *FEBS Letters*, vol. 584, no. 13, pp. 2786–2790, 2010.

[15] S. Fuentes, K. C. Tran, P. Luthra, M. N. Teng, and B. He, "Function of the respiratory syncytial virus small hydrophobic protein," *Journal of Virology*, vol. 81, no. 15, pp. 8361–8366, 2007.

[16] G. Brown, J. Aitkein, H. W. Rixon, and R. J. Sugrue, "Caveolin-1 is incorporated into mature respiratory syncytial virus particles during virus assembly on the surface of virus-infected cells," *Journal of General Virology*, vol. 83, no. 3, pp. 611–621, 2002.

[17] G. Brown, H. W. Rixon, and R. J. Sugrue, "Respiratory syncytial virus assembly occurs in GM1-rich regions of the host-cell membrane and alters the cellular distribution

of tyrosine phosphorylated caveolin-1," *Journal of General Virology*, vol. 83, no. 8, pp. 1841–1850, 2002.

[18] S. R. Roberts, R. W. Compans, and G. W. Wertz, "Respiratory syncytial virus matures at the apical surfaces of polarized epithelial cells," *Journal of Virology*, vol. 69, no. 4, pp. 2667–2673, 1995.

[19] M. J. Ciancanelli and C. F. Basler, "Mutation of YMYL in the Nipah virus matrix protein abrogates budding and alters subcellular localization," *Journal of Virology*, vol. 80, no. 24, pp. 12070–12078, 2006.

[20] M. Li, P. T. Schmitt, Z. Li, T. S. McCrory, B. He, and A. P. Schmitt, "Mumps virus matrix, fusion, and nucleocapsid proteins cooperate for efficient production of virus-like particles," *Journal of Virology*, vol. 83, no. 14, pp. 7261–7272, 2009.

[21] H. D. Pantua, L. W. McGinnes, M. E. Peeples, and T. G. Morrison, "Requirements for the assembly and release of Newcastle disease virus-like particles," *Journal of Virology*, vol. 80, no. 22, pp. 11062–11073, 2006.

[22] J. R. Patch, G. Crameri, L. F. Wang, B. T. Eaton, and C. C. Broder, "Quantitative analysis of Nipah virus proteins released as virus-like particles reveals central role for the matrix protein," *Virology Journal*, vol. 4, article 1, 2007.

[23] J. R. Patch, Z. Han, S. E. McCarthy et al., "The YPLGVG sequence of the Nipah virus matrix protein is required for budding," *Virology Journal*, vol. 5, article 137, 2008.

[24] F. Sugahara, T. Uchiyama, H. Watanabe et al., "Paramyxovirus sendai virus-like particle formation by expression of multiple viral proteins and acceleration of its release by C protein," *Virology*, vol. 325, no. 1, pp. 1–10, 2004.

[25] A. P. Schmitt, G. P. Leser, D. L. Waning, and R. A. Lamb, "Requirements for budding of paramyxovirus simian virus 5 virus-like particles," *Journal of Virology*, vol. 76, no. 8, pp. 3952–3964, 2002.

[26] M. N. Teng and P. L. Collins, "Identification of the respiratory syncytial virus proteins required for formation and passage of helper-dependent infectious particles," *Journal of Virology*, vol. 72, no. 7, pp. 5707–5716, 1998.

[27] M. Batonick, A. G. Oomens, and G. W. Wertz, "Human respiratory syncytial virus glycoproteins are not required for apical targeting and release from polarized epithelial cells," *Journal of Virology*, vol. 82, no. 17, pp. 8664–8672, 2008.

[28] M. D. Abràmoff, P. J. Magalhães, and S. J. Ram, "Image processing with imageJ," *Biophotonics International*, vol. 11, no. 7, pp. 36–41, 2004.

[29] E. M. Manders, J. Stap, G. J. Brakenhoff, R. Van Driel, and J. A. Aten, "Dynamics of three-dimensional replication patterns during the S-phase, analysed by double labelling of DNA and confocal microscopy," *Journal of Cell Science*, vol. 103, no. 3, pp. 857–862, 1992.

[30] A. G. Oomens, A. G. Megaw, and G. W. Wertz, "Infectivity of a human respiratory syncytial virus lacking the SH, G, and F proteins is efficiently mediated by the vesicular stomatitis virus G protein," *Journal of Virology*, vol. 77, no. 6, pp. 3785–3798, 2003.

[31] A. G. Oomens and G. W. Wertz, "The baculovirus GP64 protein mediates highly stable infectivity of a human respiratory syncytial virus lacking its homologous transmembrane glycoproteins," *Journal of Virology*, vol. 78, no. 1, pp. 124–135, 2004.

[32] A. G. Oomens and G. W. Wertz, "Trans-complementation allows recovery of human respiratory syncytial viruses that are infectious but deficient in cell-to-cell transmission," *Journal of Virology*, vol. 78, no. 17, pp. 9064–9072, 2004.

[33] A. G. P. Oomens, K. P. Bevis, and G. W. Wertz, "The cytoplasmic tail of the human respiratory syncytial virus F protein plays critical roles in cellular localization of the F protein and infectious progeny production," *Journal of Virology*, vol. 80, no. 21, pp. 10465–10477, 2006.

[34] K. Anderson, A. M. King, R. A. Lerch, and G. W. Wertz, "Polylactosaminoglycan modification of the respiratory syncytial virus small hydrophobic (SH) protein: a conserved feature among human and bovine respiratory syncytial viruses," *Virology*, vol. 191, no. 1, pp. 417–430, 1992.

[35] H. W. Rixon, G. Brown, J. T. Murray, and R. J. Sugrue, "The respiratory syncytial virus small hydrophobic protein is phosphorylated via a mitogen-activated protein kinase p38-dependent tyrosine kinase activity during virus infection," *Journal of General Virology*, vol. 86, no. 2, pp. 375–384, 2005.

[36] R. Ghildyal, D. Li, I. Peroulis et al., "Interaction between the respiratory syncytial virus G glycoprotein cytoplasmic domain and the matrix protein," *Journal of General Virology*, vol. 86, no. 7, pp. 1879–1884, 2005.

[37] K. W. Low, T. Tan, B. H. Tan, and R. J. Sugrue, "The RSV F and G glycoproteins interact to form a complex on the surface of infected cells," *Biochemical and Biophysical Research Communications*, vol. 366, no. 2, pp. 308–313, 2008.

[38] S. A. Feldman, R. L. Crim, S. A. Audet, and J. A. Beeler, "Human respiratory syncytial virus surface glycoproteins F, G and SH form an oligomeric complex," *Archives of Virology*, vol. 146, no. 12, pp. 2369–2383, 2001.

[39] S. Bolte and F. P. Cordelières, "A guided tour into subcellular colocalization analysis in light microscopy," *Journal of Microscopy*, vol. 224, no. 3, pp. 213–232, 2006.

[40] S. V. Costes, D. Daelemans, E. H. Cho, Z. Dobbin, G. Pavlakis, and S. Lockett, "Automatic and quantitative measurement of protein-protein colocalization in live cells," *Biophysical Journal*, vol. 86, no. 6, pp. 3993–4003, 2004.

Hindawi Publishing Corporation
Advances in Virology
Volume 2011, Article ID 650930, 6 pages
doi:10.1155/2011/650930

Research Article

The Prevalence of STIV c92-Like Proteins in Acidic Thermal Environments

Jamie C. Snyder,[1,2] Benjamin Bolduc,[2,3] Mary M. Bateson,[1,2] and Mark J. Young[1,2]

[1] *Department of Plant Sciences and Plant Pathology, Montana State University, Bozeman, MT 59717, USA*
[2] *Thermal Biology Institute, Montana State University, Bozeman, MT 59717, USA*
[3] *Department of Chemistry and Biochemistry, Montana State University, Bozeman, MT 59717, USA*

Correspondence should be addressed to Mark J. Young, myoung@montana.edu

Received 26 March 2011; Accepted 23 May 2011

Academic Editor: Claude Krummenacher

A new type of viral-induced lysis system has recently been discovered for two unrelated archaeal viruses, STIV and SIRV2. Prior to the lysis of the infected host cell, unique pyramid-like lysis structures are formed on the cell surface by the protrusion of the underlying cell membrane through the overlying external S-layer. It is through these pyramid structures that assembled virions are released during lysis. The STIV viral protein c92 is responsible for the formation of these lysis structures. We searched for c92-like proteins in viral sequences present in multiple viral and cellular metagenomic libraries from Yellowstone National Park acidic hot spring environments. Phylogenetic analysis of these proteins demonstrates that, although c92-like proteins are detected in these environments, some are quite divergent and may represent new viral families. We hypothesize that this new viral lysis system is common within diverse archaeal viral populations found within acidic hot springs.

1. Introduction

Compared to the viruses infecting organisms from the domains *Bacteria* and *Eukarya*, few viruses infecting archaeal organisms have been isolated and most are poorly understood in molecular detail. Most archaeal viruses are morphologically and genetically distinct from previously described viruses [1–4]. *Sulfolobus* turreted icosahedral virus (STIV) has emerged as a model system for examining archaeal virus replication and structure [5–15]. STIV was originally isolated from the Rabbit Creek thermal basin within Yellowstone National Park, (YNP) USA [15]. The STIV virion contains a circular double-stranded (ds) DNA genome of 17,663 base pairs (bps) which encodes for 37 open reading frames (ORFs). The cryoelectron microscopy image reconstruction of STIV particles revealed a pseudo $T = 31$ capsid, an internal membrane, and turret-like projections extending from each of the virions fivefold axes [15]. Structural analysis of the major capsid protein has suggested an evolutionary link between archaeal viruses and bacterial and eukaryotic viruses [7, 15].

Many viruses have evolved specific mechanisms for exiting their host cell at the end of their viral replication cycle. Lytic viruses of bacteria typically utilize a holin/endolysin-based mechanism for virion release [16, 17], whereas virion egress via a cellular budding mechanism is commonly used by enveloped animal viruses. A new lysis system was recently described for STIV [12, 14]. This lysis system involves the formation of unique pyramid lysis structures on the membrane of an infected cell prior to lysis (Figure 1). The lysis structures are a result of the protrusion of the cellular membrane through the S-layer surrounding the cell. A similar lysis system was more recently described in another archaeal virus, *Sulfolobus islandicus* rod-shaped virus 2 (SIRV2) [18–20], indicating that this type of lysis may be widespread among archaeal viruses. Even though these two different archaeal viruses appear to share a similar lysis mechanism, genetically they are very different from each other. Only one ORF shows any similarity between the two archaeal viruses [19]. A homologous viral protein from STIV and SIRV2 was recently identified as being responsible for

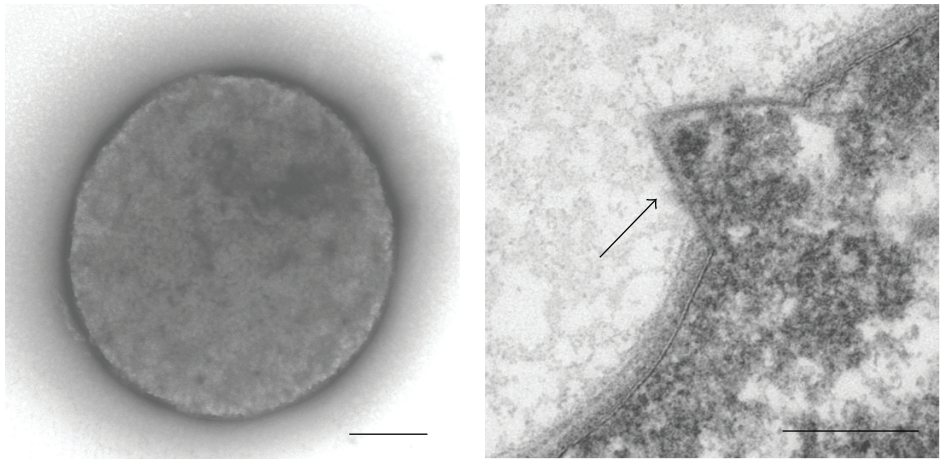

(a) (b)

Figure 1: Electron micrographs of *Sulfolobus* cells (a) not infected with STIV and (b) infected with STIV; arrow indicates the STIV-induced pyramid lysis structure. Bars: 250 nm (a) and 100 nm (b).

the formation of the pyramid lysis structures on the cell membrane [14, 18]. The STIV protein c92 [14] and the SIRV2 protein p98 [18] were independently heterologously overexpressed in *Sulfolobus* cells. Both proteins resulted in the formation of pyramid lysis structures in the absence of any other viral proteins. While the overexpression of the STIV c92 protein produced the pyramid-like structures, it did not directly lead to cell lysis, indicating there must be additional factors that are required to complete lysis of the host cell.

We are interested in examining the extent that c92-like lysis systems operate in crenarchaeal virus populations present in natural high-temperature low-pH environments. To determine whether this type of lysis system is common in crenarchaeal viruses, we compared the STIV c92 protein to archaeal cellular and viral metagenomic databases that we have produced from multiple acidic hot springs located in YNP. From this analysis, we conclude that c92-like proteins are present in the natural environment and lytic crenarchaeal viruses may be more prevalent than once thought.

2. Methods

Numerous metagenomic libraries from two geographically isolated thermal areas within YNP were used in this study. The first area is the Crater Hills thermal basin, containing an acidic (pH ~ 2.5) high-temperature (~82°C) hot spring (44.6532°N, 110.4847°W). The second thermal site is in the Nymph Lake area (44.7536°N, 110.7237°W) within Norris Geyser Basin in YNP and also contains acidic (pH ~ 3.5–4.5) and high-temperature (~91°C) hot springs. Over the course of four years we have produced a total of 39 metagenomic libraries from these two thermal areas within YNP. The metagenomes are enriched for either viral or cellular sequences by methods previously described ([21], B. Bolduc, F. F. Roberto, M. Lavin, and M. J. Young, manuscript in prep.).

The c92 protein encoded by STIV and its homologues found in a number of rudiviruses (SIRV2, SIRV1 variant XX, and SIRV1 [19]) were used to find related proteins using tBLASTn (http://blast.ncbi.nlm.nih.gov/) in a collection of 39 viral and cellular metagenomes produced from YNP acidic hot springs that contained more than 2.8 million sequencing reads and 807 megabases (Mb) of DNA sequence. An alignment of identified protein sequences from the YNP metagenomes and related proteins found in other archaeal viruses was performed using ClustalW (Blosum cost matrix) [22]. Following the alignment, phylogenetic analysis was executed using Mr. Bayes for 1.5 million generations, with a burn-in of 10,000 trees and sampling every 10,000 trees [23].

3. Results

The communities present in the acidic hot springs within YNP are dominated by archaeal organisms [21, 24, 25]. The unique viral lysis system described for STIV [12, 14] and SIRV2 [18–20] appears within the archaeal viral community associated within YNP acidic hot springs. By comparing STIV c92 and homologues in rudiviral genomes against our YNP viral and cellular metagenomic databases, we found 70 contigs coding for protein sequences that represent closely related proteins.

A tBLASTn search identified 70 contig matches to the STIV c92 protein. Alignment lengths varied from 36 to 92 (c92 full length) amino acid residues. The vast majority of matches were significant with *e*-values $<10^{-7}$ Most of the 70 contigs with matches to c92 from the metagenomic database (58 contigs representing 83% of the total number of c92 matches) aligned to at least 60 residues of the STIV c92 protein based on inferred amino acid similarity. Meanwhile, other sequences (12 contigs representing 17% of the total number of c92 matches) only aligned to less than half of the c92 sequence, because the end of the assembled contig fell within the c92-like sequence. The sequence variability within

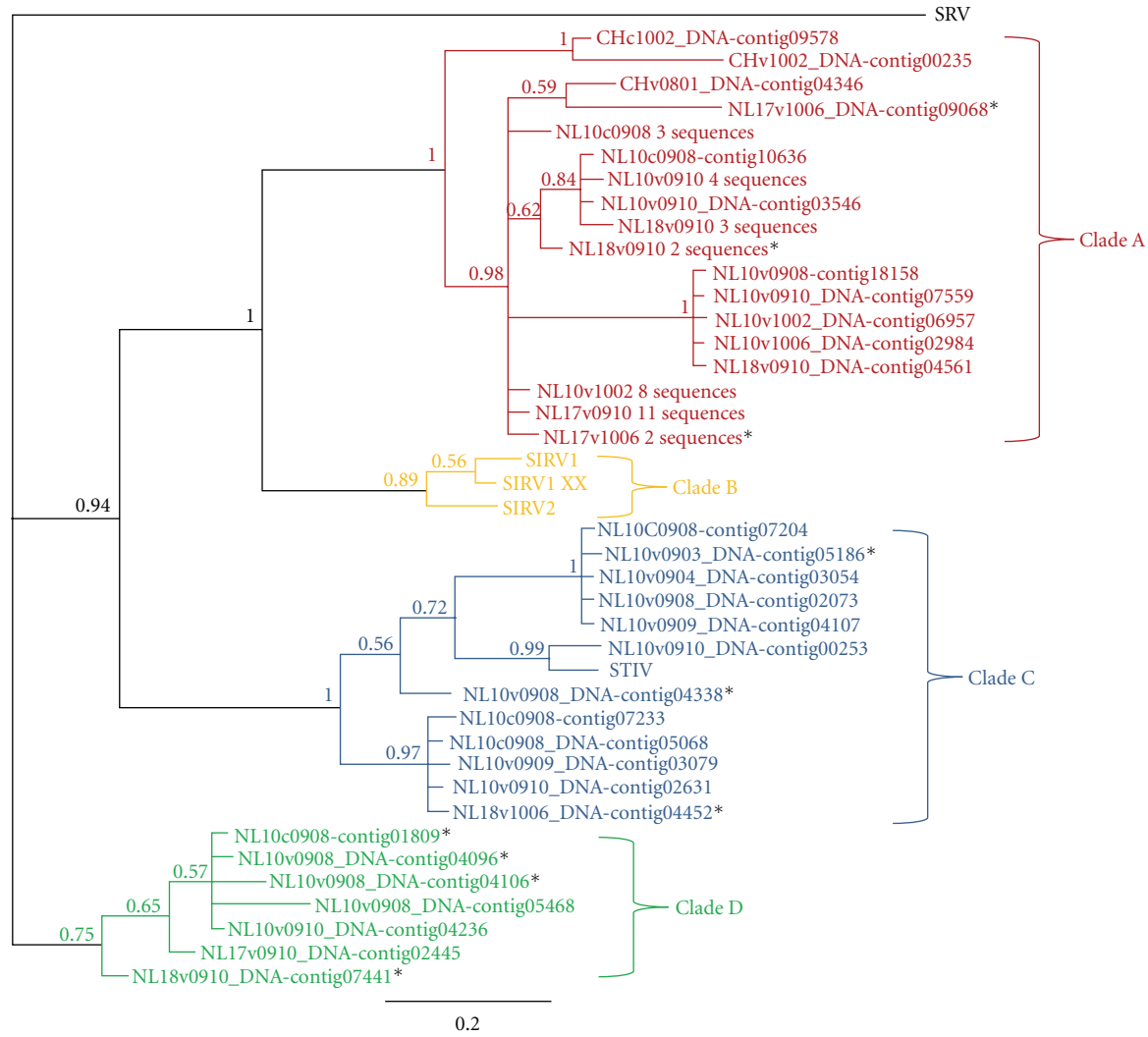

Figure 2: A maximum likelihood phylogenetic tree of c92-like proteins from YNP metagenomes illustrating three major families. SRV: *Stygiolobus* rod-shaped virus (outgroup); SIRV1: *Sulfolobus islandicus* rod-shaped virus 1; SIRV1 XX: SIRV1 variant XX; SIRV2: *Sulfolobus islandicus* rod-shaped virus 2; STIV: *Sulfolobus* turreted icosahedral virus; NL: Nymph Lake metagenomes; CH: Crater Hills metagenomes; sample names indicate cellular (c) or viral (v) metagenomes and the year followed by the month of sample collection; short contigs indicated by *. The numbers at the branches represent clade probabilities, and the scale bar represents the average number of substitutions per site.

Table 1: Sequence statistics for the three clades of c92-like proteins present in YNP.

	No. of reads	Average no. of reads/contig	Average contig length
Clade A	1153	64	592
Clade C	259	22	615
Clade D	98	14	583

the c92 protein was evenly spread through the entire length of the sequence. However, the N-terminal domains of the c92-like proteins consistently show a membrane spanning helix.

Phylogenetic analyses were performed on all contigs that aligned to c92 and on an alignment of the 58 contigs with complete c92-like proteins (Figure 2; contigs with incomplete c92-like proteins are indicated by *). Three well-supported clades of c92-like proteins were identified in the metagenomic data from Crater Hills and Nymph Lake (Figure 2). The SIRV family (Figure 2; Clade B) does not appear to have close relatives in our metagenomes. While it is likely that many of the sequences with near 100% amino acid similarity to the c92 protein represent STIV-like viruses known to exist in these environments (Figure 2; Clade C), others are more divergent representing the "c92-like" family of proteins and are present in viruses unrelated to STIV. There are two groups of contigs that are distinct from STIV and rudiviruses but, they comprise the vast majority of all the c92 matches (Figure 2; Clades A and D). The sequences with c92 matches belonging to Clade A comprise the largest group of c92-like proteins represented in our metagenomes (1,153 reads); however, all of the clades contained similar average contig lengths (Table 1).

Table 2: Characteristics of the c92 matches to YNP metagenomes.

	Total Matches	DNA viral libraries	RNA viral libraries	Cellular libraries
Crater Hills	3 (4%)[1]	2 (3%)	0 (0%)	1 (1%)
Nymph Lake	67 (96%)	56 (80%)	2 (3%)	9 (13%)
Total	70 (100%)	58 (83%)	2 (3%)	10 (14%)

[1] Indicates percentage of the total number of contigs (70) detected.

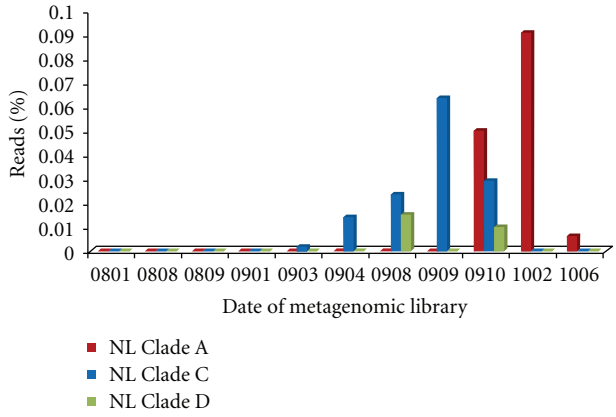

Figure 3: The temporal dynamics of c92-like protein clades in viral metagenomic data sets from a Nymph Lake (NL10) hot spring.

The characteristics of the metagenomes with matches to c92 are shown in Table 2. The contigs that matched c92 were primarily from viral DNA metagenomes created from the Nymph Lake hot springs (Table 2). For one of the Nymph Lake hot springs (NL10), the sampling dates for the libraries span from August 2008 through June 2010. The c92-like proteins from Clade A were detected in metagenomes from October 2009 through June 2010, while Clade C types were detected only from March 2009 through October 2009 (Figure 3). Clade D contained c92-like proteins that were present in August 2009, not detected in September 2009, then detected again in October 2009 (Figure 3). For the Crater Hills hot spring, the sampling dates for the libraries span from April 2007 through February 2010. The c92-like proteins from Crater Hills all belonged to Clade A but were detected only two of the five Crater Hills metagenomes (January 2008 and February 2010).

4. Discussion

Little is known about the viruses that infect organisms from the domain *Archaea*. Previously, it had been suggested that most archaeal viruses were nonlytic primarily due to the harsh conditions that many of these organisms inhabit and to the presence of integrase-like genes in many of the viral genomes. STIV was the first lytic crenarchaeal virus discovered [13], and SIRV2 was subsequently found to be lytic as well [20]. Homologous viral proteins from STIV and SIRV2 were discovered to be responsible for the formation of the unique pyramid lysis structures present on the *Sulfolobus* cellular membrane prior to viral-induced lysis [14, 18]. The presence of the viral-induced pyramid-like lysis structures on two unrelated viruses led us to investigate the prevalence of this type of viral lysis system in *Archaea*. We sought to determine the presence of c92-like proteins present in metagenomic datasets by comparing the sequenced STIV c92 protein to sequences collected from YNP.

Overall, there were three major clades of c92-like proteins detected in metagenomes from YNP (Figure 2). It surprised us that we did not detect relatives of the rudiviral clade (Figure 2; Clade B) in the YNP metagenomes even though we commonly detect SIRV-like viruses and sequences in acidic hot springs within YNP [21, 24, 26]. The majority of the c92-like sequences are in clades that are distantly related to STIV or SIRV2 (Figure 2; Clades A and D) and may represent new families of viruses that use a similar lysis mechanism. The clade that contains STIV (Figure 2; Clade C) contains sequences only from the Nymph Lake hot springs. The majority of c92-like protein sequences were detected in the Nymph Lake viral DNA metagenomes (Table 2). However, we did detect few c92-like sequences in the cellular metagenomes, which likely represent intracellular viruses.

It surprised us that we detected few c92-like sequences in Crater Hills compared to the number of c92-like sequences detected in Nymph Lake. The reason for this result is currently not understood; however, we speculate that differences in the water chemistry between these two sites may have an influence. The Crater Hills hot spring is a high-chloride, high-sulfur hot spring as compared to the Nymph Lake hot spring. The differences in water geochemistry, along with pH and temperature, may play a role in defining the microbial community composition and therefore virus community composition.

The alignments of the c92-like proteins revealed variation throughout the protein sequence. The c92-like proteins can be quite different and still function to form pyramid structures as is shown by the STIV c92 and SIRV2 p98 proteins. These homologous proteins are only 55.4% identical at the amino acid level, but both result in the formation of pyramid structures [14, 18]. The N-terminal domain of both STIV c92 and SIRV p98 is a predicted membrane spanning helix [19]. Secondary structure predictions of the c92-like proteins from the metagenomes also reveal a membrane spanning helix. Current experiments are underway to explore what residues in the STIV c92 protein are critical for the formation of the pyramid lysis structures.

The detection of c92-like proteins in our metagenomic data exhibits a dynamic pattern. Temporal analysis of the Nymph Lake metagenomic data reveals at times these c92-like proteins are undetectable, while at other times they

are persistent (although the clade that is present fluctuates) in the hot springs (Figure 3). This dynamic pattern has previously been shown for viruses within YNP [24].

This lysis system is not universal. STIV c92 homologues are not evident in the ~48 other archaeal viruses sequenced to date. Even other viruses isolated from *Sulfolobus* species do not have homologues to STIV c92 and/or SIRV2 p98 [19, 27]. This suggests that viruses in the same family may have evolved independent mechanisms to accomplish progeny virion release from infected cells. We are now challenged to isolate and further characterize archaeal viruses with phylogenetic relationships to the c92 family of proteins to confirm that they undergo host lysis mechanisms similar to STIV and SIRV2.

Acknowledgments

This research is supported by the National Science Foundation Grant nos. DEB-0936178 and EF-080220 and the National Aeronautics and Space Administration Grant no. NNA-08CN85A.

References

[1] C. M. Lawrence, S. Menon, B. J. Eilers et al., "Structural and functional studies of archaeal viruses," *Journal of Biological Chemistry*, vol. 284, no. 19, pp. 12599–12603, 2009.

[2] D. Prangishvili, P. Forterre, and R. A. Garrett, "Viruses of the Archaea: a unifying view," *Nature Reviews Microbiology*, vol. 4, no. 11, pp. 837–848, 2006.

[3] D. Prangishvili, R. A. Garrett, and E. V. Koonin, "Evolutionary genomics of archaeal viruses: unique viral genomes in the third domain of life," *Virus Research*, vol. 117, no. 1, pp. 52–67, 2006.

[4] J. C. Snyder, K. Stedman, G. Rice, B. Wiedenheft, J. Spuhler, and M. J. Young, "Viruses of hyperthermophilic Archaea," *Research in Microbiology*, vol. 154, no. 7, pp. 474–482, 2003.

[5] R. Khayat, C. Y. Fu, A. C. Ortmann, M. J. Young, and J. E. Johnson, "The architecture and chemical stability of the archaeal *Sulfolobus* turreted icosahedral virus," *The Journal of Virology*, vol. 84, no. 18, pp. 9575–9583, 2010.

[6] W. S. Maaty, A. C. Ortmann, M. Dlakić et al., "Characterization of the archaeal thermophile *Sulfolobus* turreted icosahedral virus validates an evolutionary link among double-stranded DNA viruses from all domains of life," *The Journal of Virology*, vol. 80, no. 15, pp. 7625–7635, 2006.

[7] R. Khayat, L. Tang, E. T. Larson, C. M. Lawrence, M. Young, and J. E. Johnson, "Structure of an archaeal virus capsid protein reveals a common ancestry to eukaryotic and bacterial viruses," *Proceedings of the National Academy of Sciences of the United States of America*, vol. 102, no. 52, pp. 18944–18949, 2005.

[8] E. T. Larson, B. J. Eilers, D. Reiter, A. C. Ortmann, M. J. Young, and C. M. Lawrence, "A new DNA binding protein highly conserved in diverse crenarchaeal viruses," *Virology*, vol. 363, no. 2, pp. 387–396, 2007.

[9] E. T. Larson, D. Reiter, M. Young, and C. M. Lawrence, "Structure of A197 from *Sulfolobus* turreted icosahedral virus: a crenarchaeal viral glycosyltransferase exhibiting the GT-A fold," *The Journal of Virology*, vol. 80, no. 15, pp. 7636–7644, 2006.

[10] E. T. Larson, B. Eilers, S. Menon et al., "A winged-helix protein from sulfolobus turreted icosahedral virus points toward stabilizing disulfide bonds in the intracellular proteins of a hyperthermophilic virus," *Virology*, vol. 368, no. 2, pp. 249–261, 2007.

[11] J. F. Wirth, J. C. Snyder, R. A. Hochstein et al., "Development of a genetic system for the archaeal virus *Sulfolobus* turreted icosahedral virus," *Virology*, vol. 415, no. 1, pp. 6–11, 2011.

[12] S. K. Brumfield, A. C. Ortmann, V. Ruigrok, P. Suci, T. Douglas, and M. J. Young, "Particle assembly and ultrastructural features associated with replication of the lytic archaeal virus *Sulfolobus* turreted icosahedral virus," *The Journal of Virology*, vol. 83, no. 12, pp. 5964–5970, 2009.

[13] A. C. Ortmann, S. K. Brumfield, J. Walther et al., "Transcriptome analysis of infection of the archaeon *Sulfolobus solfataricus* with *Sulfolobus* turreted icosahedral virus," *The Journal of Virology*, vol. 82, no. 10, pp. 4874–4883, 2008.

[14] J. C. Snyder, S. K. Brumfield, N. Peng, Q. She, and M. J. Young, "*Sulfolobus* Turreted Icosahedral Virus c92 protein responsible for formation of pyramid-like cellular lysis structures," *The Journal of Virology*, vol. 85, no. 13, pp. 6287–6292, 2011.

[15] G. Rice, L. Tang, K. Stedman et al., "The structure of a thermophilic archaeal virus shows a double-stranded DNA viral capsid type that spans all domains of life," *Proceedings of the National Academy of Sciences of the United States of America*, vol. 101, no. 20, pp. 7716–7720, 2004.

[16] R. Young, "Bacteriophage lysis: mechanism and regulation," *Microbiological Reviews*, vol. 56, no. 3, pp. 430–481, 1992.

[17] I.-N. Wang, D. L. Smith, and R. Young, "HOLINS: the protein clocks of bacteriophage infections," *Annual Review of Microbiology*, vol. 54, pp. 799–825, 2000.

[18] T. E. F. Quax, S. Lucas, J. Reimann et al., "Simple and elegant design of a virion egress structure in Archaea," *Proceedings of the National Academy of Sciences of the United States of America*, vol. 108, no. 8, pp. 3354–3359, 2011.

[19] T. E. F. Quax, M. Krupovic, S. Lucas, P. Forterre, and D. Prangishvili, "The *Sulfolobus* rod-shaped virus 2 encodes a prominent structural component of the unique virion release system in Archaea," *Virology*, vol. 404, no. 1, pp. 1–4, 2010.

[20] A. Bize, E. A. Karlsson, K. Ekefjärd et al., "A unique virus release mechanism in the Archaea," *Proceedings of the National Academy of Sciences of the United States of America*, vol. 106, no. 27, pp. 11306–11311, 2009.

[21] J. C. Snyder, M. M. Bateson, M. Lavin, and M. J. Young, "Use of cellular CRISPR (clusters of regularly interspaced short palindromic repeats) spacer-based microarrays for detection of viruses in environmental samples," *Applied and Environmental Microbiology*, vol. 76, no. 21, pp. 7251–7258, 2010.

[22] J. D. Thompson, D. G. Higgins, and T. J. Gibson, "CLUSTAL W: improving the sensitivity of progressive multiple sequence alignment through sequence weighting, position-specific gap penalties and weight matrix choice," *Nucleic Acids Research*, vol. 22, no. 22, pp. 4673–4680, 1994.

[23] J. P. Huelsenbeck and F. Ronquist, "MRBAYES: Bayesian inference of phylogenetic trees," *Bioinformatics*, vol. 17, no. 8, pp. 754–755, 2001.

[24] J. C. Snyder, B. Wiedenheft, M. Lavin et al., "Virus movement maintains local virus population diversity," *Proceedings of the National Academy of Sciences of the United States of America*, vol. 104, no. 48, pp. 19102–19107, 2007.

[25] W. P. Inskeep, D. B. Rusch, Z. J. Jay et al., "Metagenomes from high-temperature chemotrophic systems reveal geochemical controls on microbial community structure and function," *PLoS One*, vol. 5, no. 3, article e9773, 2010.

[26] G. Rice, K. Stedman, J. Snyder et al., "Viruses from extreme thermal environments," *Proceedings of the National Academy of Sciences of the United States of America*, vol. 98, no. 23, pp. 13341–13345, 2001.

[27] L. J. Happonen, P. Redder, X. Peng, L. J. Reigstad, D. Prangishvili, and S. J. Butcher, "Familial relationships in hyperthermo- and acidophilic archaeal viruses," *The Journal of Virology*, vol. 84, no. 9, pp. 4747–4754, 2010.